Universidad Austral de Chile
Facultad de Ciencias Veterinarias

Austral Journal of Veterinary Sciences

ISSN 0719-8000 / ISSN 0719-8132

Fotografía: Juan Ramírez

VOLUME 55 / VALDIVIA - CHILE / 2023 / Nº 3

This journal is subsidised by
Vicerrectoría de Investigación, Desarrollo y Creación Artística (VIDCA)
Periodicity: Triannual (January-May-September). Funded in 1969.

Indexed in:

- Current Contents Agriculture, Biology and Environmental Sciences (CC/AB and ES)
- Commonwealth Agricultural Bureau, International (C.A.B.I.)
- Dairy Science Abstracts
- Veterinary Bulletin
- Animal Breeding Abstracts
- Helminthological Abstracts S.A.
- Agrindex
- Biological Abstracts
- Periódica
- Focus on: Veterinary Sciences and Medicine
- Science Citation Index Expanded
- Scielo - Chile
- Google Scholar
- Ebsco
- Scopus

Austral Journal of Veterinary Sciences

VOL. 55, Nº 3, 2023

Universidad Austral de Chile
Facultad de Ciencias Veterinarias
Casilla 567 - Valdivia - Chile

VOLUME 55, Nº 3, 2023

Austral Journal of Veterinary Science

Austral J Vet Sci 55, 153-154 (2023)
https://doi.org/10.4206/ajvs.553.00

EDITORIAL

In Memory of Dr. med. vet. Gerold Sievers Prekehr (1943–2023)

Miguel Peña-Espinoza[1*], Pamela Muñoz[2]

[1] Institute of Parasitology, Department of Pathobiology, University of Veterinary Medicine Vienna, Vienna, Austria

[2] Laboratorio de Parasitología, Instituto de Patología Animal, Facultad de Ciencias Veterinarias, Universidad Austral de Chile, Valdivia, Chile

Corresponding author
*Miguel Peña-Espinoza
miguel.pena@vetmeduni.ac.at

"Scientific curiosity makes you wonder: what's underneath that rock? And when you finally raise that rock to discover what is below, you will always find many more little rocks – and now you want to know what's beneath each one of them"

Gerold Sievers Prekehr

Gerold Sievers Prekehr was an eminent veterinary parasitologist and former Full Professor at the Faculty of Veterinary Sciences of the Universidad Austral de Chile (UACh) in Valdivia. After obtaining his veterinary degree at the UACh, Prof. Sievers joined the University's Veterinary Hospital as lecturer. He obtained his doctorate (Dr. med. vet.) in 1973 at the University of Veterinary Medicine Hannover (TiHo), Germany, with a thesis describing a novel method to isolate infective larvae of parasitic nematodes from pasture[1]. Following a period as scientist in the German pharmaceutical industry, Prof. Sievers returned to Chile in 1975 to take a position as Professor and Director of the Laboratory of Parasitology in the Institute of Animal Pathology at the UACh, roles that he held until his retirement in 2009.

During his academic and scientific career of over 40 years, Prof. Sievers studied the biology, epidemiology, diagnosis, prevention and control of several parasites of veterinary and zoonotic importance in Chile. He performed long-term research studies on the seasonal dynamics of parasite egg excretion and development of infective stages of parasitic nematodes of cattle, sheep, horses and cervids in different environments in southern Chile[2,3,4]. Prof. Sievers also investigated the life cycles and epidemiology of the cattle horn fly *Haematobia irritans* and the equine bot flies *Gasterophilus*[5], as well as the biology and economic impact of the salmon parasites *Ceratothoa gaudichaudii*[6] and *Caligus rogercresseyi*. This seminal work provided new understanding on local infection dynamics of several parasite-host systems, allowing the design of prevention and control strategies of endoparasites and ectoparasites based on the principles of "prophylaxis" (management practices of contaminated areas and of animals to avoid clinical parasitoses) and "metaphylaxis" (strategic administration of antiparasitic drugs to reduce the parasite infective stages in the environment). Furthermore, Prof. Sievers performed extensive studies on the field efficacy of anthelmintics in cattle and horses, reporting the first cases of anthelmintic resistance in equine and bovine nematodes in Chile[7,8], as well as testing the effects of bioactive forages as complementary parasite control strategy in cattle[9]. In addition, he conducted investigations on the fertility and viability of hydatid cysts of *Echinococcus granulosus* in cattle[10] and on the environmental contamination with *Toxocara canis* eggs.

For almost 40 years, the didactic and engaging teaching classes of Prof. Sievers captivated the attention of many generations of veterinary students, often combining the

[1] *Sievers G. 1973. Methode zur Gewinnung von III. Strongylidenlarven aus dem Weidegras. Diss. Dr. med. vet., Tierärztliche Hochschule Hannover*
[2] *Sievers G. 1982. Epizootiología de las trichostrongilidosis de los terneros en Chile. En: VIII Jornadas Médico-Veterinarias, 26-28 de agosto de 1982, Valdivia, Chile, 93-112*
[3] *Sievers G et al. 1998. Annual variation in the distribution of bovine trichostrongyle infective larvaeon pasture grass in Valdivia, Chile. Arch. med. vet. 30 (1), 47-54*
[4] *Sievers G et al. 2002. Annual study of the of egg and oocyst outputs of gastrointestinal parasites and lungworm larvae in a sheep station of Magallanes, Chile. Arch. med. vet. 34 (1), 37-47*
[5] *Sievers G and Weber, B. 2005. Egg laying period of Gasterophilus nasalis and G. intestinalis on horses. 8th Region, Chile. Arch. med. vet. 37 (2), 169-172*
[6] *Sievers G et al. 1996. The effect of the isopod parasite Ceratothoa gaudichaudii on the body weight of farmed Salmo salar in southern Chile. Aquaculture 143, 1-6*
[7] *Sievers G and Alocilla A. 2007. Anthelminthic resistance of bovine nematodes against ivermectin in two farms of the south of Chile. Arch. med. vet. 39 (1), 67-69*
[8] *von Samson-Himmelstjerna et al. 2002. Comparative use of faecal egg count reduction test, egg hatch assay and beta-tubulin codon 200 genotyping in small strongyles (Cyathostominae) before and after benzimidazole treatment. Vet. Parasitol. 108, 227-235*
[9] *Sievers G and Nannig S. 2006. Effect of the supplementary feeding with Plantago lanceolata on the egg output of gastrointestinal nematodes in calves. Arch. med. vet. 38 (3), 233-238*
[10] *Muñoz JP and Sievers G. 2005. Study of the fertility and viability of bovine hydatid cysts in Chile. Parasitol. Latinoam. 60, 69-73*
[11] *Sievers G. 2022. Parasitosis del Bovino: Epidemiología y Posibilidades de Control. Valdivia*

explanation of the sophisticated parasites' life cycles with related (classical) musical pieces. In parallel to his academic activities, Prof. Sievers was a regular guest speaker on parasite control for veterinarians and livestock producers, always very keen to translate scientific findings to the end users, giving more than 140 talks to different audiences between Santiago and Punta Arenas.

Prof. Sievers published his works in 40 scientific articles in indexed journals, several of these in the predecessor of this Journal (Archivos de Medicina Veterinaria), and as supervisor of more than 80 undergraduate theses and postgraduate dissertations. He presented his research at many international and national scientific conferences, including presentations at the International Congresses of the World Association for the Advancement of Veterinary Parasitology (WAAVP), at the Chilean Society of Parasitology (SOCHIPA) and in the symposiums of the Rioplatense Meeting of Veterinary Endoparasitologists with experts from Argentina, Uruguay, Brazil and Chile. He was a member of the Colegio Médico Veterinario of Chile (1969–2009) and of SOCHIPA (1977–2009), which awarded him a recognition for his work in 2004.

After his retirement from the UACh, Prof. Sievers remained active as supervisor of veterinary theses and as an independent scientific consultant, always developing innovative methods for his new research studies, and in 2022 published a book for veterinary practitioners summarising his knowledge on the epidemiology and control of cattle parasites in Chile[11]. He died in Valdivia on August 22, 2023. He will be remembered as a man devoted to his family and to his friends, as a dedicated and passionate teacher, supervisor and veterinary parasitologist with ceaseless scientific curiosity, and as an example of consequence, modesty and intellectual honesty.

Dr. med. vet. Gerold Sievers Prekehr (1943–2023).

Austral Journal of Veterinary Science

Austral J Vet Sci 55, 155-166 (2023)
https://doi.org/10.4206/ajvs.553.01

ORIGINAL ARTICLE

Cesarean surgery and ovariohysterectomy in a precocial rodent *Octodon degus*

Loreto A. Correa[1*], Ángelo Espinoza[2], O. Alejandro Aleuy[3], Mauricio Soto-Gamboa[4]

[1] Escuela de Medicina Veterinaria, Facultad de Medicina y Ciencias de la Salud, Universidad Mayor, Santiago, Chile.

[2] Centro de Rehabilitación de Fauna Silvestre (CEREFAS), Facultad de Ciencias Veterinarias, Universidad Austral de Chile, Valdivia, Chile.

[3] Department of Biological Sciences, University of Notre Dame, Notre Dame, Indiana, USA.

[4] Laboratorio de Ecología Conductual y Conservación, Instituto de Ciencias Ambientales y Evolutivas, Facultad de Ciencias, Universidad Austral de Chile. Valdivia, Chile.

Article History
Received: 12.12.2022
Accepted: 24.04.2023
Published: 01.09.2023

Corresponding author
*Loreto A. Correa
lcorreak@bio.puc.cl
loreto.correa@umayor.cl

ABSTRACT. The common degu (*Octodon degus*) is a trendy rodent pet in Europe and the USA, but is also widely used in scientific research. Information about degu housing, nutrition, behavior, disease diagnosis, and disease treatment is abundant in scientific literature. However, information on reproductive management, such as cesarean section, ovariohysterectomy, ovariectomy, and orchiectomy, is scarce and anecdotal. Our general objective was to develop a protocol for cesarean section and ovariohysterectomy for degus. Our results indicated that cesarean post-surgical survival was 100% for mothers and 97% for offspring, while ovariohysterectomy female postsurgical survival was 100%. Cesarean surgeries lasted an average of 61.82 min, while ovariohysterectomies lasted an average of 32.65 min. The initial recovery times for cesarean sections and ovariohysterectomies were an average of 8.18 and 5.53 min, respectively. The full recovery time for cesarean section was an average of 50.18 min, whereas that for ovariohysterectomies was an average of 15.38 min. These results suggest that both protocols are viable for use in veterinary clinics that use mid-level equipment. We discuss our results with data from other rodent species and rabbits and with orchiectomy and ovariectomy procedures practiced in degu. Finally, we discuss in detail four critical considerations for cesarean and ovariohysterectomy surgeries performed on small mammals such as degu.

Keywords: cesarean surgery; ovariohysterectomy surgery; common degu; *Octodon degus*.

INTRODUCTION

The common degu (*Octodon degus*), a caviomorph rodent endemic to Central Chile, has several characteristics that make it an exciting animal model. Degu has interesting life-history traits, including being long-lived (under laboratory conditions, ~ 8 years), having large litters, and giving birth to precocial pups (Rojas *et al*., 1982). Degu is a social breeder in which females share nests and offspring care, including nursing, for both their own and unrelated offspring (Ebensperger *et al*., 2004). Male degu can also provide offspring care (Ebensperger *et al*., 2010; Aspillaga-Cid *et al*., 2021). Degu has been widely used in laboratory experiments because it can be easily acclimatized to laboratory conditions (Weir, 1970; 1974), making it the most studied native Chilean species (Labra *et al*., 2021). Additionally, degu is an excellent model for biomedical research; degus has been used in studies of diabetes (Wright & Kern, 1992), amyloidosis (Nishi & Steiner, 1990), Alzheimer's disease (Castro-Fuentes & Socas-Pérez, 2012), and aging (Cuenca-Bermejo *et al*., 2020). Finally, degu is common as a pet and zoo in Europe and the USA (Jekl *et al*., 2010).

Due to the prevalence of degu living in captivity (houses, zoos, and research colonies), it is possible to find several studies that provide varied information relative to degu housing (Palacios & Lee, 2013), nutrition and behavior (Gutiérrez & Bozinovic, 1998; Edwards, 2009), disease diagnosis and treatment (Richardson, 2003; Jekl *et al*., 2010), and reproductive management and breeding (Palacios & Lee, 2013). However, only two studies have provided relevant information regarding the reproductive management of degu. The first study (Malbrue *et al*., 2019) assessed two orchiectomy techniques (pre-scrotal open technique vs. scrotal open technique) and one ovariectomy technique (bilateral technique). The second study corresponds to a case report of pregnancy failure, which concluded with the extraction of two dead fetuses and the uterus from a very young (3-month-old) female (Mancinelli *et al*., 2013). To date, studies relevant to female reproductive management such as ovariohysterectomy (OVH) and cesarean section (CS) are not available in the literature. Studying and describing these procedures is essential for implementing efficient reproductive management programs in captive settings such as research colonies, zoo colonies, breeding programs, and pet trade (Malbrue *et al*., 2019). Procedures such as OVH and CS have been described in other rodent species including hamsters (Fleischman, 1981), rats (Redobre, 2002), guinea pigs (Richardson & Flecknell, 2006; Prior, 1986; Jones, 1990), gerbils (Mighell & Baker, 1990) and rabbits (Richardson & Flecknell, 2006). These reports concluded that there are four critical aspects to consider during OVH and CS procedures: i) respiratory compromise due to pres-

sure of the visceral organs on the diaphragm, ii) difficulty in maintaining proper body temperature during the procedure due to decreased thermoregulatory ability under anesthesia, exacerbated by incision of the abdominal cavity and small body size, iii) suture dehiscence due to gnawing behavior, and iv) cessation or decreased motility of the small intestine (paralytic ileus) as a consequence of abdominal pain (Redobre, 2002; Richardson & Flecknell, 2006; Malbrue *et al*., 2019). Degu is a caviomorph rodent; thus, the chinchilla and guinea pig protocols have also been used for degu. However, degus is much smaller (170–250 g) (Ebensperger *et al*., 2004) than chinchillas (400–600 g) (Richardson, 2003) and guinea pigs (700–1100 g) (Terril & Clemons, 1998), and anesthesia and surgery are more complicated due to the difficulty of accessing the vascular and respiratory system function and because of the rapid loss of heat from such small-sized caviomorph rodents (Malbrue *et al*., 2019).

Relevant reproductive aspects of *degus*

Degu is a small-to medium-sized (ranging from 170 to 250 g) diurnal rodent that inhabits scrubland areas of arid central Chile (Ebensperger *et al*., 2004). Sexual maturity in degus occurs ~6 months after birth but can occur as early as 2 months or as late as 9 months of age (Rojas *et al*., 1982), with the primary mating season occurring during the late austral fall (June). Occasionally, degus undergoes a second breeding event as a result of post-partum estrus, with birth during late December and lactation extending through January (Ebensperger *et al*., 2013). After a gestation period of 87 ± 3 days (Rojas *et al*., 1982), females give birth an average of 3.42 ± 2.71 (SD) offspring, with a range of 0–10 offspring (Ebensperger *et al*., 2019). Degus has a chorioallantoic placenta (Mess, 2007), which corresponds to a haemomonochorial structure (Kanashiro *et al*., 2009). Degus has a long pregnancy period in rodents, likely because it produces precocial offspring (Long & Ebensperger, 2010). Offspring are born with open eyes and ears, well-developed incisors, an entire body covered with hair, long and stained nails, and large vibrissae (Reynolds & Wright, 1979; Rojas *et al*., 1982; Jekl *et al*., 2010). Lactation is relatively short, lasting for approximately 30 days, and corresponds to the most energetically demanding life-history stage for degu dams (Veloso & Bozinovic, 2000). In captivity, degus can live for 7 to 10 years (Edwards, 2009), females reproduce for four years, and males remain fertile until death (Palacios & Lee, 2013).

The main objective of this study was to describe a protocol for CS and OVH in degus. Our specific objectives were to determine: 1) percentage of maternal and neonatal survival, 2) duration of the procedure, and 3) time to initial and full recovery for both procedures. For the duration of both procedures, we determined whether surgeon expertise (i.e., measured as the order in which procedures were practiced, first last) and, in the case of CS, the size of the litter could be associated with the procedure duration. In addition, we provided descriptive data related to the reproductive traits of degu. Finally, based on our experience with degu CS and OVH, we discuss the critical points reported in other rodent species during CS and OVH.

MATERIAL AND METHODS

Study subjects and animal housing

The study was conducted between March 2011 and March 2012. A total of 38 pregnant females were included in the study (11 females with CS and 27 with OVH). CS females were two years old (born in 2009), and the procedure was performed at their second birth. OVH females were one-year-old (born in 2010) with one previous birth. To impregnate the females, we used two-year-old reproductive males (born in 2009) with records of reproductive success. All animals were born in captivity at the Universidad Austral de Chile (UACh) animal colony. The parents of these individuals were obtained from the animal colony of the Pontificia Universidad Católica de Chile (PUC) and corresponded to the third generation of captive animals born from wild specimens captured in Rinconada de Maipú, Chile (33°23'S, 70°31'W) in 2006. Each individual was maintained in a standard polycarbonate transparent rat box (45 × 23 × 21 cm) with hardwood chip bedding, water, and food (Cisternas® commercial rabbit pellets) provided *ad libitum*. The animals were provided with sticks, cardboard, and wood to gnaw. The vivarium room had an active ventilation system and an artificial photoperiod of 12:12 hour light-dark. The Ambient temperature and humidity were maintained at 18 ± 2 °C and 49% ± 3%, respectively.

Cesarean context

CS surgeries were performed in a behavioral ecology study (Correa, 2012), the objective of which was to determine whether intrauterine position (the position in utero occupied by each pup) relative to male siblings was related to differential exposure to androgens (for details, see Correa *et al*., 2013; Correa *et al*., 2016). CS was performed one day before the estimated parturition date (mean pregnancy period of 87 days from visible sperm plugs) (Rojas *et al*., 1982).

Cesarean surgery protocol

Pre-surgical management. We did not apply pre-surgical fasting, as we wanted to avoid hypoglycemia, and vomiting and regurgitation are unlikely in rodents (Redobre, 2002; Richardson & Flecknell, 2006). One hour before surgery, we treated the females with analgesics (tramadol 2 mg/kg of body weight, SC Tramadol Clorhidrato®, Sanderson Lab, Santiago, Chile) and fluids (10 ml 0.9% NaCl, SC) to reduce pain and improve hemodynamics (Redobre, 2002; Richardson, 2003).

Surgical procedure. Anesthetic induction was performed in an induction chamber (plastic box) with an oxygen flow of 1 L/min, and the initial percentage of isoflurane (Isofluorano USP®, Baxter Lab Santiago, Chile) of 2% gradually rising to 4% during the first minute. Once the animal was unconscious, it was removed from the chamber and placed

in a stretcher. Anesthesia was continued using an inhalation anesthesia machine (Surgivet/Anesco; model 100) and a face mask (non-rebreathing system Mapleson type B) specially designed to decrease nose size (a plastic perfume bottle cut and padded with gauze in the area in contact with the face). Anesthesia was maintained with an oxygen flux of 0.6 liter/min and 3% isoflurane throughout the surgical procedure.

To assess the depth of anesthesia, we squeezed the skinfold between the toes. Forceps were used to tighten the skin folds. If the animal did not move its leg, the absence of deep pain and the existence of a deep plane of anesthesia were assumed. Once anesthetized, we positioned the animal in dorsal recumbency, with the head and thorax raised at 45° to reduce visceral pressure (degus has a well-developed cecum) on the thorax and promote pulmonary ventilation (Redobre, 2002; Mancinelli *et al*., 2013). The arms and legs were maintained in a stretched position by using cotton ropes tied to a stretcher. After applying an ophthalmic ointment to maintain eye hydration, we covered the eyes of each female with a cotton hood (made by cutting the top of a baby sock), but left the nostrils exposed. Each female was placed in a slightly warm seed bag throughout surgery. Each degu was supported by seed bags that were placed on either side of the body. Only the degu head was left without moderate heat supply. The abdomen of the female was shaved with an electric razor and the skin was disinfected with iodinated alcohol (70%).

We initiated surgery with an abdominal midline laparotomy on the white line, exposing the gravid uterine horns one at a time (Figure 1). The pups were removed from the uterus one at a time, from the ovarian end to the cervical extreme of the uterine horn, starting with a horn with fewer pups. Using tissue scissors, we opened the fetal membranes and removed the pups by tearing the umbilical cord. Immediately after each pup was removed from the uterus, a second surgeon assisted the newborn by wiping the oronasal superficial secretions with soft gauze, gently shaking in short, up-and-down motions with the pup's head pointing downwards to eliminate nasal fluids, gently drying the pup's coat with a paper towel, and finally disinfecting and cauterizing the umbilical cord with a cotton swab soaked in a 10% iodine solution. Newborns were then placed in a box with bedding 60 cm beneath a red heat lamp. Female degus allonurse and provide maternal care indiscriminately to biological and foreign offspring (Ebensperger *et al*., 2006), thus we placed newborn pups with a second lactating female until the mother recovered from anesthesia.

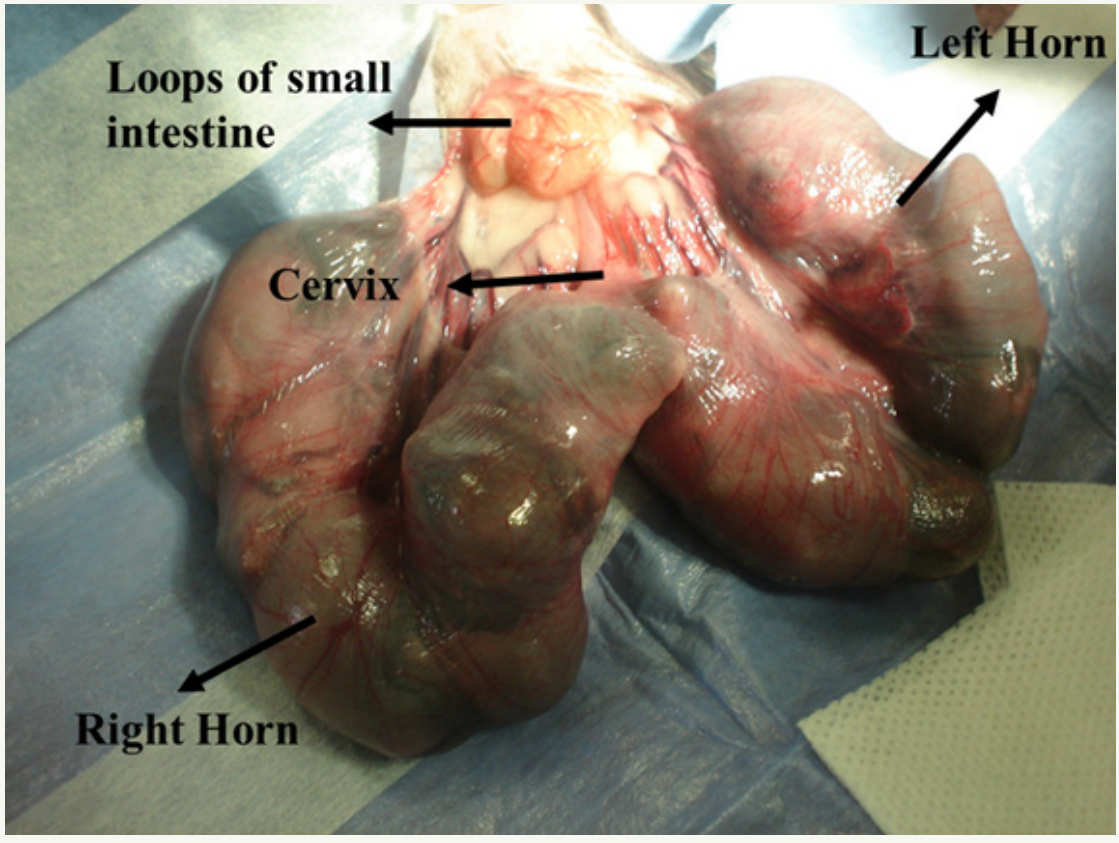

Figure 1. Gravid uterus of degu, exposed during a cesarean surgery. In addition to the cervix, the right horn and left horn of the uterus are indicated.

During surgery, we administered slightly warm and sterile intraperitoneal fluid (10 ml sterile 0.9% NaCl) to improve hydration and maintain abdominal visceral moisture (Redobre, 2002; Richardson, 2003). This procedure was repeated three times (total, 30 ml), with 20 minutes between each infusion period. After the removal of the pups, the uterus and ovaries were removed from the ovarian end to the cervix. Ligation of the uterine and ovarian stumps was performed with polyglycolic acid (Vycril®) 3-0, following the recommendations (Redobre, 2002; Richardson & Flecknell, 2006). Polyglycolic acid (Vycril®) 3-0 was also used for peritoneum and muscle sutures. We performed a discontinuous skin suture using nylon 3-0 attached to 23G needles. Anesthesia was closed when the skin suture was started. After finishing the skin sutures, the females remained on the face mask and received oxygen for 5–10 minutes (depending on the latency to wake up). Finally, the sutures were disinfected with iodinated alcohol (70%). Surgeries were performed by well-trained veterinarians (A.E, O.A.A, L.A.C) at the minor surgical pavilion of the Veterinary Teaching Hospital Facilities, Faculty of Veterinary Sciences, Universidad Austral de Chile.

Post-surgical management. Once the females woke up from the anesthesia, they were allocated to the same box with their litter and the nursing female. Wood chip bedding was used with pieces of tissue paper in each corner to provide a comfortable nest (Richardson & Flecknell, 2006). Once the two nursing females were together with the litter, a red heat lamp was placed 80 cm above the box to provide a warm environment (Richardson, 2003). The family was kept under a red heat lamp for one night, and the mother was offered an isotonic hydrating solution (Gatorade®) and palatable food (sunflower seeds and crushed oats) to encourage gut motility (Richardson & Flecknell, 2006). After surgery, all females were injected with an antibiotic (enrofloxacin, 5 mg/kg, SC Baytril®, Bayer Lab, Santiago, Chile) (Richardson, 2003), anti-inflammatory (ketoprofen 2 mg/kg, SC, Ketofen®, Merial Lab, Santiago, Chile), and analgesic (tramadol at the same dose as before surgery) every 12 hours for five days. Analgesics, anti-inflammatory drugs, and antibiotics were administered during the post-operative stage, as CS corresponds to invasive surgery that requires postoperative pain management and infection control, given the opening of the abdominal cavity. Postoperative pain was monitored for five days, during which analgesics and anti-inflammatory drugs were administered. The pain assessment was qualitative and involved analysis of the presence or absence of the following behaviors and postures: i) anorexia, ii) hunched posture, iii) bristly fur, iv) contraction of the abdominal muscles, which are indicative of discomfort and pain in rodents and rabbits (Richardson & Flecknell, 2006), and v) ocular secretions with a milky appearance that corresponds to a specific sign of stress and discomfort in degus (Correa, personal communication, March, 2012). The suture line was monitored and disinfected once daily with iodinated alcohol (70%). While suture dehiscence due to gnawing can be an issue in rodents, we did not see any evidence of this in degus; therefore, we did not use soft Elizabethan collars made of cloth (Redobre, 2002; Richardson & Flecknell, 2006). The nylon suture was removed six days (range, 5–7 days) after surgery. One person gently restricted the female, while the other removed the suture by using blunt scissors. However, chemical sedation is not required. Females and pups were monitored daily for the first 10 days and twice at night during the first two days after surgery. The substitute mother remained in the group until three days after surgery. Various food items, including fruits, honey cereals, sunflower seeds, crushed oats, and both rat and rabbit pellets, were offered during the post-surgical period.

Ovariohysterectomy context

OVH surgeries were performed as part of a behavioral ecology study (Correa, 2012), in which the objective was to evaluate whether intrauterine position determines litter traits in adulthood, including the size of the litter (see Correa *et al.*, 2016). For this purpose, we needed to know if there was reabsorption of embryos in the uterus, which can be evaluated by counting the scars that remain on the uterine mucosa, indicating failed implantation in first-time mothers (Krackow, 1992; Zielinski *et al.*, 1992). A total of 27 OVH surgeries were performed, in which we removed the uterus and ovaries of one year-old females after their first pregnancy and birth. After a typical gestation, parturition, and lactation period, the pups were weaned at 49 d of age. Females were then separated from their pups and left alone for ~41 days with *ad libitum* food and water, which allowed them to recover from reproductive processes. OVH surgery was performed at 90 days postpartum.

Ovariohysterectomy surgical procedure

Pre-surgical management. Females were treated with an analgesic (tramadol 2 mg/kg, SC) 1 h before surgery. The protocols for anesthetic induction, anesthesia, positioning of the degus on the surgical bed, and thermoregulatory variables were the same as those used for the CS procedure described above.

Surgical procedure. Skin preparation was identical to that for CS, but the abdominal midline incision was shorter (~1.5 cm). The small intestine was then gently displaced to expose the cervix. Once the cervix was identified, bifurcation of the horns was followed to reach the ovary. Uterine and ovarian stump ligations were performed as outlined in the CS protocol. Once the ovaries and uterus were removed, slightly warm and sterile saline fluid was administered intraperitoneally (5 ml 0.9% NaCl). A second dose of intraperitoneal fluid (5 ml 0.9% NaCl) was administered immediately before the last stitch to close the peritoneum and muscle. Peritoneal, muscular, and skin sutures were applied as described for CS. Recovery and postprocedural management were identical to those of CS. Similarly, OVH surgeries were performed by the same professionals and at the same facilities as the CS surgeries. During recovery, females were housed in standard rat boxes with the same bedding material as

in the CS protocol. In this study, we did not use red heat lamps because the females were housed in a room with a controlled temperature of 18–22°C. Once the females were fully awake, they were offered an isotonic hydrating solution (Gatorade®) to drink and palatable food (honey cereals, sunflower seeds, crushed oats, apple pieces, and rat pellets).

Procedure Durations, Recovery Times, And Survival Of Mothers And Pups

The duration of CS and OVH was defined as the time between the first abdominal incision and when the female was rotated from dorsal to ventral recumbency for post-surgical recovery (Malbrue *et al.*, 2019). The initial recovery time was defined as the time between ventral recumbency and the first leg movement. Full recovery time was defined as the time between the first leg movement and when the female was able to stand and walk in a coordinated manner. Neonatal and maternal survival were determined at two time points: i) once the CS and OVH were over, and ii) at weaning. These data are presented as percentages ((number of individuals surviving/total number of pups per litter) × 100). Finally, for CS, we determined i) the litter size, ii) male percentage of the litter, iii) female percentage of the litter, iv) number of pups per uterine horn, v) pup body weight, vi) litter weight, and vii) maternal reproductive investment (MRI). MRI was calculated as ((((litter weight at birth + uterus and membrane weight)/maternal weight before CS) × 100). As the CS procedure provided data on the intrauterine position (IUP) of each pup, we analyzed whether the IUP (cranial end, middle on, and caudal end of the uterine horn) is associated with the body weight of the pups.

Statistical analyses

We conducted descriptive statistical analyses for i) CS duration correlated with litter size, ii) CS duration correlated with the order in which different CS were performed (i.e., the last CS surgery was significantly shorter than the first CS surgery), and iii) OVH duration correlated with the order in which different OVHs were performed. For these determinations, we conducted a Spearman's correlation analysis. To analyze the potential effect of IUP on pup body weight, we performed a one-way ANOVA, with IUP (cranial end, middle, and caudal end) as the independent variable and pup body weight as the dependent variable. Before carrying out a one-way ANOVA, we confirmed that the dependent variable had a normal distribution using the Kolmogorov-Smirnov test. Tukey's test was used for a posteriori analyses. Statistical analyses were performed using STATISTICA 7 software (StatSoft). All data are reported as mean ± SD.

RESULTS

Maternal and pup survival rates

For the CS surgeries, we measured 83 pups distributed across 11 litters. All pups were extracted alive from the uterus, except for one mummified pup, which probably died because of umbilical cord compression (Figure 2b). At the end of CS, the maternal and neonatal survival rates were 100% and 97.3%, respectively. Of the 83 pups born by CS, three died shortly after being extracted. These three pups came from two large litters (mother 161, one male pup dead, litter size 10; female 612, two male pups dead, litter size 10). All three pups that did not survive showed signs of delayed development. The pups remained with their mothers until natural weaning (~49 days), and no pups died during the lactation stage; thus, the mother and pup survival at weaning was 100%. Relative to OVHs, maternal survival was 100%.

Procedure duration

The CS procedures took, on average, 61.82 ± 8.62 min. The fastest CS surgery lasted 51 min, while the slowest CS surgery took 79 min (n= 11, Table 1). CS duration and litter size were positively correlated (Spearman correlation= 0.92, $P<0.05$), CS duration was not correlated with the order in which different CS surgeries were performed (Spearman correlation= –0.33, $P>0.05$). The OVH procedures had an average duration of 32.89 ± 4.26 min. The fastest OVH lasted 26 min, whereas the slowest lasted 42 min (n= 27; Table 2). In this case, OVH duration and order were negatively correlated (Spearman correlation= -0.39, $P<0.05$), such that early OVH surgeries were generally performed more slowly than later OVH surgeries.

Times to initial and full recovery

The average time to initial recovery for CS surgeries was 8.18 ± 2.79 min with a range of 4–13 min (n=11). The average full recovery time was 50.18 ± 41.00 min. The high variability observed in this variable was associated with one female patient (612), who presented with a full recovery time of 171 min. When excluding this extreme value, the time to full recovery was 38.10 ± 9.13 min with a range of 21–52 min (Table 1, n=10). For OVH surgeries, the average time to initial recovery was 5.59 ± 2.08 min with a range of 2–10 min (n=27). The average time to full recovery was 15.11 ± 5.82 min, with a range of 7–27 min (Table 2, n=27).

Descriptive data relative to reproductive traits

For CS surgeries, the average litter size was 7.55 ± 1.63 (ranging 5–10 pups, n=11). The average percentage of males per litter was 53.8 ± 20.8% (33.3-100%), whereas the average percentage of females per litter was 46.2 ± 20.8% (0-66.7%). Left uterine horns had 3.90 ± 1.44 pups (ranging 1–6, n=11), whereas right uterine horns had 3.63 ± 1.28 pups (ranging 2–6, n=11). Thus, the pups were homogeneously distributed between the horns. Details of each litter type are presented in Table 3. The average pup body weight at CS was 10.19 ± 1.14 g (ranging from 8.20–12.40 g, n= 83). while average litter weight was 75.90 ± 13.53 g (ranging 58.00–106.40 g, n=11). The average maternal reproductive investment was 26.6 ± 3.6% (20.8–32.3). Details of the reproductive investment of each female are presented in Table 4. The results of one-way ANOVA indicated that IUP use was associated

Table 1. Descriptive data regarding surgery duration and times to initial and full wake up from cesarean surgeries in female degus.

Mother ID	Order	Litter size	Cesarean duration (min)	Time to initial recovery (min)	Time to full recovery (min)
56	1	9	71	11	44
61	2	7	61	9	33
161	3	10	79	11	52
246	4	7	60	4	21
841	5	5	51	9	35
10A	6	6	55	8	41
811	7	7	57	6	37
612	8	10	72	13	171
H40	9	8	59	5	49
827	10	6	54	8	39
427	11	8	61	6	30
Average		7.55	61.82	8.8	50.18
Standard deviation		1.63	8.62	2.79	41.00

with pup body weight (ANOVA, F (2.80) = 5.376, p= 0.006). Tukey's posteriori analysis showed that pups located at the cervical end of the uterine horn were heavier (mean, 10.784 g) than those located in the middle (mean, 9.581 g) of the uterine horn (Figure 3).

DISCUSSION

In this study, we outlined the detailed protocols for CS and OVH surgeries in degus, including pre-surgical, surgical, and post-surgical management. These details expand on previously reported orchiectomy, ovariectomy, and OVH procedures in degus (Mancinelli *et al.*, 2013; Malbrue *et al.*, 2019). Compared with the available information from other rodent and rabbit species (Redobre, 2002; Richardson & Flecknell, 2006), our protocols differed in four major aspects. First, we did not consider the intravenous route for the administration of fluids and drugs because degus are too small, and rodent cannulation techniques (caudal and jugular veins) are unreliable (Redobre, 2002; Richardson & Flecknell, 2006). Degus has a very short neck and caudal skin autotomy (spontaneous tail self-mutilation as an anti-predator strategy) occurs when the tail is manipulated (Shargal *et al.*, 1999). Intravenous routes have also not been used in orchiectomy, ovariectomy, or OVH procedures performed in degus (Mancinelli *et al.*, 2013; Malbrue *et al.*, 2019). Second, we used a face mask instead of an endotracheal tube to maintain anesthesia, as recommended in the anesthetic protocol for other rodent species (Redobre, 2002; Richardson & Flecknell, 2006). Maintenance of anesthesia by mask was the chosen methodology for orchiectomy, ovariectomy, and OVH procedures previously performed in degus (Mancinelli *et al.*, 2013; Malbrue *et al.*, 2019). Third, we used tramadol to provide analgesia, although it has not been used in previous degu orchiectomy, ovariectomy, or OVH procedures (Mancinelli *et al.*, 2013; Malbrue *et al.*, 2019). Mancinelli *et al.* (2013) used buprenorphine to provide analgesia for OVH procedures, whereas Malbrue *et al.* (2019) used butorphanol tartrate for analgesia during orchiectomy and ovariectomy surgeries in degus. Our results indicate that tramadol is an effective analgesic in degus, as we did not observe any evidence of post-surgical acute pain, such as anorexia, hunched posture, bristly fur, contraction of the abdominal muscles (Richardson & Flecknell, 2006), or ocular secretions with a milky appearance (Correa, personal communication, March 2012). Degu mothers also displayed normal post-partum behaviors including eating, drinking, and nursing. Although tramadol is not the first choice of analgesic in other small mammals such as rabbits (Hedenqvist, 2008), our results suggest that this drug could be an effective analgesic for degus. Fourth, nylon was used for skin sutures instead of skin staples, as recommended for rodents and rabbits to decrease suture dehiscence from gnawing (Redobre, 2002; Richardson & Flecknell, 2006). However, in previously reported OVH, orchiectomy, and ovariectomy procedures in degus, the skin was closed with sutures and sometimes with surgical glue as a second barrier to close the skin (Mancinelli *et al.*, 2013; Malbrue *et al.*, 2019). No suture dehiscence was observed among the OVH (n=27), and CS (n=11) surgeries performed in this study, as Mancinelli *et al.* (2013) and Malbrue *et al.* (2019) also did not detect suture dehiscence during their surgical procedures. We observed that mothers licked but did not gnaw the stitches, and that pups suckled without

Table 2. Descriptive data regarding surgery duration and times to initial and full wake up from ovariohysterectomy surgeries in female degus.

Mother ID	Order OVH	OVH duration (min)	Time to initial recovery (min)	Time to full recovery (min)
368	1	39	7	8
415	2	35	5	13
Short tail	3	37	5	25
417	4	42	7	15
405	5	41	7	26
447	6	38	6	7
424	7	32	3	11
370	8	29	4	11
418	9	35	4	21
411	10	27	6	9
324	11	32	8	13
427	12	29	2	9
421	13	32	5	19
429	14	28	6	10
305	15	35	4	16
61A	16	33	10	27
61B	17	28	5	21
848	18	31	5	12
White ear	19	29	2	9
446	20	28	8	17
401	21	36	3	10
404	22	26	7	22
428	23	34	4	11
448	24	31	10	14
437	25	36	7	16
H5	26	33	6	21
506	27	32	5	15
Average		32.89	5.59	15.11
Standard deviation		4.26	2.08	5.82

any problem or interest in the stitches. Therefore, we suggest that good surgical techniques and gentle tissue handling are sufficient for preventing suture dehiscence.

Additionally, in comparison to our CS and OVH protocols, previous OVH, orchiectomy, and ovariectomy procedures in degus: i) used sevofluoerane as an anesthetic (Mancinelli *et al.*, 2013), ii) used a subcutaneous route to hydration during surgery (Mancinelli *et al.*, 2013; Malbrue *et al.*, 2019), iii) administered local anesthetic blocks (Malbrue *et al.*, 2019), iv) permanently controlled degu body temperature (Mancinelli *et al.*, 2013; Malbrue *et al.*, 2019), v) used meloxicam to manage inflammation (Mancinelli *et al.*, 2013; Malbrue *et al.*, 2019), vi) did not use antibiotics during pre-surgical, surgical, or post-surgical management (Malbrue *et al.*, 2019), and vii) had problems finding ovaries during ovariectomy via the flank, likely as consequence of the high volume and surface area of degu

Table 3. Descriptive data of degu litters obtained by cesarean section.

Mother ID	Litter size	Male/female pups ratio	Male pup percentage	Female pup percentage	N° of pups in left horn	N° of pups in right horn
56	9	3/6	33.3	66.7	6	3
61	7	4/3	57.1	42.9	1	6
161	10	4/6	40	60	5	5
246	7	5/2	71.4	28.6	5	2
841	5	3/2	60	40	3	2
10A	6	2/4	33.3	66.7	3	3
811	7	3/4	42.9	57.1	3	4
612	10	7/3	70	30	5	5
H40	8	4/4	50	50	5	3
827	6	2/4	33.3	66.7	3	3
427	8	8/0	100	0	4	4
Average	7.55		53.75	46.25	3.91	3.64
Standard deviation	1.63		20.83	20.83	1.45	1.29

Table 4. . Descriptive data regarding degu litter weight and maternal reproductive investment. Maternal reproductive investment was calculated as ((litter weight at birth + uterus and membranes weight)/maternal weight before CS) x 100.

Mother ID	Female body weight (g) before cesarean	Female body weight (g) after cesarean	Uterus weight (g)	Maternal Reproductive investment (%)	Litter weight (g) at birth	Mean offspring body weight (g) at birth
56	373.9	264.2	15.5	25.1	78.3	8.7
61	372	232.7	17.1	25.5	77.7	11.1
161	360.7	273.8	15	26.8	81.7	8.2
246	383	246.3	14.5	21.6	68.2	9.7
841	393.5	297.3	20.2	20.8	61.8	12.4
10A	301.4	217.9	15.4	24.4	58	9.7
811	279.5	199.2	10.4	29.7	72.7	10.4
612	380.5	187.8	16.4	32.3	106.4	10.6
H40	358.4	260.2	16.3	28.6	86.1	10.8
827	291.5	204.6	14.2	26.8	63.8	10.6
427	307.6	194.2	15.3	31.1	80.3	10
Average	345.64	234.38	15.48	26.61	75.91	10.20
Standard deviation	41.83	36.60	2.35	3.65	13.53	1.15

intestines (Malbrue *et al*., 2019). However, similar to Mancinelli *et al*. (2013) and Malbbrue *et al*. (2019), we also utilized heat sources throughout the entire surgery to maintain degu body temperature (Mancinelli *et al*., 2013; Malbrue *et al*., 2019) and administered analgesic and anti-inflammatory medications during the pre-and post-operative stages (Mancinelli *et al*., 2013). Finally, similar to Mancinelli *et al*. (2013), we positioned the degus with the thorax elevated during the surgical steps, which required them to lie on their backs.

As our first objective was to report survival rates related to our surgical protocols, our protocols resulted in high maternal and neonatal survival rates (100% and 97.3%, respectively). As reported in the Results section, the three mortality events corresponded to underdeveloped individuals within a very large litter. The asymmetry of development in the littermates of recently born degu pups is a common phenomenon (Rojas *et al*., 1982) (Figure 2c), which is also observed in guinea pigs, which are the closest related domestic species to degus (Scott, 1937).

Our results indicated that individuals in the middle of the uterine horns were lighter than those in the cervical ends of the uterine horns (Figure 2a,c, and Figure 3). Individuals in the ovarian ends of the uterine horns had an intermediate body weight but were not statistically different from those in the middle and cervical ends of the uterine horns. This pattern has been previously described in domestic pigs (Dziuk, 1992), European rabbits (Bautista *et al*., 2015) and Sprague Dawley laboratory rats (D'Errico *et al*., 2021), but in different ways than in degus. In Sprague-Dawley rats, individuals in the middle of the horn were lighter than those in the cervical and ovarian ends, and the horn (left, right) also affected individual body weight, with the lightest individuals located in the middle of the left horn (D'Errico *et al*., 2021). In domestic pigs, individuals in the ovarian end are heavier than those in the middle or cervical end of the uterine horns (Dziuk, 1992), whereas in European rabbits, individuals located at both ends of the uterine horns are heavier than those in the middle (Bautista *et al*., 2015).

From these studies and our results, only one pattern emerged: the individuals located in the middle of the uterine horns were light. Dziuk (1992) suggested that lower body weight in these individuals could be a consequence of high fetal density, leading to less space for growth, while Bautista *et al*. (2015) also suggested that differences in pup body weight, depending on the IUP, could be a consequence of differences in vascular supply and placental efficiency. Raz *et al*. (2012) suggested that individuals at both ends of the uterine horns receive more blood supply and, therefore, more nutrients, having an advantage to grow, which may explain our findings.

The second objective was to calculate the duration of the CS and OVH procedures. Our results indicate that these average times (CS 61 min and OVH 32 min) are reasonable. It is difficult to compare these times with those of similar species, as we have only found anecdotal reports of CS and OVH in different rodent species (Fleischman, 1981; Prior, 1986; Jones, 1990; Mighell & Baker, 1990) and rabbit species (Richardson & Flecknell, 2006). Therefore, we only can compare our results with the ovariectomy procedure performed previously in degus (Malbrue *et al*., 2019), which reported an average duration of 12.56 ± 4.09 min (considering only the surgical time) for an ovariectomy using the bilateral flank technique. As this duration is shorter than that of our OVH protocol via a midline approach, we suggest using the ovariectomy protocol from Malbrue *et al*. (2019) if the objective is only to sterilize the females without removing the uterus. We observed a positive correlation between the litter size and CS duration. The lack of correlation between CS surgery order and duration and the negative correlation between the order of OVH surgeries and duration suggest that surgeon expertise can help decrease OVH, but not CS duration. We suggest that these relationships are a consequence of OVH being very similar between each degu, whereas CS is more variable as female degus vary in litter size.

Our third objective was to report that the time to initial and full recovery from anesthesia was relatively short in degus (average initial: CS, 8 min; OVH, 5 min; average full:38 min; OVH, 15 min). These results are similar to those reported by Malbrue *et al*. (2019), who found that the average ovariectomy recovery time was 14.14 ±3.12 min. These fast recovery times are not surprising as degus, similar to other small mammals, exhibit rapid metabolism and drug elimination (Zhao *et al*., 2016).

Finally, in relation to the reproductive traits of degu, we highlight that degu mothers make high maternal investments. Our results indicated that the summed litter, uterus, and membrane weights corresponded to 1/5 to 1/3 of the mother's total body weight. This trait is notable, as close caviomorph relatives of degus (chinchillas and guinea pigs) generally deliver smaller litters, but with well-developed pups (chinchillas average two offspring, ranging 1–4 (Kuroiwa & Imamichi, 1977); guinea pigs average two offspring, ranging 1–5 (Peaker & Taylor, 1996)). However, degus delivers larger litters (average six, range 1–10) (Ebensperger *et al*., 2019), and at the same well-developed pups (Rojas *et al*.,1982), which implies a higher energy expenditure. In terms of surgical management, this trait could be relevant because removal of 1/5 to 1/3 of female body weight could cause acute decompression of abdominal organs, blood redistribution, and changes in abdominal pressure. Therefore, during CS, we administered intraperitoneal fluid three times, exposed only one horn at a time, and started pup extraction with a uterine horn containing fewer pups.

In conclusion, relative to our four critical points, we used previous information to control for i) respiratory compromise, ii) body temperature fluctuations, iii) suture dehiscence, and iv) reduced intestinal motility during reproductive surgery in degus. (Redobre, 2002; Richardson, 2003; Richardson & Flecknell, 2006) The individuals included in this study did not encounter any of the four critical problems listed above, and we want to highlight that degu are good patients during all stages of the detailed surgeries.

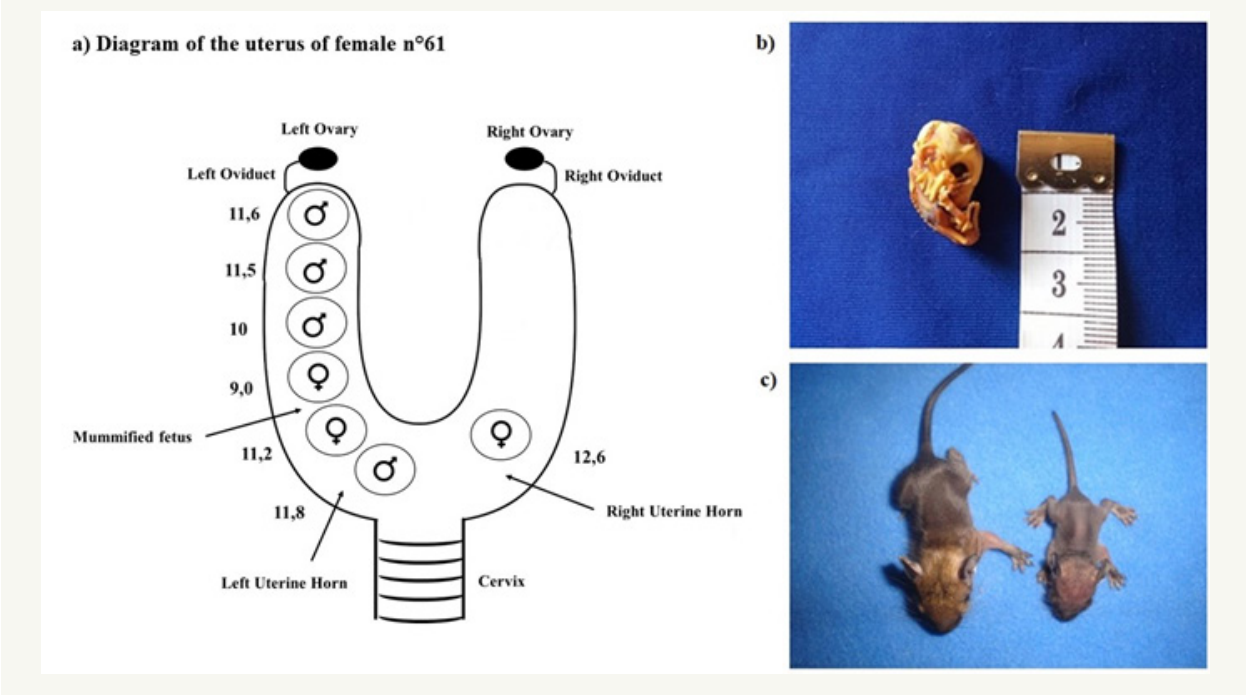

Figure 2. a) Diagram of the uterus of female n°61, which includes the real weights of the offspring extracted by cesarean section, the real fetus distribution, and the position in which mummified was located. Males and females are indicated with man and woman symbols. b) Photograph of mummified pup with cm scale. c) Example of asymmetry in body size and developmental levels of degu littermates. The pup on the left side of the photo corresponds to the 12.6 g female that was alone in the right horn. The pup on the right side of the photo corresponds to the 9.0 g female that was in fourth position, counting from the ovary to the cervix, in the left horn.

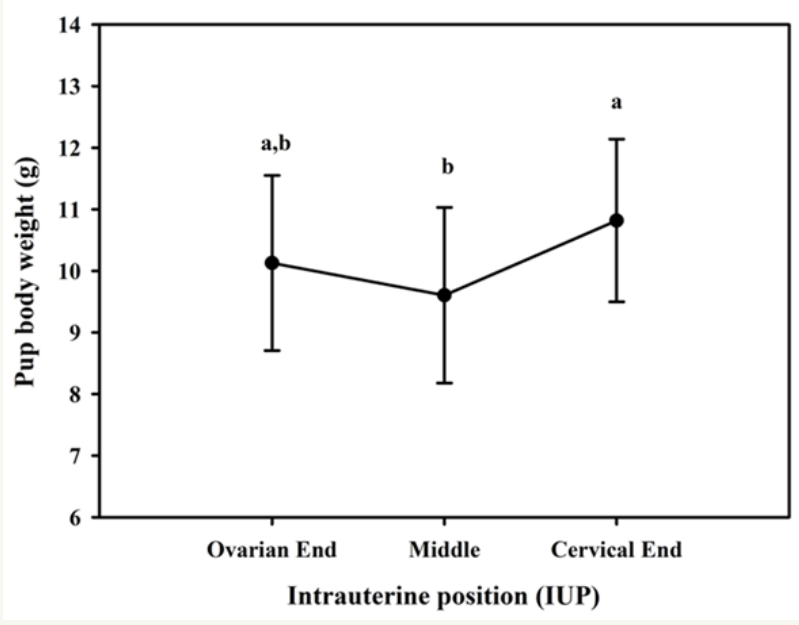

Figure 3. Intrauterine position and pup body weight at cesarean. Letters represent significant differences between groups using a Tukey posteriori test with $p < 0.05$.

Competing interests statement

The authors declare that they have no competing interests.

Author contribution

Conception: Loreto A. Correa and Mauricio Soto-Gamboa. Data acquisition: Ángelo Espinoza, O. Alejandro Aleuy, and Loreto A. Correa. Data analysis and interpretation: Loreto A. Correa. Original draft: Loreto A. Correa. Revisions: Ángelo Espinoza, O. Alejandro Aleuy, and Mauricio Soto-Gamboa.

Ethical statement

In this study, we followed all protocols, animal handling techniques, and suggestions by the Ethics Committee of the Universidad Austral de Chile (report 03/09) and followed the Chilean Ethical Legislation required by CONICYT. Animal handling, injections, and surgeries were performed by veterinarian staff (A. E., O.A.A, and L.A.C).

Funding information

This study was funded by FONDECYT grant 10900302 (to M.S-G) and CONICYT Fellowship (to L. A. C.).

Acknowledgements

We are grateful to Aline Barrera Aguirre and Maria Jose Frugone for their help in maintaining *O. degus* colonies, and Luis A. Ebensperger for providing us with the founding animals of our colony. We thank the Center of Rescue and Rehabilitation of Wildlife (CEREFAS) and Veterinary Teaching Hospital of the Faculty of Veterinary Sciences, Universidad Austral de Chile. We also thank the Ecology Institute Faculty of Science for providing us with the dependencies to maintain our colonies. We are grateful to Carolyn Bauer and the three anonymous reviewers and editor for providing useful suggestions regarding the previous version of this manuscript.

REFERENCES

Aspillaga-Cid, A., Vera, D.C., Ebensperger, L.A., & Correa, L.A. (2021). Parental care in male degus (*Octodon degus*) is flexible and contingent upon female care. *Physiology & Behaviour*, *238*, 113487. https://doi.org/10.1016/j.physbeh.2021.113487

Bautista, A., Rödel, H.G., Monclús, R., Juárez-Romero, M., Cruz-Sánchez, E., Martínez-Gómez, M., & Hudson, R. (2015). Intrauterine position as a predictor of postnatal growth and survival in the rabbit. *Physiology & Behaviour*, *138*, 101-106. http://dx.doi.org/10.1016/j.physbeh.2014.10.028

Castro-Fuentes, R., & Socas-Pérez, R. (2012). *Octodon degus*: A Strong Attractor for Alzheimer Research. *Basic and Clinical Neuroscience*, *4*, 91-96. PMC4202560

Correa, L.A. (2012). *Mecanismos de regulación del tamaño de camada y razón de sexos en Octodon degus: efectos de la alostasis prenatal en la variación fenotípica de las crías y sus consecuencias en la estabilidad de los grupos sociales*. [PhD tesis, Universidad Austral de Chile, Valdivia, Chile].

Correa, L.A., Frugone, M.J., & Soto-Gamboa, M. (2013). Social dominance and behavioral consequences of intrauterine position in female groups of social rodent, *Octodon degus*. *Physiology & Behaviour*, *119*, 161-167. https://doi.org/10.1016/j.physbeh.2013.06.002

Correa, L.A., León, C., Ramírez-Estrada, J., Sepúlveda, R., Soto-Gamboa, M., & Ebensperger, L.A. (2016). Masculinized females produce heavier offspring in a group living rodent. *Journal of Animal Ecology*, *85*, 1552-1562. https://doi.org/10.1111/1365-2656.12588

Cuenca-Bermejo, L., Pizzichini, E., González-Cuello, A.M., De Stefano, M.E., Fernández-Villalba, E., & Herrero, M.T. (2020). *Octodon degus*: a natural model of multimorbidity for ageing research. *Ageing Research Reviews*, *64*, 101204. https://doi.org/10.1016/j.arr.2020.101204

D'Errico, J.N., Fournier, S.B., & Stapleton, P.A. (2021). Considering intrauterine location in a model of fetal growth restriction after maternal titanium dioxide nanoparticle inhalation. *Frontiers in Toxicology*, *3*, 643804. https://doi.org/10.3389/ftox.2021.643804

Dziuk, P. (1992). Survival of Peas, Peaches, and Prenatal Pigs. *Perspectives in Biology and Medicine*, *35*, 357–360. https://doi.org/10.1353/pbm.1992.0035

Ebensperger, L.A., Hurtado, M.J., Soto-Gamboa, M., Lacey, E.A., & Chang, A.T. (2004). Communal nesting and kinship in degus (*Octodon degus*). *Naturwissenschaften*, *91*, 391–395. https://doi.org/10.1007/s00114-004-0545-5

Ebensperger, L.A., Ramírez-Otárola, N., León, C., Ortiz, M.E., & Croxatto, H.B. (2010). Early fitness consequences and hormonal correlates of parental behavior in the social rodent, *Octodon degus*. *Physiology & Behaviour*, *101*, 509–517. http://dx.doi.org/10.1016/j.physbeh.2010.07.017

Ebensperger, L.A., Tapia, D., Ramírez-Estrada, J., León, C., Soto-Gamboa, M., & Hayes, L.D. (2013). Fecal cortisol levels predict breeding but not survival of females in the short-lived rodent, *Octodon degus*. *General and Comparative Endocrinology*, *186*, 164–171. http://dx.doi.org/10.1016/j.ygcen.2013.02.044

Ebensperger, L.A., Correa, L.A., Ly-Prieto, A., Pérez de Arce, F., Abades, S., & Hayes, L.D. (2019). Multiple mating is linked to social setting and benefits the males in a communally rearing mammal. *Behavioral Ecology*, *30*, 675–687. http://dx.doi.org/10.1093/beheco/arz003

Edwards, M.S. (2009). Nutrition and behavior of degus (*Octodon degus*). *Veterinary Clinics of North America: Exotic Animal Practice*, *12*, 237-253. http://dx.doi.org/10.1016/j.cvex.2009.01.003

Fleischman, R.W. (1981). A technique for performing an ovariectomy in a hamster. *Veterinary medicine, small animal clinician*, *76*, 1006-1007.

Gutiérrez, J., & Bozinovic, F. (1998). Diet selection in captivity by a generalist herbivorous rodent (*Octodon degus*) from the Chilean costal desert. *Journal of Arid Environment*, *39*, 601-607. https://doi.org/10.1006/jare.1998.0412

Hedenqvist, P. (2008). *Anesthesia and analgesia for surgery in rabbits and rats: A comparision of effects of different compounds*. [Thesis for doctoral degree. Karolinska Intitutet, Stockholm, Sweden].

Jekl, V., Hauptman, K., & Knotek, Z. (2010). Diseases in pet degus: a retrospective study in 300 animals. *Journal of Small Animal Practice*, *52*, 107–112. https://doi.org/10.1111/j.1748-5827.2010.01028.x.

Jones, A.K. (1990). Caesarean section in a chinchilla. *Veterinary Record*, *126*, 441. PMID: 2386590.

Kanashiro, C., Santos, T.C., Miglino, M.A., Mess, A.M., & Carter, A.M. (2009). Growth and development of the placenta in the capibara (Hydrochaeris hydrochaeris). *Reproductive Biology and Endocrinology*, *7*, 57. https://doi.org/10.1186/1477-7827-7-57

Krackow, S. (1992). Sex ratio manipulation in wild house mice: the effect of fetal resorption in relation to mode of reproduction. *Biology of Reproduction*, *47*, 541-548. https://doi.org/10.1095/biolreprod47.4.541

Kuroiwa, J., Imamichi, T. (1977). Growth and reproduction of the chinchilla-age at vaginal opening, oestrous cycle, gestation period, litter size, sex ratio, and diseases frequently encountered (author's transl). *Jikken Dobutsu*, *26*, 213-222. https://doi.org/10.1538/expanim1957.26.3_213

Labra, A., Pérez de Arce, F., Ebensperger, L.A. (2021). *Estudios conductuales en la fauna nativa de Chile: posibles especies modelos*. In L.A. Ebensperger, & A. Labra, (Eds), *Comportamiento social de la fauna nativa de Chile* (pp. 25-45). Ediciones UC, Santiago, Chile.

Long, C., Ebensperger, L. (2010). Pup growth rates and breeding female weight changes in two populations of captive bred degus (*Octodon degus*), a precocial caviomorph rodent. *Reproduction in Domestic Animals*, *45*, 975–982. https://doi.org/10.1111/j.1439-0531.2009.01470.x

Malbrue, R.A., Arsuga-Zorrilla, C.B., Bidot, W., Molitor, L.E., Mendoza, K.A., Shateenah, K.B., Alexander, D.J., Bova, J.F., Evans, D.E. (2019). Evaluation of orchiectomy and ovariectomy surgical technique in degus (*Octodon degus*). *Journal of Exotic Pet Medicine*, *30*, 22–28. https://doi.org/10.1053/j.jepm.2018.08.003

Mancinelli, E., Eatwell, K., Meredith, A. (2013). Successful management of a case of pregnancy failure in a degu (*Octodon degus*). *Journal of Exotic Pet Medicine*, *22*, 293–300. https://doi.org/10.1053/j.jepm.2013.08.012

Mess, A. (2007). Development of the chorioallantoic placenta in *Octodon* degus—a model for growth processes in caviomorph rodents? *Journal of Experimental Zoology*, *308B*, 371–383. https://doi.org/10.1002/jez.b.21160

Mighell, J.S., & Baker, A.E. (1990). Caesarean section in a gerbil. *Veterinary Record*, *126*, 441. PMID: 2345947

Nishi, M., & Steiner, D.F. (1990). Cloning of complementary DNAs encoding islet amyloid polypeptide, insulin, and glucagon precursors from a new world rodent, the degu, *Octodon degus*. *Molecular Endocrinology*, *4*, 1192–1198. https://doi.org/10.1210/mend-4-8-1192

Palacios, A.G., & T.M, Lee. (2013). Husbandry and Breeding in the Octodon degu (Molina 1782). *Cold Spring Harbor Protocols*, 350-353. https://doi.org/10.1101/pdb.prot073577.

Peaker, M., & Taylor, E. (1996). Sex ratio and litter size in the guinea-pig. *Journal of Reproduction and Fertility*, *108*, 63-67. https://doi.org/10.1530/jrf.0.1080063

Prior, J.E. (1986). Caesarean section in the chinchilla. *Veterinary Record*, *119*, 408. https://doi.org/10.1136/vr.119.16.408

Raz, T., Avni, R., Addadi, Y., Cohen, Y., Jaffa, A.J., Hemmings, B., Garbow, J.R., & Neeman, M. (2012). The hemodynamic basis for positional- and inter-fetal dependent effects in dual arterial supply of mouse pregnancies. *PLoS ONE*, *7*, e52273. https://doi.org/10.1371%2Fjournal.pone.0052273

Redobre, S. (2002). Soft tissue surgery of rabbits and rodents. *Seminars in Avian and Exotic Pet Medicine*, *11*, 231-245. https://doi.org/10.1053/SAEP.2002.126570

Reynolds, T.J., & Wright, J.W. (1979). Early postnatal physical and behavioural development of degus (*Octodon degus*). *Laboratory Animals*, *13*, 93-99. https://doi.org/10.1258/002367779780943576.

Richardson, V.C.G. (2003). *Diseases of Small Domestic Rodents*, Oxford, UK, Blackwell.

Richardson. C., & Flecknell, P. (2006). Routine neutering of rabbits and rodents. *In Practice*, *28*, 70-79. https://doi.org/10.1136/inpract.28.2.70

Rojas, M.A., Montenegro, M.A., & Morales, B. (1982). Embryonic development of the degu, *Octodon degus*. *Journal of Reproduction and Fertility*, *66*, 31-38. https://doi.org/10.1530/jrf.0.0660031

Scott, J.D. (1937). The embryology of the guinea-pig. *American Journal of Anatomy*, *60*, 397-432. https://doi.org/10.1002/aja.1000600304

Shargal, E., Rath-Wolfson, L., Kronfeld, N., & Dayan, T. (1999). Ecological and histological aspects of tail loss in spiny mice (Rodentia: Muridae, Acomys) with a review of its occurrence in rodents. *Journal of Zoology*, *249*, 187-193. https://doi.org/10.1111/j.1469-7998.1999.tb00757.x

Terril, L., & Clemons, D. (1998). *The Laboratory Guinea Pig*. Boca Raton, Florida: CRC Press LLC.

Veloso, C., & Bozinovic, F. (2000). Effect of food quality on the energetics of reproduction in a precocial rodent, *Octodon degus*. *Journal of Mammalogy*, *81*, 971-978. https://doi.org/10.1644/1545-1542(2000)081%3C0971:EOFQOT%3E2.0.CO;2

Weir, B.J. (1970). The management and breeding of some more hystricomorph rodents. *Laboratory Animals*, *4*, 83-97. https://doi.org/10.1258/002367770781036562.

Weir, B.J. (1974). Reproductive characteristics of hystricomorph rodents. *Symposium Zoological Society of London*, *34*, 265-301.

Wright, J.W., & Kern, M.D. (1992). Stereotaxic atlas of the brain of *Octodon degus*. *Journal of Morphology*, *214*, 299-320. https://doi.org/10.1002/jmor.1052140306

Zhao, M., Lepak, A.J., & Andes, D.R. (2016). Animal models in the pharmacokinetic/pharmacodynamic evaluation of antimicrobial agents. *Bioorganic & Medicinal Chemistry*, *24*, 6390-6400. https://doi.org/10.1016/j.bmc.2016.11.008

Zielinski, W.J., vom Saal, F.S., Vandenbergh, J.G. (1992). The effect of intrauterine position on the survival, reproduction and home rage size of female house mice (Mus musculus). *Behavioral Ecology and Sociobiology*, *30*, 185-191. https://doi.org/10.1007/BF00166702

Austral Journal of Veterinary Science

Austral J Vet Sci 55, 167-175 (2023)
https://doi.org/10.4206/ajvs.553.02

ORIGINAL ARTICLE

Determination of copro-prevalence of *Echinococcus granulosus* and associated factors in domestic dogs: a household cross-sectional study in Huancarama, Peru

Aldo A. Valderrama[1*], Graciela Mamani[1], Falcon J. Uzuriaga[1]

[1] Facultad de Medicina Veterinaria y Zootecnia, Universidad Nacional Micaela Bastidas de Apurímac, Abancay, Perú.

Article History
Received: 04.11.2022
Accepted: 02.05.2023
Published: 04.09.2023

Corresponding author
*Aldo A. Valderrama
avalderrama@unamba.edu.pe

ABSTRACT. Echinococcosis is an important disease with regard to public health and the leading role that humans have in fulfilling the transmission cycle. The objective of this study was to determine the copro-prevalence of *Echinococcus granulosus* in dogs from homes in Huancarama, Peru, and the factors associated with this infection. The research was basic, prospective, quantitative, observational, cross-sectional, and analytical. This study was approved by the Institutional Ethics Committee for the Use of Animals (CIEA) and the Institutional Research Ethics Committee (CIEI) of the Universidad Peruana Cayetano Heredia. The sample comprised of 519 homes. A geographic information system (GIS) was used to develop layers of information on the study area with georeferencing of the locations of these homes. Information processing was performed using Excel for Windows 2010, Statistical Package for the Social Sciences SPSS 25 software, and ArcGIS 10.8. Univariate and multivariate logistic regression tests were performed to determine the possible associations. Categorical variables were statistically contrasted using the chi-square test with 95% confidence intervals and $P \leq 0.05$, which indicated the extreme degree of significance. It was found that 94.4% of the houses had dogs and that the prevalence of *E. granulosus* was 27.7% (95/343; 95% CI 22.8-32.6). The distance from the house to the cattle slaughterhouse was associated with disease occurrence ($P < 0.01$). Locations in the Suni altitude zone presented a higher prevalence (41.8%) ($P < 0.05$). Lack of knowledge that humans can contract echinococcosis was associated with disease occurrence ($P < 0.05$).

Keywords: Echinococcosis; dogs; prevalence; copro-ELISA; spatial distribution.

INTRODUCTION

Cystic echinococcosis (CE) is a parasitic zoonotic infection caused by the larval stage of the cestode *Echinococcus granulosus sensu lato*. This parasite fulfills its biological cycle between domestic dogs and some wild canids (definitive hosts) and livestock animals (intermediate hosts). Humans act as aberrant hosts after the accidental ingestion of parasite eggs (Sierra-Ramos & Valderrama-Pomé, 2017). This parasite is distributed worldwide and occurs in many parts of South America, including Argentina, Peru, Bolivia, Chile, Uruguay, and southern Brazil. The Andean localities of the central and southern highlands of Peru present conditions that enable the maintenance of the biological cycle of the parasite, which is endemic for cystic echinococcosis in both animals (sheep and cattle) and humans (Sanchez *et al*., 2022). In South America, dogs are the definitive hosts with the greatest epidemiological significance (in which the strobilar or adult stage develops) (Larrieu *et al*., 2014). Therefore, the diagnosis of *E. granulosus* infection in dogs is very important. This plays a key role in epidemiological studies and control programs for cystic echinococcosis (Frison de Costas *et al*., 2014).

Cystic echinococcosis is a neglected disease that manifests in poor and rural populations (Harada *et al*., 2019), and the main factors that lead to transmission and persistence of infection include the close coexistence of animals or humans with dogs, poor hygienic-sanitary conditions, cultural customs, and low socioeconomic status. Persistence of the biological cycle of *E. granulosus* is favored by the coexistence of intermediate and definitive hosts; some habits of the inhabitants of such regions, such as feeding dogs with viscera, close contact with dogs, drinking untreated water or eating unwashed raw vegetables and fruits, ignorance of hygiene rules, and lack of veterinary surveillance for deworming of dogs and controlling the slaughter of intermediate hosts (Ramírez *et al*., 2018; Apt *et al*., 2000; Carrión-Ascarza *et al*., 2021).

In the larval stage of the parasite, hydatid cysts develop in the viscera of the host, especially in the lungs and liver of humans and herbivorous animals. This reduces the productivity of these animals. Death of an infected herbivore or its slaughter for human consumption and release of infected viscera into the environment completes the life cycle of the parasite if dogs have access to infected organs and eat them. This gives rise to dog-domestic species cycles (Zuñiga-A *et al*., 1999). Such cycles are so common that in some non-endemic areas of Peru, up to 6.3% prevalence of echinococcosis is reported among dogs that ingest viscera from slaughterhouses, since the

animals slaughtered in these facilities may have come from endemic areas (Montalvo *et al*., 2018). One such area is the Huancarama district, where an average prevalence of 19% in slaughtered animals has been reported (Peña & Valderrama, 2022). This situation worsens when slaughterhouses in human settlements are small and poorly equipped (Khan *et al*., 2018), thereby becoming sources of infection.

On the other hand, long distances in rural areas may preclude the transportation of animals to rural slaughterhouses in the area. In such situations, slaughter is carried out almost exclusively at home and by the owner himself (Frison de Costas *et al*., 2014). However, unsupervised slaughter of herbivorous animals constitutes the main transmission route for infection in the canine host (Pavletic *et al*., 2017).

Given the significance of this disease with regard to public health and the leading role that humans have in fulfilling the transmission cycle, it is necessary to understand the social and cultural environment of people affected by cystic echinococcosis and determine the level of knowledge that they have in this regard (Khan *et al*., 2018; Ramírez *et al*., 2018). This can be achieved through surveys. Hence, the objective of the present study was to determine the copro-prevalence of *E. granulosus* in dogs from homes in Huancarama and the factors associated with this infection.

MATERIALS AND METHODS

Description of the research ethics setup

The study protocol, which included the interview guide and the informed consent statement for the owners of the dogs, was approved by the following committees of the Universidad Peruana Cayetano Heredia: Institutional Ethics Committee for the Use of Animals (Certificate 008-03-21) and the Institutional Research Ethics Committee (Certificate 064-01-21), under the category of expedited review. In addition, respondents signed an informed consent statement as a sign of acceptance. The survey was conducted under anonymous conditions, and the respondents' participation was voluntary. The District Municipality of Huancarama and the National University Micaela Bastidas de Apurímac authorized the research to be conducted.

Population and sample

The houses in Huancarama were considered the population units to be analyzed. To establish the number of households potentially involved in the research, the 2017 National Census (XII of Population, VII of Housing, and III of Indigenous Communities) (INEI, 2022) was taken into account, considering both the urban-rural and rural sectors. In this case, the only village considered to be marginally urban was Huancarama, which is the capital of the district and its most populated area. All dwellings in the district were identified and listed. Dwellings were selected through proportional random stratified sampling, considering each village as a stratum. Thus, it was ensured that the number of households surveyed and sampled was equitable according to the number of dwellings in each village to avoid any bias. The following formula was used for this purpose.

$$n = (NZ^2P[1-p]) / (E^2[N-1]+Z^2P[1-p])$$

Where:

n = Sample size: 519

N = Population size: 2366

Z = Confidence level (99%): 2.58

P = Baseline prevalence: 0.5

E = Tolerable upper limit of error (5%): 0.05

All the buildings in these dwellings were plotted on a district map so that they could be randomized. Through this, it was aimed to achieve greater efficiency in assigning samples using Google Maps (web map application server belonging to Alphabet Inc.) The population studied corresponded to the total number of existing dwellings in all locations of the Huancarama district (2,366). From these, a sample size of 519 dwellings was selected, and fecal samples were taken only from the dwellings where dogs were kept (490 dwellings), as indicated in Table 1.

Procedure

The team of interviewers was trained to complete the questionnaire. In addition, identification credentials and biosafety clothing (latex gloves, waterproof hooded protective suits, respirators with particle filters, and face shields, among others) were provided in accordance with the recommendations of the Pan-American Health Organization (OMS, 2020).

The interviewers toured all the randomly selected dwellings. If a given home did not respond when the team members called, they went to the adjoining house, to the left or right, if necessary. Observations of echinococcosis in homes in Huancarama district were based on the collection of dog fecal samples from residences in both rural and urban areas. Consequently, the observational unit was a household unit.

Fresh fecal samples were collected from dogs. The samples were collected in the form of one excreta per bottle.

Table 1. Sample size among households in the Huancarama district, Peru

Village	Dwellings	Sample	%
Huancarama	749	171	32.9
Llactabamba	52	11	2.2
Pampahura	107	24	4.6
Matecclla	71	16	3.0
Acco	65	14	2.8
Tunyabamba	35	8	1.5
Tambo	33	7	1.4
Chihuarque	67	15	2.9
Arcahua	71	15	3.0
Sayhua	125	28	5.3
Karhuakahua	78	17	3.3
Pichiupata	223	50	9.7
Ahuanuqui	45	10	1.9
Lambraspata	92	20	3.8
California	38	8	1.6
Los Ángeles	94	21	4.0
Sotapa Pararani	110	24	4.7
Other	311	59	11.3
Total	2366	519	100

The team searched for feces both inside and outside the house. One fecal sample was collected from each household. The biological sample collection bottles had a capacity of 120 cc, with a wide mouth and hermetic sealing. The sample placed in each bottle did not exceed the capacity of the bottle. Care was taken not to externally soil the bottle such that the sample would not have to be discarded later.

The samples were labeled according to the enumeration of the files. When the feces sample form had been completed with all the necessary information, the samples were refrigerated until they were transferred to the laboratory. General standards for the transportation of biological materials were followed. The samples were sent within 10 days, and the reasons for sample referral were informed via telephone.

For sample referral, it was verified that the fecal samples from the dogs were properly identified and labeled with a complete identification form. The bottles were carefully cleaned and sealed externally using 1% bleach. The bottles were individually wrapped in absorbent paper and packed in cardboard boxes, in which they were properly distributed to prevent spillage. The empty spaces between bottles were immediately filled with absorbent paper. The cardboard boxes were then placed inside a Styrofoam box and refrigerants were placed in this box.

In the laboratory, samples that were kept for 48 h were frozen at -80 °C, those that were kept for over 4 days were maintained at -70 °C, and those that were kept for ≥ 7 days were maintained at -20 °C. The samples were processed using a copro-ELISA technique. The laboratory issued a report detailing the number of samples that tested positive using the copro-ELISA. Dog feces containing traces of the parasite represented evidence and was supported by this method of immunodiagnosis (copro-ELISA), which has been used in control programs in many countries, including Cyprus, Spain, Peru, and Argentina (Frison de Costas *et al.*, 2014).

The results were reported to the Huancarama Health Center, with the recommendation to carry out activities of mass deworming of dogs and to diagnose the owners of the dogs and any person living in the homes where a dog tested positive, as recommended by Larrieu *et al.* (2014).

Technique and instruments

The copro-ELISA test was performed using the techniques and instruments described in the study by Jara *et*

al. (2019), who indicated that this test had a sensitivity of 96.1% (95% CI:85.9-99.6) and a specificity of 98.2% (95% CI:89.5-100). Likewise, they indicated that its negative predictive value (NPV) was 96.5% (95% CI:91.7-100) and its positive predictive value (PPV) was 98% (95% CI:94.1-100).

Georeferencing of dogs raised in the sampled homes

To visualize the spatial distribution of echinococcosis on the corresponding map, a geographic information system (GIS) was used to develop data layers obtained from all locations in Huancarama district. Through this, georeferencing of 343 points corresponding to the houses where the owners had dogs was achieved, using the ArcGIS software (version 10.8) and GPS (GARMIN eTrex® 10) to generate the corresponding coordinates.

Statistical analysis.

Observations and processing of the information were carried out using Excel for Windows 2010 and the Statistical Package for the Social Sciences SPSS 25 software. Categorical variables were statistically contrasted using the chi-square test and odds ratios with 95% confidence intervals, and a value of $P \leq 0.05$ was taken to indicate the extreme degree of significance. Univariate and multivariate logistic regression tests were performed to determine possible associations between echinococcosis and the following: location of the home; distance from the slaughterhouse; altitude of the home; number, sex, and age of the dogs; veterinary control; lockdown; sterilization; and feeding with viscera. The lowest number was used as the reference value to seek the best biological model, with the following details: $g(x) = \beta0 + \beta1x1 + \beta2x2 + \beta3x3 + \beta4x4 + \beta5x5 + \beta6x6 + \beta7x7 + \beta8x8 + \beta9x9 + \beta10x10$. The variables of dog owners' knowledge of echinococcosis, domestic animal species sensitive to this infection, and transmission from dogs to people were not included in the model.

RESULTS

The study showed that 94.4% of households had dogs (490/519; 95% CI:92.3-96.5). On average, there were 0.6 dogs per home. In addition, it was estimated that there was a ratio of three people for each dog. The prevalence of *E. granulosus* in dogs in the Huancarama district was 27.7% (95/343; 95% CI:22.8-32.6).

Univariate logistic regression analysis showed that the distance from the dwellings to the slaughterhouse was associated with *E. granulosus* infection in dogs. The highest prevalence of echinococcosis occurred in households in the rural sector, which were more than 1000 m away from the population center of Huancarama (33.2%) ($P < 0.05$). Likewise, the altitude of the house was associated with *E. granulosus* in dogs, such that locations in the Suni altitude zone had a higher prevalence of echinococcosis in dogs (41.8%) than in the Quechua zone (25%) ($P < 0.05$). However, the slaughtering of animals in homes did not show any statistically significant association with echinococcosis in dogs. In addition, the characteristics of the dogs raised in Huancarama, such as the number of dogs kept, sex, age, veterinary control, confinement, sterilization, and feeding with viscera, also did not show any statistically significant association with echinococcosis ($P > 0.05$) (Table 2). Furthermore, as shown in Figure 1, fecal samples of dogs with *E. granulosus* (red dots) were distributed across all locations in the Huancarama district.

Table 3 shows that lack of knowledge that humans can contract echinococcosis was associated with *E. granulosus* in dogs (22.6%) ($P < 0.05$). However, unawareness of the existence of echinococcosis and that dogs can transmit this infection to people did not show any statistically significant association with *E. granulosus* in dogs ($P > 0.05$).

The multivariate logistic regression analysis showed that dogs whose homes were more than 1000 m away from the district slaughterhouse had a protective factor against echinococcosis (OR = 0.37; $P = 0.006$). The other factors studied did not show any statistically significant association ($P > 0.05$).

DISCUSSION

The majority of households in the Huancarama district had dogs (70%). This was similar to the findings of studies conducted in Bucaramanga, Colombia (67%) (Florez & Solano, 2019) and Coquimbo, Chile (63-89%) (Acosta-Jamett *et al.*, 2010). However, this proportion was higher than in Peruvian cities such as Abancay (47.8%) (Valderrama & Serrano, 2020), Lima (55.6-60.4%) (Soriano *et al.*, 2017; Esparza *et al.*, 2020) and Callao (56.1-61.9%) (Rendón *et al.*, 2018; Harada et al., 2019); as well as in the cities of Havana, Cuba (63%) (Pino-Rodríguez *et al.*, 2017), Buenos Aires, Argentina (47.9-57%) (Brusoni *et al.*, 2007; Zumpano *et al.*, 2011; Tortosa *et al.*, 2016), Viña del Mar, Chile (57%) (Morales *et al.*, 2009) and Chapecó, Brazil (52.5%) (Paula *et al.*, 2018).

The average number of dogs per dwelling in urban and rural areas estimated in the present study was 0.6. This was similar to what was found in Neuquén, Argentina (0.6) (Brusoni *et al.*, 2007), but lower than what was reported in Coquimbo, Chile (0.8-2.8) (Acosta-Jamett *et al.*, 2010) and in Lima, Peru (1.6-1.7) (Esparza *et al.*, 2020; Soriano *et al.*, 2017). In addition, the canine population density was high, considering that the human-to-dog ratio determined was very close (3:1), i.e. exceeding the 10:1 ratio recommended by the WHO (2020). The locations surveyed in the Huancarama district were mostly rural, with deficient socioeconomic development and a precarious standard of living, which increases the risk to human health from such a large canine population.

The high percentage of dog ownership found in this study may have been related to local cultural factors, the lack of animal population control, and responsible surveil-

Table 2. Characteristics of dog ownership, homes and *E. granulosus* in the Huancarama district, Peru

Factors	Dogs with *E. granulosus* n (%)	Dogs without *E. granulosus* n (%)	Total (100%)	OR	95% CI	*P*
Characteristics of the house						
Distance to slaughterhouse (m)						
< 200	3 (15.8)	16 (84.2)	19			0.026
200-400	14 (27.5)	37 (72.5)	51	0.49	0.2-1.2	0.11
401-1000	11 (15.5)	60 (84.5)	71	0.98	0.2-3.9	0.975
> 1000	67 (33.2)	135 (66.8)	202	0.37	0.2-0.8	0.006
Species slaughtered in the house						
Cattle	5 (45.5)	6 (54.5)	11	2.39	0.6-9.6	0.181
Sheep	5 (27.8)	13 (72.2)	18	0.57	0.2-2.2	0.994
Goats	4 (36.4)	7 (63.6)	11	1.44	0.4-5.9	0.514
Pigs	27 (31.4)	59 (68.6)	86	1.22	0.7-2.2	0.376
Altitude of the house (m)						
Suni zone 3500-4000)	23 (41.8)	32 (58.2)	55			
Quechua zone (2300-3500)	72 (25.0)	216 (75.0)	288	2.16	1.2-3.9	0.012
Dog ownership						
Number of dogs						
> 4	-	5 (100.0)	5			0.662
2-4	49 (30.2)	113 (69.8)	162	-	-	0.999
1	46 (26.1)	130 (73.9)	176	-	-	0.999
Sex of dogs						0.344
Female	26 (24.3)	81 (75.7)	107			
Male	69 (29.2)	167 (70.8)	236	0.77	0.5-1.3	0.344
Age of dogs (years)						
> 8	2 (25.0)	6 (75.5)	8			0.182
2-8	80 (30.1)	186 (69.9)	266	1.85	0.9-3.6	0.066
< 2	13 (18.8)	56 (81.2)	69	1.44	0.3-7.9	0.678
No veterinary control	85 (29.5)	203 (70.5)	288	1.88	0.9-3.9	0.089
No confinement	78 (28.1)	200 (71.9)	278	1.1	0.6-2	0.758
Unsterilized	95 (28.3)	241 (71.7)	336	-	-	0.999
Fed with viscera	13 (22.4)	45 (77.6)	58	0.72	0.4-1.4	0.326

lance policies (Paula *et al*., 2018). All locations surveyed in the Huancarama district, except for the location of Huancarama itself, were located in rural areas, where the number of dogs tended to be higher (WHO, 1990; Pino-Rodríguez *et al*., 2017; Rendón *et al*., 2018), despite socioeconomic conditions that tended to be poorer (Harada *et al*., 2019). On the other hand, the human-animal interaction generated through possession of dogs would benefit the people who cohabit with them, such as reduced stress, increased self-esteem, and increased psychological well-being, etc. (Rendón *et al*., 2018). Dogs can perform functions of guardianship, companionship, or hunting (Esparza *et al*., 2020); however, the high percentage of ownership reported in the present survey shows the importance of for-

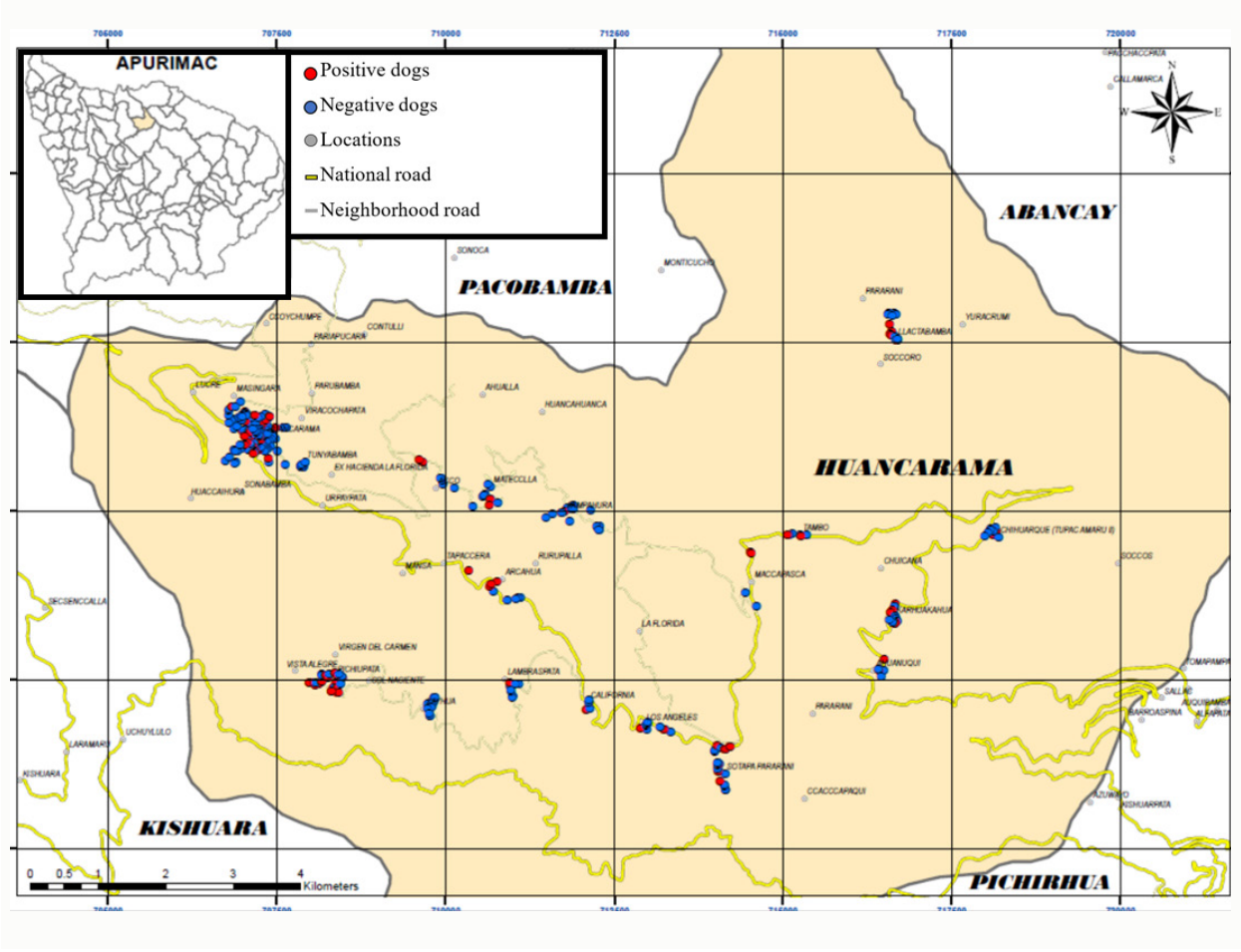

Figure 1. Map of distribution of fecal samples from dogs with owners, with (in red) and without (in blue) *E. granulosus* infection, in different locations in the Huancarama district.

tifying responsible ownership of companion animals and prevention of zoonotic diseases in the population of the District Municipality of Huancarama and its Health Center, pursuant to Law No. 30407 on Animal Protection and Welfare (Valderrama & Serrano, 2020).

The prevalence of *E. granulosus* in the dogs in this study was high (27.7%). It was much higher than that reported among dogs belonging to slaughterhouse workers and viscera traders in metropolitan Lima (13.8%) (Merino *et al.*, 2017); or among dogs in the provinces of Rio Negro (6.5%) (Larrieu *et al.*, 2014), La Rioja (15.9%) (Amaya *et al.*, 2016) and Jujuy, in Argentina (2-27.7%) (Frison de Costas *et al.*, 2014), and in the XII Region of Chile (1.8%) (Álvarez *et al.*, 2005). In addition, the locations of Pichiupata, California, and Sotapa Pararani presented exceedingly high prevalence (73.3%, 50%, and 43.5%, respectively), comparable only with what was reported from towns in the district of San José de Quero in Junín, Peru (50%) (Santivañez *et al.*, 2010).

This high prevalence in the most remote rural sectors probably occurred due to the precarious nutritional status of dogs. However, access to raw viscera containing hydatid cysts from cattle slaughtered at home is the main risk factor (Merino *et al.*, 2017). People tend to dispose of solid waste behind their homes, including household waste, thereby contaminating the environment and increasing the risk of contagion (Montalvo *et al.*, 2018). Along these lines, it can also be noted that the percentage of echinococcosis infection among pigs slaughtered in the slaughterhouse of Huancarama was 77%, probably as a result of poor knowledge and deficient practices among pork producers (Sierra-Ramos & Valderrama-Pomé, 2017). It is also worth mentioning that there is only one municipal slaughterhouse located in the capital of the Huancarama district, which means that for the most remote rural residents, slaughtering animals in their own homes is preferred, in order to avoid the complication of moving the animals to the district capital.

The distance from the houses to the slaughterhouse was associated with *E. granulosus* in dogs, such that the highest prevalence occurred in sectors that were more than 1000 m away from the village of Huancarama, where the slaughterhouse is located ($P < 0.05$). This is because most remote locations do not have a municipal slaughterhouse,

Table 3. Dog owners' knowledge about the parasite cycle of *E. granulosus* and its presence in dogs in the Huancarama district

Factors	Dogs with *E. granulosus* n (%)	Dogs without *E. granulosus* n (%)	Total (100%)	OR	95% CI	*P*
Echinococcosis	87 (28.7)	216	303	1.61	0.7-3.6	0.251
Species that can contract *E. granulosus:*						
Cattle	95 (28.9)	234 (71.1)	329	-	-	0.998
Goats	95 (28.3)	241 (71.7)	336	-	-	0.999
Dogs	94 (28.2)	239 (71.8)	333	3.54	0.4-28.3	0.234
Sheep	93 (28.0)	239 (72.0)	332	1.75	0.4-8.3	0.479
Pigs	88 (27.9)	227 (72.1)	315	1.16	0.5-2.8	0.74
Humans	43 (22.6)	147 (77.4)	190	0.57	0.4-0.9	0.02
that dogs can transmit *E. granulosus* to people	1 (11.1)	8 (88.9)	9	0.32	0-2.6	0.26

so slaughtering of animals is done at home, thus facilitating the consumption of viscera by dogs and increasing disease prevalence (Merino *et al*., 2017; Montalvo *et al*., 2018).

The locations in the Suni altitude zone (3500-4000 m.a.s.l.) presented a higher prevalence of echinococcosis in dogs than those in the Quechua zone (2300-3500 m.a.s.l.) ($P < 0.05$). This finding differs from that reported in other studies, such as in the Quebrada area (2200-2700 m.a.s.l.) and the Puna area (3000 m.a.s.l.) of Jujuy, Argentina, where the prevalence was similar (11.7-14% and 2-14.8%, respectively) (Frison de Costas *et al*., 2014). Similarly, in a previous study on pigs slaughtered in the slaughterhouse of Huancarama in 2013, the percentage of cystic echinococcosis infection was higher in pigs from Andahuaylas (2926 m.a.s.l.) than in pigs from Huancarama (2965 m.a.s.l.), Pacobamba (2720 m.a.s.l.), and Kishuara (3665 m.a.s.l.), with no relationship with altitude (Sierra-Ramos & Valderrama-Pomé, 2017).

Contrary to what several authors have suggested (Frison de Costas *et al*., 2014; Amaya *et al*., 2016; Merino *et al*., 2017; Montalvo *et al*., 2018), neither the characteristics of dogs raised in the locations of Huancarama (such as the number of dogs bred, sex, age, veterinary control, confinement, sterilization, and feeding with viscera) nor the slaughter of animals in homes showed any association with echinococcosis in dogs. This was probably because infection with this parasite spread endemically throughout the district. However, it was difficult to observe the owners' habits regarding their feeding of their dogs because the residents of this district were very suspicious about letting strangers into their homes.

The lack of knowledge on whether cattle and humans can contract echinococcosis is associated with echinococcosis in dogs. This is a concern considering that this disease is zoonotic. The inhabitants neglect their self-care to avoid contracting the infection by maintaining contact with their dogs or feeding them with raw viscera contaminated with hydatid cysts (Amaya *et al*., 2016), especially from cattle slaughtered at home. It should be noted that the Apurimac region, where the Huancarama district is located, is not a sheep area, but backyard breeding of species such as cattle and pigs is practiced especially (INEI, 2017).

The multivariate logistic regression analysis showed that dogs whose homes were more than 1000 m from the district slaughterhouse had 63% protection against echinococcosis. This was because, unlike homes in the urban-rural area where the slaughterhouse is located, homes in rural areas are far from each other, which would make it difficult for a dog to travel to eat some viscera with hydatid cysts that had been improperly disposed of in another household. Therefore, dogs that were found to be infected would not have become infected by eating raw viscera supplied by their owners, considering that these owners were aware of the risks that this implies. Rather, they would mainly have become infected from viscera that had been improperly discarded by residents of neighboring houses in the urban-rural sector.

It should be emphasized that this was the first survey on the presence of echinococcosis in dogs in the Huancarama district. There is a latent risk factor due to deficient possession of dogs that are usually fed raw viscera, fruits,

or waste from the slaughterhouse of the city (Reyes *et al*., 2012; Larrieu *et al*., 2014; Amaya *et al*., 2016). However, this survey presented some limitations, considering that even though the surveys were carried out using an interview guide, the interviewee's responses had to be trusted. Moreover, if there had been prior knowledge of the number of dogs in the district and in each village would have helped in designing a more accurate sample size and thus to obtain more precise results.

The lack of echinococcosis control strategies has allowed for the spread of infection in the study area. The results of this study demonstrated that *E. granulosus* is present throughout the district, highlighting that echinococcosis constitutes a public health problem. The present results may form a useful basis for subsequent studies and are valuable with regard to the implementation of mitigation and control strategies in the district studied and in the province of Andahuaylas. For this reason, the results from this research have been reported to the Huancarama Health Center, with a view to undertaking deworming programs for dogs and people who were living in homes from which canine fecal samples were positive for *E. granulosus*.

Competing interests statement

The authors declare that they did not have any conflict of interest.

Author contributions

GM and FJU were involved in the data collection, analysis, and interpretation. AAV participated in the study conception, data analysis and interpretation, writing, design, critical review of the article, statistical advice, and technical or administrative advice. All authors approved the final version of the manuscript.

Ethics statement

The study protocol was approved by the Institutional Ethics Committee for the Use of Animals (Certificate 008-03-21) and the Institutional Research Ethics Committee (Certificate 064-01-21), of the Universidad Peruana Cayetano Heredia, under the expedited review category.

Funding

This research was funded by the Universidad Nacional Micaela Bastidas de Apurimac through the "III Contest of Scientific and Technological Research Projects for Teachers, financed with Funds from Canon, Sobrecanon and Mining Royalties" (Resolution no. 496-2019-CU-UNAMBA).

REFERENCES

Acosta-Jamett, G., Cleaveland, S., Cunningham A. A., & Bronsvoort B. M. (2010). Demography of domestic dogs in rural and urban areas of the Coquimbo region of Chile and implications for disease transmission. *Preventive Veterinary Medicine*, *94*(3-4), 272–281. https://doi.org/10.1016/j.prevetmed.2010.01.002

Álvarez, F., Tamayo, R., & Ernst, S. (2005). Estimación de la prevalencia de equinococosis canina en la XII Región, Chile, 2002. *Parasitología Latinoamericana*, *60*(1-2), 74-77. https://doi.org/10.4067/S0717-77122005000100013

Amaya, J. C., Moreno, N., Salmaso, N., Bazan, E., Ricoy, G., Córdoba, P., & Santillan. G. I. (2016). Estudio de infestación de caninos con Echinococcus granulosus en la provincia de La Rioja, Argentina. *Revista Argentina Microbiología*, *48*(1), 38-42. https://doi.org/10.1016/j.ram.2015.11.003

Apt, W., Pérez, C., Galdamez, E., Campano, S., Vega, F., Vargas D., Rodríguez, J., Retamal, C., Cortés, P., Zulantay, I., & Rycke, PH. (2000). Equinococosis/hidatidosis en la VII Región de Chile: diagnóstico e intervención educativa. *Revista Panamericana de Salud Pública* *7*(1), 8-16.

Brusoni, C., Dezzotti, A., Fernández, J., & Lara, J. (2007). Tamaño y estructura de la población canina en San Martín de los Andes (Neuquén). *Analecta Veterinaria*, *27*(1), 11-23.

Carrión-Ascarza, Y. P., Bustinza-Cardenas, R. H., & Valderrama-Pomé, A. A. (2021). Comiso de vísceras por fascioliasis y equinococosis quística en bovinos, ovinos y caprinos faenados en Apurímac, Perú. *Revista MVZ Córdoba*, *26*(2), 1-10. https://doi.org/10.21897/rmvz.2056

Esparza, B., León, D., & Falcón, N. (2020). Conocimientos y prácticas potencialmente riesgosas en la tenencia de animales relacionadas a exposición a zoonosis en un Sector de Lomas de Carabayllo, Lima - Perú. *Revista de Investigaciones Veterinarias del Perú*, *31*(3), 1-15. https://doi.org/10.15381/rivep.v31i3.18170

Florez, A. A., & Solano, J. A. (2019). Estudio demográfico de la población de perros y gatos domiciliados en el sector suroriental de Bucaramanga, Colombia. *Revista de Investigaciones Veterinarias del Perú*, *30*(2), 828-835. https://doi.org/10.15381/rivep.v30i2.15087

Frison de Costas, S., Riveros, N., Ricoy, G., Sosa, S., & Santillan, G. (2014). Diagnóstico de situación de la equinococosis quística en heces dispersas en las zonas de Quebrada y Puna, provincia de Jujuy, Argentina. *Revista Argentina de Microbiología*, *46*(2), 80-84. https://dx.doi.org/10.1016/S0325-7541(14)70052-5

Harada, C., León, D., Gamarra, N., & Falcón, N. (2019). Indicadores demográficos y estimación de la población de canes en el distrito de Bellavista, Callao - Perú. *Salud y Tecnología Veterinaria*, *7*(1), 27-32. https://doi.org/10.20453/stv.v7i1.3565

INEI (2022). IV Censo Nacional Agropecuario 2012. INEI, Lima. http://censos.inei.gob.pe/cenagro/tabulados/.

INEI (2017). Censos Nacionales 2017: XII de Población, VII de Vivienda y III de Comunidades Indígenas. INEI, Lima. http://censo2017.inei.gob.pe/

Jara, L. M., Rodriguez, M., Altamirano, F., Herrera, A., Verastegui, M., Gımenez-Lirola, L. G., Gilman, R. H., & Gavidia, C. M. (2019). Development and Validation of a Copro-Enzyme–Linked Immunosorbent Assay Sandwich for Detection of Echinococcus granulosus–Soluble Membrane Antigens in Dogs. *American Journal of Tropical Medicine and Hygiene*, *100*(2), 330-335. https://doi.org/10.4269/ajtmh.18-0645

Khan, A., Naz, K., Ahmed, H., Simsek, S., Afzal, S. M., Haider, W., Ahmad S. S., Farrakh, S., Weiping, W., & Yayi, G. (2018). Knowledge, attitudes and practices related to cystic echinococcosis endemicity in Pakistan. *Infectious Diseases of Poverty*, *7*(4), 1-15. https://doi.org/10.1186/s40249-017-0383-2

Larrieu, E., Seleiman, M., Herrero, E., Mujica, G., Labanchi, J. L., Araya D., Grizmado, C., Sepúlveda, L., Calabro, A., Talmón, G., Crowleya, P., Albarracína, S., Arezo, M., Volpe M., Ávila, A., Pérez, A., Uchiumi, L., Salvitti, J. C., & Santillan, G. (2014). Vigilancia de la equinococosis quística en perros y niños en la provincia de Río Negro, Argentina. *Revista Argentina de Microbiología*, *46*(2), 91-97. https://doi.org/10.1016/S0325-7541(14)70054-9

Merino, V., Falcón, N., More, N., & González, G. (2017). Detección de coproantígenos de Echinococcus granulosus en canes de trabajadores de camales y comercializadores de vísceras en Lima metropolitana. *Revista Panamericana de Salud Pública*, *41*, e10.

Montalvo, R., Clemente, J., Castañeda, L., Caro, E., Ccente, Y., & Nuñez M. (2018). Coproprevalencia de infestación canina por Echinococcus granulosus en un distrito endémico en hidatidosis en Perú. *Revista de Investigaciones Veterinarias del Perú*, *29*(1), 263-269. https://doi.org/10.15381/rivep.v29i1.14189

Morales, M.A., Varas, C., & Ibarra, L. (2009). Caracterización demográfica de la población de perros de Viña del Mar, Chile. *Archivos de Medicina Veterinaria*, *41*(1), 89-95. https://doi.org/10.4067/S0301-732X2009000100013

OMS (2020). Orientaciones de bioseguridad en el laboratorio relacionadas con la COVID-19 [Internet]. OMS, Ginebra. https://apps.who.int/iris/bitstream/handle/10665/332285/WHO-WPE-GIH-2020.3-spa.pdf

Paula, J., Santos, C. G., Canalli, V., Fritzen, D. M., Busato, M. A., & Lutinski, J. A. (2018). Perfil populacional de cães e gatos e bem-estar animal em Chapecó, SC. *Revista Brasileira de Higiene e Sanidade Animal*, *12*(4), 437-449.

Pavletic, C. F., Larrieu, E., Guarnera, E. A., Casas, N., Irabedra, P., Ferreira, C., Sayes, J., Gavidia, C. M., Caldas, E., Laurence, L. M., Melody, M., Marcos, A., Navarro, A. M., Vigilato, M. A. N., Cosivi, O., Espinal, M., & Del Rio V.

J. (2017). Cystic echinococcosis in South America: a call for action. *Revista Panamericana de Salud Pública*, *41*(42). https://doi.org/10.26633/RPSP.2017.42

Peña, Y., & Valderrama, A. A. (2022). Equinococosis quística en animales faenados en mataderos municipales de la provincia de Andahuaylas, Perú. *Revista de Investigaciones Veterinarias del Perú*, *33*(5), e23777. https://doi.org/10.15381/rivep.v33i5.23777

Pino-Rodríguez, D., Márquez-Álvarez, M., & Rojas-Hoyos, N. A. (2017). Aspectos demográficos de la población de perros con dueños del municipio Boyeros, Cuba. *Revista de Salud Animal*, *39*(2), 1-8.

Ramírez, D. Y., Jefferson, M. E., Hernández, I. H., León C., D., & Falcón, P. N. (2018). Conocimientos, percepciones y prácticas relacionados a equinococosis quística en familias con antecedentes de la enfermedad. *Revista de Investigaciones Veterinarias del Perú*, *29*(1), 240-252. https://doi.org/10.15381/rivep.v29i1.14193

Rendón, D., Quintana, E., Door, I., Vicuña, F., León, D., & Falcón, N. (2018). Parámetros demográficos en la población de canes y gatos domésticos en asentamientos humanos del distrito de Ventanilla, Callao-Perú. *Revista de Investigaciones Veterinarias del Perú*, *29*(1), 217-225. https://doi.org/10.15381/rivep.v29i1.14191

Reyes, M. M., Taramona, C. P., Saire-Mendoza, M., Gavidia, C. M., Barron, E., Boufana, B., Craig, P. S., Tello, L., Garcia, H. H., & Santivañez, S. J. (2012). Human and canine echinococcosis infection in informal, unlicensed abattoirs in Lima, Peru. *PLoS Neglected Tropical Diseases*, *6*(4), 1-6. https://doi.org/10.1371/journal.pntd.0001462

Sanchez, L., Mayta, H., Jara, L. M., Verástegui, M., Gilman, R. H., Gómez-Puerta, L. A., & Gavidia, C. M. (2022). Echinococcus granulosus sensu stricto and E. canadensis are distributed in livestock of highly endemic area in the Peruvian highlands. *Acta Tropica*, *225*, 1-6. https://doi.org/10.1016/j.actatropica.2021.106178

Santivañez, S. J., Naquira, C., Gavidia, C. M., Tello, L., Hernandez, E., Brunetti, E., Kachani, K., Gonzalez, A. E., & Garcia, H. H. (2010). Factores domiciliarios asociados con la presencia de hidatidosis humana en tres comunidades rurales de Junín, Perú. *Revista Peruana de Medicina Experimental y Salud Pública*, *27*(4), 498-505. https://doi.org/10.17843/rpmesp.2010.274.1519

Sierra-Ramos, R. G., & Valderrama-Pomé, A. A. (2017). Hiperendemia de equinococosis y fertilidad quística en porcinos del valle interandino de Huancarama, Perú. *Revista Peruana Medicina Experimental Salud Publica*, *34*(2), 250-254. https://doi.org/10.17843/rpmesp.2017.342.2500

Soriano, J. F., Núñez, J., León, D., & Falcón, N. (2017). Estimación de la población de canes con dueño en el distrito de Comas, Lima - Perú. *MV Revista de Ciencias Veterinarias*, *3*(2), 5-10.

Tortosa, A., Zumpano, R., Ardiles, I., Berra. Y., Faigenbaum, A. N., Guido, G. G., Castro, J., Molina, J. L., Marcos, E. R., & Degregorio, O. J. (2016). Caracterización de la Tenencia de Animales de Compañía en la Ciudad de Buenos Aires, Argentina. *Revista de Investigaciones Veterinarias del Perú*, *27*(4), 631-643. https://doi.org/10.15381/rivep.v27i4.11997

Valderrama, A. A., & Serrano, K. J. I. (2020). Estimación poblacional de perros y gatos con propietario en la ciudad de Abancay, Perú (2017). *Revista de Investigaciones Veterinarias del Perú*, *31*(3), 1-8. https://doi.org/10.15381/rivep.v31i3.17294

WHO (1990). Guidelines for dog population management. Veterinary Public Health Unit. WHO, Ginebra. https://apps.who.int/iris/handle/10665/61417

WHO (2020). Guidelines for dog population management. WHO, Ginebra. https://apps.who.int/iris/handle/10665/61417?locale-attribute=en&

Zumpano, R., Tortosa, A., & Degregorio, O. J. (2011). Estimación del impacto de la esterilización en el índice de crecimiento de la población de caninos. *Revista de Investigaciones Veterinarias del Perú*, *22*(4), 336-341. https://doi.org/10.15381/rivep.v22i4.333

Zuñiga-A, I., Jaramillo-A, C. J, Martínez-M J. J., & Cárdenas-L, J. (1999). Investigación experimental de la equinococosis canina a partir de quiste hidatídico de origen porcino en México. *Revista de Saúde Pública*, *33*(3), 302-308.

Austral Journal of Veterinary Science

Austral J Vet Sci 55, 176-181 (2023)
https://doi.org/10.4206/ajvs.553.03

ORIGINAL ARTICLE

Clinicopathological investigations among recurrent camelpox outbreaks in Omanis' Arabian camels (*Camelus dromedarius*)

Amal Alkharusi[1], Nadia Al Khaldi[1], Nada Al-Sharji[1], Khalsa Altoubi[1], Taha Alsubhi[1], Maged A. Al-Garadi[2], Naif Al-Gabri[3], Haytham Ali[4],[5*]

[1] Ministry of Agriculture, Fisheries Wealth and Water Resources, Muscat, 100, Sultanate of Oman

[2] Department of Animal Production, College of Food and Agriculture Sciences, King Saud University, Saudi Arabia

[3] Laboratory of Salam Veterinary Group, Buraydah 51911, Al-Qassim, Saudi Arabia

[4] Department of Animal and Veterinary Sciences, College of Agricultural and Marine Sciences, Sultan Qaboos University, Muscat 123, Sultanate of Oman.

[5] Department of Pathology, Faculty of Veterinary Medicine, Zagazig University, Zagazig, Egypt

Article History
Received: 03.02.2023
Accepted: 28.06.2023
Published: 06.09.2023

Corresponding author
*Haytham Ali
h.ali@squ.edu.om

ABSTRACT. Camelpox remains a widespread viral disease in camelids, with socioeconomic relevance. The present study explored the hematological, biochemical, and histopathological alterations in dromedary-racing camels from the North of Oman infected with camelpox virus diagnosed by real-time PCR. Blood and skin samples were collected from camels with clinical signs and skin lesions (n=4) and from healthy camels (n=3) from 10 different camel herds. The results indicated that the infected camels showed clinical signs, including pyrexia, lacrimation, nasal mucus discharge, affixed and swollen eyelids, emaciation, and pimples on the skin of the head, legs, and abdomen. Hemoglobin, hematocrit, and platelets were significantly greater, with a significant reduction in leukocyte and lymphocyte counts in infected camels than in healthy camels. Infected camels had higher CK and creatinine levels and hepatic-related metabolites, including AST, ALP, AST, GGT, and LDH, than the apparently healthy camels. Histopathological examination of skin scab samples revealed ballooning degeneration of epidermal cells in the presence of typical large eosinophilic intracytoplasmic inclusion bodies and suppurative dermatitis following secondary bacterial infection in all examined infected camels. Camelpox viral DNA was detected using real-time PCR in the blood and skin samples of all infected camels. These findings in dromedary-racing camels associated with a molecular diagnosis of camelpox are described for the first time in the Sultanate of Oman. Therefore, further studies are warranted.

Keywords: Camelpox; Camel; hematological; Oman; Outbreak; Molecular detection.

INTRODUCTION

Camels have socioeconomic importance in Arabian countries as food safety nets owing to their milk and meat consumption. Viral outbreaks are recurrent in camels and are triggered by pathogenic or environmental factors that can restrict vaccination competence. Camelpox virus, a highly contagious disease of camelids, is the etiological agent of this disease. This virus is a member of the genus Orthopoxvirus of the family Poxviridae. Camel keepers encounter significant losses due to morbidity and mortality in infected camels, as well as weight loss in the body and reduction in milk yield (Bhanuprakash *et al*., 2010b). The disease has erupted in almost every region that practices camel husbandry, and many outbreaks have been reported in several countries in Africa, the Middle East, and Asia (Wernery & Kaaden, 2002), including the Oman (Fassi-Fehri, 1987; Shommein & Osman, 1987; Kumar *et al*., 2012; Hussain *et al*., 2015). Camelpox outbreaks have led to huge economic losses through deaths, milk loss, aborted infected camels, and the cost of supportive treatment and prevention of the spread of the disease (Wernery & Zachariah, 1999; Bhanuprakash *et al*., 2010a).

Camelpox presents with clinical signs, including pyrexia, enlarged lymph nodes, and characteristic pox skin lesions (Bhanuprakash *et al*., 2010b). Moreover, Camelpox disease appears in either a generalized or a localized form. In the generalized form, pox lesions spread all over the skin and extend to the esophagus, trachea, and lungs (Wernery & Kaaden, 2002; Narnaware *et al*., 2021). In the localized form, the lesions are strictly in the skin and start as papules that transform into vesicles and pustules, followed by scab formation, which may take up to 4–6 weeks to heal. Histopathological lesions include typical cytoplasmic vacuolation of epidermal stratum spinosum keratinocytes, with large eosinophilic intracytoplasmic inclusions. Vesicles form following the rupture of swollen cells, and lesions are usually associated with the infiltration of mononuclear cells and neutrophils. Hyperplastic epithelium may be observed at the rim of the skin lesions (Balamurugan *et al*., 2013). Rainy seasons, common watering sources, and the introduction of new camels into herds are risk factors for a higher incidence of camelpox disease. The transmission of camel poxvirus usually occurs by direct or indirect contact, as the virus is secreted in various body fluids, including nasal and ocular discharges, milk, and saliva of infected

animals. Infection is caused by inhalation, skin abrasion, and mechanical transmission through ticks (Bhanuprakash *et al*., 2010b; OIE, 2021). Camelpox is clinically diagnosed on the basis of the identification of classical signs. However, confirmation is required to exclude similar effects such as contagious ecthyma (Orf), papillomavirus, and insect bites (Khalafalla *et al*., 2015; OIE, 2021). Camelpox can be confirmed by several tests like transmission electron microscopy, immunohistochemistry, virus isolation, serological tests, and molecular tests like PCR (Bhanuprakash *et al*., 2010a; Bayisa, 2019).

Camelpox has been reported in many developing countries in Asia and Africa (Mohammadpour *et al*., 2020). The disease has been reported among camels in the Sultanate of Oman; however, there is a lack of reports regarding clinicopathological data on the disease. This is the first study to report hematological, bichemical, histopathological, and molecular investigations related to camelpox infection in camels from the Sultanate of Oman.

MATERIALS AND METHODS

Samples collection

In October 2020, an outbreak of skin lesions in camels was reported on ten farms in the Sultanate of Oman. Samples were collected from camel herds reared in Aswad, Shinas Province, Al Batinah North Governorate, Sultanate of Oman. The animals were kept under a closed rearing system of a dromedary camel herd. Infected camels were male and female, aged between 1 and 10 years. The infected camels showed clinical signs. Blood samples (n=7) of both apparently healthy (n=3) and infected (n=4) camels from each farm were collected to study hematological and biochemical alterations and DNA extraction. Skin scabs were collected and deposited in 10% neutral buffered formalin for histopathological examination.

Hematological and plasma biochemical assessment

Blood samples (5 ml) were collected from the jugular vein in heparin tubes and stored at 4 °C until examination. Once in the laboratory, the samples were further separated into two subsamples. The first was used for hematological examinations. The second sub-tube was centrifuged (3000 rpm for 20 min) for plasma separation and stored at -20 ºC for blood metabolites. Using the automated Haematology Veterinary Analyser (ABX Micros ES 60®, Horiba Company, UK), the total of white blood cells (WBC), differential leucocyte (DLC), red blood cell count (RBC), hemoglobin (Hb), hematocrit (PCV), and platelets count were measured.

The plasma components of the protein fractions (total protein and albumin), creatinine, creatinine kinase, alkaline phosphatase (ALP), lactate dehydrogenase (LDH), gamma-glutamyl transferase (GGT), aspartate aminotransferase (AST), and alanine transaminase (ALT) were assessed using commercially available kits (Pars Azmun Corporation Ltd., Tehran, Iran) according to the manufacturer's instructions, using auto-analyzer biochemistry (Chem 299, Gesan, Italy).

Histopathological examination

To assess the histopathological alterations, specimens were fixed in 10% neutral buffered formalin and then dehydrated with increasing concentrations of alcohol (65%, 75%, 90%, and 100%). Fixed specimens were embedded in paraffin using an automated processor (MTM-SLEE, Germany), sectioned with a Leica® microtome into 5 µm sections, and routinely stained with hematoxylin and eosin according to the method described by Suvarna *et al*. (2018). Images of tissues were captured using a Nikon ECLIPSE E200 microscope.

DNA extraction and real-time PCR

DNA was extracted from whole blood samples of healthy and infected camels. DNA was isolated using a DNeasy Blood & Tissue kit (Qiagen, Germany) following the manufacturer's instructions (Alhaddad *et al*., 2019). The quality and quantity of DNA were then determined. Extracted DNA from blood and skin scab tissue samples was tested by real-time PCR using a commercial Genetic PCR Solutions (GPSTM) Camelpox virus MONODOSE dtec-qPCR kit (Alicante, Spain), following the manufacturer's protocol. The thermal cycling conditions were 95°C for 1 min, followed by 40 cycles of denaturation at 95°C for 10 s, extension, and data collection at 60°C for 1 min.

Statistical analysis

The differences between the means of the two groups (infected and apparently healthy) were tested for significant differences using a t-test (Proc T-test; SAS Institute Inc., 2012). Statistical significance between means was set at a p-value less than 0.05. The results are expressed as the mean ±SEM.

RESULTS

Clinical signs and treatment

Our data revealed that the infected camels exhibited clinical signs of different severity, including anorexia, pyrexia, lacrimation, swollen eyelid, nasal mucus discharge, and pock lesions at various skin parts such as nostrils, mouth, head, legs, and abdomen, especially in the end periods (Figure 1 A, B, and C). No mortality was recorded from any of the camels during data collection from the camel herds. Clinically infected camels were isolated and treated successfully with three doses of long-acting oxytetracycline (20 mg/kg every two days) with a topical antibiotic spray (chloramphenicol/gentian violet).

Haematological and biochemical profile

The hematological values of the infected and apparently healthy camels are presented in Table 1. Hb, PCV, WBC,

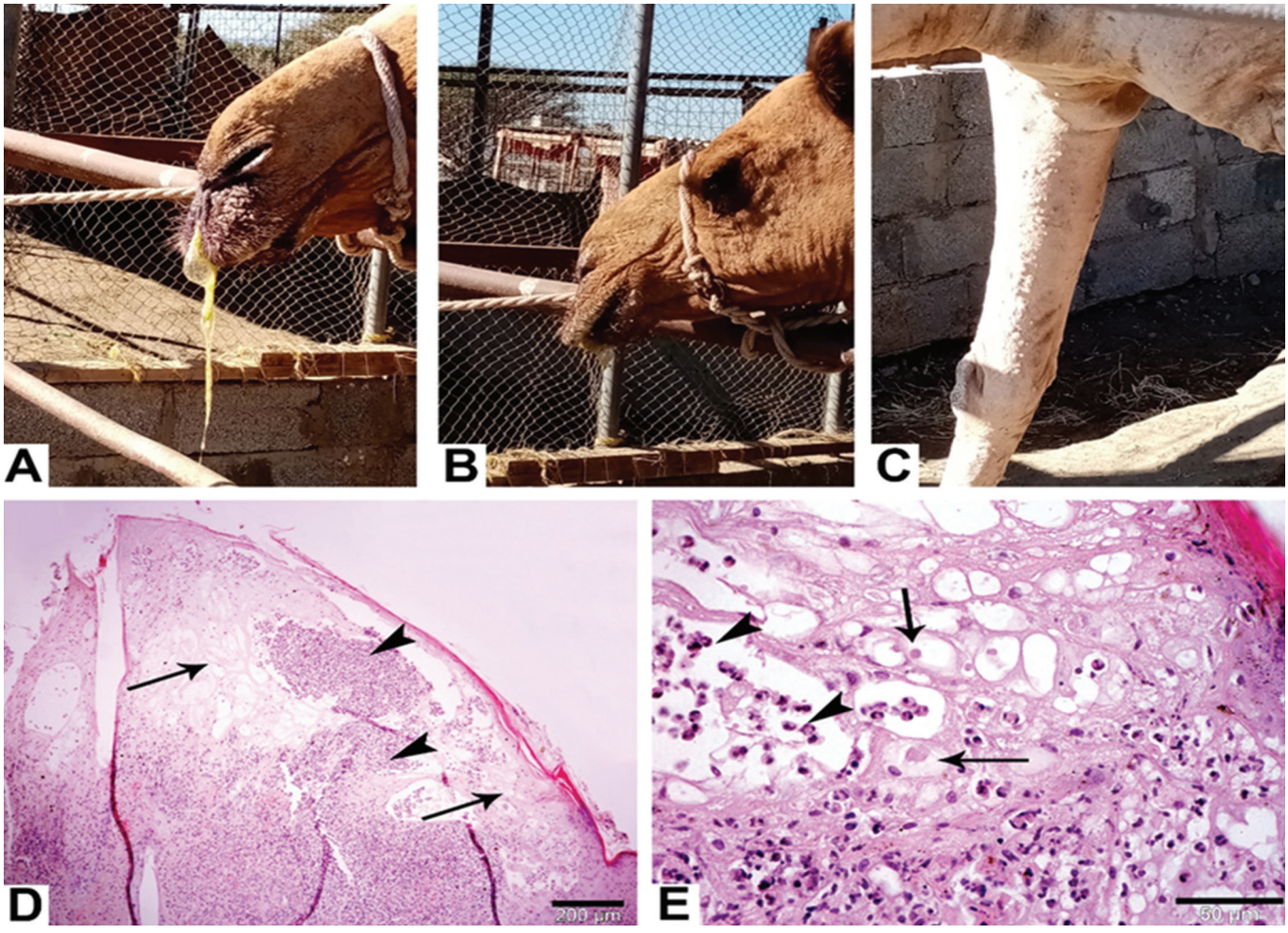

Figure 1. An adult racing dromedary camel showing nasal discharges along with papules over the head and the forelimb (A, B, C); Skin scabs from camelpox infected animal showing marked hydropic and ballooning degeneration (arrows) of the epidermal cell layer with large aggregates of dead and living neutrophils forming microabscesses (arrowheads) (D) (H&E stain, Bar= 200µm); Large eosinophilic intracytoplasmic inclusion bodies (arrows) in the degenerated cells of the stratum spinosum along with aggregates of neutrophils (arrowheads) (E) (H&E stain, Bar= 50µm).

platelet, and neutrophil levels were significantly different between the two groups. Hb, PCV, and platelet values significantly increased by 24.8%, 27.6%, and 5.0%, respectively, in the infected group compared to those in the healthy group. Infected camels had lower ($p < 0.05$) WBC and lymphocyte counts by 33.05% and 14.4%, respectively, than apparently healthy camels (Table 1). The plasma biochemical values of infected and healthy camels are shown in Table 2. The values of creatinine and CK were significantly increased ($p < 0.05$) in infected camels by 55.5% and 41.08%, respectively, compared with those in the healthy camel group. In contrast to the healthy camel group, all hepatic-related enzymes, ALP, LDH, AST, and GGT, were significantly increased in the infected camels by 70.4%, 48.9%, 58.3%, and 51.7%, respectively. No significant effects were detected for ALT levels.

Histopathological examination

As shown in Figure 1(D) and 1(E), examination of the skin scab tissues revealed marked hydropic and ballooning degeneration of the epidermal cell layer, with large eosinophilic intracytoplasmic inclusion bodies. The scabs also exhibited large aggregates of dead and living neutrophils that formed microabscesses.

Molecular detection of camelpox virus

Camelpox viral DNA was successfully detected using a commercial kit for real-time PCR from the blood and skin scab tissue samples of camels that exhibited clinical signs and only one of the apparently healthy camels.

Table 1. Haematological values of camels infected by campelpox virus showing skin lesions and apparently healthy. Results are expressed as means ± SE.

Variable[1]	Infected	Apparently healthy
Erythrocytes		
Hb (g/dl)	15.1 ± 0.83*	12.1 ± 0.72*
RBC (10^6/µl)	9.9 ± 0.62	7.7 ± 0.69
PCV%	41.3 ± 1.14*	32.4 ± 1.07*
Platelets	607.5 ± 2.46*	578 ± 2.17*
Leucocytes		
WBC (10^3/µl)	8.7 ± 0.80*	13.1 ± 0.57*
Neutrophil (%)	74.8 ± 0.75*	65.4 ± 0.54*
Lymphocyte (%)	17.3 ± 0.76	19.4 ± 1.38

Hb: hemoglobin; RBC, red blood cell; PCV, packed cell volume; WBC, white blood cells. * $p \leq 0.05$ is statistically significant.

Table 2. Plasma biochemical values obtained from camels infected with the Camelpox virus showing skin lesions and apparently healthy. Results are expressed as means ± SE.

Variable[1]	Infected	Apparently healthy
Protein fraction		
Total protein (g/dl)	7.8 ± 1.09	6.55 ± 0.27
Albumin (g/dl)	2.92 ± 0.51	3.54 ± 0.92
Cardiac indices		
CK (U/L)	179.6 ± 1.14*	115.5 ± 1.32*
Kidney indices		
Creatinine (mg/dL)	2.21 ± 0.05*	1.57 ± 0.1*
Hepatic indices		
ALP (U/L)	154.4 ± 0.95*	90.6 ± 1.04*
LDH (U/L)	1176 ± 6.92*	591 ± 4.83*
AST (U/L)	79.4 ± 3.73*	50.15 ± 2.28*
ALT (U/L)	6.24 ± 0.270	6.4 ± 0.31
GGT (U/L)	11.5 ± 1.75*	7.58 ± 1.95*

[1] CK, creatinine kinase; ALP, alkaline phosphatase; LDH, lactate dehydrogenase; GGT, gamma-glutamyl transferase; AST, aspartate aminotransferase; ALT, alanine transaminase. * $p \leq 0.05$ is statistically significant.

DISCUSSION

This study investigated outbreaks of camelpox disease in camel herds in Oman. All infected camels had localized skin lesions on their head, neck, abdomen, and limbs. No mortality was recorded for any of the affected animals. The outbreak occurred in October, a hot and humid month in the coastal Al-Batinah North Governorate, which may have played a role in initiating the infection. Our data are in agreement with previous investigations, where a higher incidence and more severe form of camelpox outbreaks were observed in the rainy season than in the dry season, in addition to its association with calf weaning and poor nutrition (Wernery *et al*., 1997; Wernery & Kaaden, 2002; Bhanuprakash *et al*., 2010; Mohammadpour *et al*., 2020).

As reported in our study, infected camels typically show

clinical signs of localized camelpox infection. These clinical signs, including pyrexia, anorexia, lacrimation, swollen eyelids, and pock lesions on the skin of the head, neck, legs, and abdomen, which form pustules and scabs, are in agreement with other reported camel pox outbreaks (Narnaware *et al*., 2021; OIE, 2021; Mohammadpour *et al*., 2020). Moreover, similar studies (Wernery & Kaaden, 2002) have mentioned that skin lesions initially appear as erythematous macules, develop into papules and vesicles, and later turn into pustules. Lacrimation and excess salivation in camels have been previously described by several authors (Aregawi & Feyissa, 2016; Dahiya *et al*., 2017; Narnaware *et al*., 2018). Additionally, we detected camelpox viral DNA in all camels showing clinical signs and in one of the apparently healthy camels that could be carriers or during the incubation period.

Significant changes in Hb, PCV, WBC, neutrophil, and platelet counts were observed between the infected and healthy camels. In this study, infected camels had higher levels of Hb, PCV, and platelets, and lower levels of WBCs and leukocytes. In agreement with previous reports (Kachhawaha *et al*., 2014; Narnaware *et al*., 2018), hyperproteinemia in camels infected with the camelpox virus in India was attributed to anorexia related to mouth lesions. Moreover, Bhanuprakash *et al*. (2010) indicated that camels infected with camelpox exhibited an increase in Hb and PCV and a significant reduction in WBC and lymphocyte counts. In addition, hepatic metabolites, such as GGT and AST, were higher in camelpox-infected camels (Hussein & Al-Mufarrej, 1999). This may be associated with the attachment of the virus to blood cells and prevention of their mobility and functionality. However, other studies have indicated that camelpox has no considerable impact on biochemical and hematological parameters (Bhanuprakash *et al*., 2010). In line with our data, De *et al*. (2020) reported that leukocyte counts were significantly reduced in camelpox-infected camels than in healthy camels. During the initial period of infection, leukopenia has been detected in ruminants and is associated with augmented tissue requests and neutrophil margination (Hussein & Al-Mufarrej, 1999). The presence of other antigens in systemic infectious syndromes may lead to lymphopenia due to the lymph node confiscation of peripheral blood lymphocytes (Bhanuprakash *et al*., 2010; Du *et al*., 2020). Moreover, exposure of camels to Trypanosoma evansi infection, as evidenced by the detection of specific antibodies against the parasite, might have a role in suppressing animal immunity and hence be vulnerable to camelpox virus infection (OIE, 2021). However, our results partially agree with those of Narnaware *et al*. (2015), who reported that the blood and biochemical parameters in camel calves infected with para-poxvirus (camel contagious ecthyma) were not significantly affected.

In addition to the clinical signs and haematological changes induced by camelpox, it is critical to explore the histopathological changes in camel skin lesions to select a more appropriate treatment strategy. In the current study, marked hydropic and ballooning degeneration of the epidermal cell layer, with large aggregates of dead and living neutrophils, formed microabscesses in addition to large eosinophilic intracytoplasmic inclusion bodies in the degenerated cells of the stratum spinosum. Histopathological changes associated with campelpox infection have been previously described (Dahiya *et al*., 2017; Narnaware *et al*., 2018). Moreover, marked acanthosis, ballooning degeneration, and vacuolation of the prickle cell layer, in addition to homogenous eosinophilic inclusion bodies, were reported by Khalafalla *et al*. (1998), as indicated in our present investigation. Similarly, Narnaware *et al*. (2021) revealed marked epithelial hyperplasia in infected camel`s tongue with noticeable vacuolation and hydropic/ballooning degeneration with the presence of oval-shaped intracytoplasmic eosinophilic inclusion bodies in large numbers.

Very few records are available on the review of results related to molecular detection by PCR of camelpox viral DNA in camel species. PCR revealed the presence of genomic virus in all infected camels. Consistent with our data, many authors (Nagarajan *et al*., 2013; Khalafalla *et al*., 2015; Dahiya *et al*., 2017) have demonstrated that PCR amplification of camelpox viral DNA from blood samples is a rapid, sensitive, and specific assay for the early detection of camelpox infection. Moreover, the assay detected viral particles in an apparently healthy camel. Molecular identification of Camelpox virus DNA is reported in this study to provide more evidence for clinical, histological, and blood biochemical changes. This molecular diagnostic method should be applied, especially in dromedary racing camels. In this regard, we expect that this study will incetivate the use of molecular techniques for the diagnosis of viral or bacterial infections in dromedary-racing camels.

The detection of camelpox virus in dromedary-racing camels using molecular and histopathological techniques ensures early intervention by veterinarians for better treatment and prevention of disease occurrence. This could also help in selecting a suitable treatment and prevention strategy, and invite other researchers to develop new therapies for this disease.

Ethics statement

All procedures in this study were in accordance with the regulations of the Ethics Committee for Animal Use in Research, Sultan Qaboos University, Sultanate of Oman.

Conflict of interest

The authors declare no conflicts of interest regarding the publication of this manuscript.

Funding

Research support project (RSPD2023R690), King Saud University, Riyadh, Saudi Arabia.

REFERENCES

Alhaddad, H., Maraqa, T., Alabdulghafour, S., Alaskar, H., Alaqeely, R., Almathen, F., & Alhajeri, B. H. (2019). Quality and quantity of dromedary camel DNA sampled from whole-blood, saliva, and tail-hair. *PLoS One*, *14*(1), e0211743. https://doi.org/10.1371%2Fjournal.pone.0211743

Aregawi, W. G., & Feyissa, P. T. (2016). Diagnostic approaches towards camelpox disease. *Journal of Veterinary Science and Animal Husbandry*, *4*, 303. https://www.annexpublishers.com/articles/JVSAH/4303-Diagnostic-Approaches-towards-Camelpox-Disease.pdf

Balamurugan, V., Venkatesan, G., Bhanuprakash, V., & Singh, R. K. (2013). Camelpox, an emerging orthopox viral disease. *Indian Journal of Virology*, *24*(3), 295–305. https://doi.org/10.1007/s13337-013-0145-0

Bayisa, D. (2019). Review on Camel Pox: Epidemiology, Public Health and Diagnosis. *ARC Journal of Animal and Veterinary Sciences*, *5*(4), 22–33. http://dx.doi.org/10.20431/2455-2518.0504003

Bhanuprakash, V., Balamurugan, V., Hosamani, M., Venkatesan, G., Chauhan, B., Srinivasan, V. A., Chauhan, R. S., Pathak, K. M., & Singh, R. K. (2010a). Isolation and characterization of Indian isolates of camelpox virus. *Tropical Animal Health and Production*, *42*(6), 1271–1275. https://doi.org/10.1007/s11250-010-9560-z

Bhanuprakash, V., Prabhu, M., Venkatesan, G., Balamurugan, V., Hosamani, M., Pathak, K. M., & Singh, R. K. (2010b). Camelpox: epidemiology, diagnosis and control measures. *Expert Review of Anti-infective Therapy*, *8*(10), 1187–1201. https://doi.org/10.1586/eri.10.105

Dahiya, S. S., Kumar, S., Mehta, S. C., Singh, R., Nath, K., Narnaware, S. D., & Tuteja, F. C. (2017). Molecular characterization of Camelpox virus isolates from Bikaner, India: Evidence of its endemicity. *Acta Tropica*, *171*, 1–5. https://doi.org/10.1016/j.actatropica.2017.03.011

De, U. K., Chander, V., Akhilesh, Mahajan, S., Sharma, G. K., Nandi, S., Singh, K. P., & Gupta, V. K. (2020). Alterations of hemogram, serum biochemistry, oxidative/nitrosative balance, and copper/zinc homeostasis in dromedary camels naturally infected with poxvirus. *Tropical Animal Health and Production 52*, 2997–3003. https://doi.org/10.1007/s11250-020-02318-2

Fassi-Fehri, M. M. (1987). Les maladies des camélidés. *Revue scientifique et technique (International Office of Epizootics)*, *6*(2), 337-354. https://doi.org/10.20506/rst.6.2.305

Hussain, M. H., Saqib, M., Al-Maawali, M. G., Al-Makhladi, S., Al-Zadjali, M. S., Al-Sidairi, T., Asubaihi, S., Al-Rawahi, A., & Mansoor, M. K. (2015). Seroprevalence of Mycobacterium avium subspecies paratuberculosis (MAP) and evaluation of risk factors in camels of the Sultanate of Oman. *Tropical Animal Health and Production*, *47*(2), 383-389. https://doi.org/10.1007/s11250-014-0734-y

Hussein, M. F., & Al-Mufarrej, S. L. (1999). Some clinicopathological aspects of camelpox in Saudi Arabia. *Journal of King Saud University Agricultural Sciences*, *11*(2), 113–120 http://masder.kfnl.gov.sa/bitstream/123456789/12663/2/U01M05V11I02A05.pdf?locale=ar?locale=ar

Kachhawaha, S., Srivastava, M., Kachhawa, J. P., Tanwar, M., Sharma, A., Singh, N. K., Kachwaha, K., Rathore, S. S., & Tanwar, R. K. (2014). Therapeutic Management of Camel Pox - A Case report. *Advances in Animal and Veterinary Sciences*, *2*(4), 239–241. http://dx.doi.org/10.14737/journal.aavs/2014/2.4.239.241

Khalafalla, A. I., Al-Busada, K. A., & El-Sabagh, I. M. (2015). Multiplex PCR for rapid diagnosis and differentiation of pox and pox-like diseases in dromedary Camels. *Virology Journal 12*, 102. https://doi.org/10.1186/s12985-015-0329-x

Khalafalla, A. I., Mohamed, M. E. M., & Ali, B. H. (1998). Camel pox in the Sudan: Part 1. Isolation and identification of the causative virus. *Journal of Camel Practice and Research*, *5*(2), 229-233.

Kumar, S. M., Johnson, E. H., & Tageldin, M. H. (2012, January 29). *Most Common Medical Conditions of Camels in Oman as Observed by Veterinarians in Private Practice: A Practitioner Survey* [Paper presentation]. Proceedings of the Third Conference of the International Society of Camelid Research and Development, Oman.

Mohammadpour, R., Champour, M., Tuteja, F., & Mostafavi, E., (2020). Zoonotic implications of camel diseases in Iran. *Veterinary Medicine and Science*, *6*, 359–381. https://doi.org/10.1002%2Fvms3.239

Nagarajan, G., Swami, S. K., Dahiya, S. S., Sivakumar, G., Yadav, V. K., Tuteja, F. C., Narnaware, S. D., & Patil, N. V. (2013). Phylogenetic analysis of immunomodulatory protein genes of camelpoxvirus obtained from India. Comparative Immunology, *Microbiology & Infectious Diseases*, *36*(4), 415–424. https://doi.org/10.1016/j.cimid.2013.03.001

Narnaware, S. D., Ranjan, R., Dahiya, S. S., Panchbuddhe, A., Bajpai, D., Tuteja, F. C., & Sawal, R. K. (2021). Pathological and molecular investigations of systemic form of camelpox in naturally infected adult male dromedary camels in India. *Heliyon*, *7*(2), e06186. https://doi.org/10.1016/j.heliyon.2021.e06186

Narnaware, S. D., Nagarajan, G., & Dahiya, S. S. (2015). Hemato-biochemical studies in Indian camel (Camelus dromedarius) affected with contagious ecthyma. *Indian Journal of Veterinary Pathology*, *39*(2), 168-170. http://dx.doi.org/10.5958/0973-970X.2015.00038.3

Narnaware, S. D., Ranjan, R., & Dahiya, S. S. (2018). Clinicopathological investigations during an outbreak of camelpox in a dromedary camel herd in India. *Comparative Clinical Pathology*, *27*(6), 1497-1500. https://doi.org/10.1007/s00580-018-2763-9

OIE (2021). *Camelpox. In: Terrestrial Manual Online Access* [accessed 2022 May 19]. https://www.oie.int/fileadmin/Home/eng/Health_standards/tahm/3.05.01_CAMELPOX.pdf

SAS Institute Inc. (2012). *SAS/STAT Statistics user's guide. Statistical analytical system.* 5th ed. Cary, NC, USA. SAS Institute Inc.

Shommein, A. M., & Osman, A. M. (1987). Diseases of camels in the Sudan. *Revue scientifique et technique (International Office of Epizootics)*, *6*(2), 481–486. https://doi.org/10.20506/rst.6.2.298

Suvarna, S. K., Layton, C., & Bancroft, J. D. (2018). *Bancroft's Theory and Practice of Histological Techniques.* (8th ed.) Churchill Livingstone. Elsevier, England.

Wernery, U., & Kaaden, O. R. (2002). *Infectious diseases in camelids*. (2nd, rev. and enl. ed.) Berlin: Blackwell-Wiss.-Verl.

Wernery, U., Meyer, H., & Pfeffer, M. (1997). Camel pox in the United Arab Emirates and its prevention. *Journal of Camel Practice and Research*, *4*, 135–139.

Wernery, U., & Zachariah, R. (1999). Experimental camelpox infection in vaccinated and unvaccinated dromedaries. *Journal of Veterinary Medicine, Series B*, *46*(2), 131-135. https://doi.org/10.1111/j.0931-1793.1999.00250.x

Austral Journal of Veterinary Science

Austral J Vet Sci 55, 182-188 (2023)
https://doi.org/10.4206/ajvs.553.04

ORIGINAL ARTICLE

Investigating mutations in the genes *GDF9* and *BMP15* in Pelibuey sheep through the amplification-refractory mutation system with tetra-primers

Canuto Muñoz-García[1], Obdulia L. Segura-León[2], Julio C. Gómez-Vargas[1], Juan González-Maldonado[3], Juan A. Quintero-Elisea[4], Juan F. Martínez-Montoya[5] and César Cortez-Romero[5,6*]

[1] Facultad de Medicina Veterinaria y Zootecnia, Universidad Autónoma de Guerrero, Altamirano, Guerrero, México.

[2] Colegio de Postgraduados, Entomología y Acarología, Campus Montecillo, Montecillo, Texcoco, Estado de México, México.

[3] Instituto de Ciencias Agrícolas, Universidad Autónoma de Baja California, Mexicali, México.

[4] Departamento de Ciencias Veterinarias, Instituto de Ciencias Biomédicas, Universidad Autónoma de Ciudad Juárez, Chihuahua, México.

[5] Colegio de Postgraduados, Innovación en Manejo de Recursos Naturales, Campus San Luis Potosí. San Luis Potosí, México.

[6] Colegio de Postgraduados, Recursos Genéticos y Productividad-Ganadería, Campus Montecillo, Montecillo, Texcoco, Estado de México, México.

Article History
Received: 14.03.2023
Accepted: 04.07.2023
Published: 22.09.2023

Corresponding author
* César Cortez-Romero
ccortez@colpos.mx

ABSTRACT. Single Nucleotide Polymorphisms (SNP) or mutations are variations with a broad distribution in the genome and, as part of genetic studies, SNP allow the identification of allelic variants related to characteristics of economic importance in sheep production. However, the identification of SNP and their genotypes through sequencing is expensive, as it requires specialized materials and equipment. The objective of this study was to identify polymorphisms and their genotypes in the growth differentiation factor 9 (*GDF9*) and bone morphogenetic protein 15 (*BMP15*) genes in Pelibuey sheep using the tetra-primer amplification-refractory mutation system through polymerase chain reaction (T-ARMS-PCR). DNA extraction and amplification of *BMP15* and *GDF9* were conducted from blood samples contained in Whatman™ FTA™ cards from 60 multiparous Pelibuey ewes with reproductive records. The T-ARMS-PCR methodology allowed the identification of wild-type genotypes and mutated homozygous genotypes in polymorphisms *G4* and *G6* of *GDF9*, whereas mutations in the *BMP15* gene were not found. These results were confirmed by sequencing. In conclusion, the T-ARMS-PCR methodology allowed the identification of mutated and wild-type genotypes in SNP *G4* and *G6* of *GDF9*, although no mutations were found in *BMP15* in Pelibuey sheep. This technique was found to be reliable, rapid, and easily applied to identify polymorphic genotypes.

Keywords: gene, mutation, T-ARMS-PCR, genotyping, sequencing.

INTRODUCTION

Many studies have reported that the ovulation rate and litter size in sheep are regulated by genes that affect ovarian function. These are known as fertility genes (Davis, 2005; Fabre *et al*., 2006) and include the bone morphogenetic protein receptor (*BMPR-IB*), bone morphogenetic protein 15 (*BMP15*), and growth differentiation factor 9 (*GDF9*), which are intra-ovarian regulators of folliculogenesis (Ahlawat *et al*., 2014; Aboelhassan *et al*., 2021) expressed in follicle oocytes during development (Hanrahan *et al*., 2004; Strauss III & Williams, 2019). The *BMP15*, *BMPR-IB*, and *GDF9* genes belong to a large family of transforming growth factor β (TGFβ) and, with their mutations or Single Nucleotide Polymorphisms (SNP), heterozygous sheep generally increase their ovulation rate and prolificacy, whereas homozygous sheep present infertility and primary failures in folliculogenesis (Hanrahan *et al*., 2004; Nicol *et al*., 2009; Gootwine, 2020).

In *BMP15*, the mutations found in the gene coding region are *FecX*^{I} (Inverdale), *FecX*^{H} (Hanna) (Galloway *et al*., 2000), *FecX*^{B} (Belclare), *FecX*^{G} (Galway) (Hanrahan *et al*., 2004), *FecX*^{L} (Lacaune) (Bodin *et al*., 2007), *FecX*^{R} (Roa) (Martínez-Royo *et al*., 2008), *FecX*^{Gr} (Grivette), *FecX*^{O} (Olkuska) (Demars *et al*., 2013), and *FecX*^{Bar} (Tunisian Bárbara) (Lassoued *et al*., 2017). In most of these mutations, there was an average increase of 0.6 offspring per ewe compared to the wild genotype (Galloway *et al*., 2000; Hanrahan *et al*., 2004; Fabre *et al*., 2006; Bodin *et al*., 2007; Martinez-Royo *et al*., 2008). In contrast, 11 specific mutations have been reported in the gene *GDF9* in the coding region, but not all of these affect ovarian function (G2 and G3) (Hanrahan *et al*., 2004), and only nine affect ovulation rate and litter size: *FecG*^{H} (high fertility or *G8*) (Hanrahan *et al*., 2004), *FecG*^{T} (Thoka) (Nicol *et al*., 2009), *FecG*^{E} (Embrapa) (Silva *et al*., 2010), *FecG*^{1} (Baluchi or G1) (Moradband *et al*., 2011), *FecG*^{V} (Vecaria) (Souza *et al*., 2014), *FecG*^{F} (Finnish or G7) in white Norwegian sheep (Våge *et al*., 2013), *FecG*^{A} (Araucana or G5, *G6*) (Bravo *et al*., 2016), and *G4* (Dash *et al*., 2017).

Polymorphism is the main source of variation in the DNA of an organism and can be used as a molecular marker to identify allelic variants associated with economically important characteristics (Niciura *et al*., 2018). In the recognition of these allelic variants, some methodologies have been used to identify SNP and their genotypes in ewes. These methods

include DNA sequencing, restriction fragment length polymorphism through Polymerase Chain Reaction (PCR-RFLP), single-strand conformation polymorphism (SSCP), hybridization with TaqMan fluorescence probes, and DNA Microarrays, among others (Ahlawat *et al*., 2014; Niciura *et al*., 2018). The disadvantage of these methodologies is the high cost of reagents as well as the requirement for specialized materials and equipment for sample processing (Niciura *et al*., 2018). In this context, Newton *et al*. (1989) developed an Amplification-Refractory Mutation System (ARMS-PCR). This, together with the tetra-primer procedure (Ye *et al*., 2001), was found to be an economical, reliable, and easy-to-use methodology for identifying mutations in genotypes (Nicol *et al*., 2009; Polley *et al*., 2010).

In the Tetra-primer Amplification Refractory Mutation System through Polymerase Chain Reaction (T-ARMS-PCR), a fragment of the gene of interest and each internal primer are combined with an opposing external primer in a single reaction to amplify the wild-type, mutated, and control fragment forms in a single PCR reaction (Polley *et al*., 2010). Thus, the objective of this study was to identify polymorphisms in *GDF9* and *BMP15* in Pelibuey ewes by using T-ARMS-PCR.

MATERIALS AND METHODS

Collection and conservation of samples

Sterile syringes were used to collect three mL of blood from the jugular veins of sixty multiparous ewes of the Pelibuey breed, from the agriculture and livestock production unit "El Gargaleote", property of Universidad Autónoma Chapingo; under the criteria of the Mexican Official Norm (*Norma Oficial Mexicana*, NOM-062-ZOO-1999) [SAGARPA, 2001] on technical specifications for the production, care, and use of laboratory animals, and following the regulations for the use and care of research animals, as approved by the General Academic Council of Colegio de Postgraduados, Mexico (COLPOS, 2016). From the collected blood, a 0.5 mL subsample was placed in a Whatman™ FTA™ mini card (WB 120055, GE Healthcare©, United Kingdom). The cards were dried in the shade according to the manufacturer´s instructions (GE Healthcare©, United Kingdom) until subsequent processing. The laboratory phase was conducted in the facilities of the Molecular Biology Laboratory of common use in the Postgraduate Program in Plant Health, at Campus Montecillo, Colegio de Postgraduados, Texcoco, State of Mexico.

Sample processing

For DNA extraction, sections of approximately one mm^2 were cut from the Whatman FTA mini card impregnated with blood and deposited in an Eppendorf tube of 0.2 mL. They were then washed three times with 200 µL of FTA purification reagent (GE Healthcare©, United Kingdom) at room temperature, for seven minutes each, and the purification reagent was discarded after each wash. Two further washes were then carried out with 200 µL of Tris (hydroxymethyl aminomethane)-EDTA (ethylenediaminetetraacetic acid) buffer or TE (10 mM Tris, 0.1 mM EDTA, pH 8.0) at room temperature for seven min, and the TE buffer was discarded after each wash, according to the manufacturer's instructions and the methodology followed by Muñoz-García *et al*. (2021). On average, the ratio of the absorbance of DNA at 260 and 280 nm was 1.8 with a concentration of 452.98 ng μL^{-1}.

Polymorphisms and genotypes in the *BMP15* and *GDF9* genes by T-ARMS-PCR

This study used the T-ARMS-PCR methodology described by Ye *et al*. (2001) for the detection of polymorphisms and their genotypes in the *BMP15* and *GDF9* genes of Pelibuey sheep. Fragments of these genes were amplified by PCR, using the sequences listed in Table 1, as reported by Polley *et al*. (2010). The reaction mixture for the T-ARMS-PCR of the genes was produced separately; each reaction mixture had a final volume of 13.75 µL, containing 6.25 µL of GoTaq® Colorless Master Mix 2X (Promega© Madison, WI, USA), 0.625 µL of each primer (two Forward and two Reverse; IDT®, Illinois, USA) at a concentration of 10 µM and five µL of trehalose dihydrate at 10% (Merck© KGaA 64271, Darmstadt, Germany). The tubes containing the reaction mixture and fragment of the processed FTA mini card were introduced into a Biometra® thermal cycler.

The amplification conditions programmed for each allele (wild-type and mutated) are detailed below. For exon 2 of the gene *GDF9*: initial denaturation was performed at 93 °C for three min; 35 cycles of denaturation at 93 °C for 40 s; alignment, Table 1, 40 s; extension, 72 °C, 40 s; and a final extension at 72 °C for five min. For exon 2 of *BMP15*, initial denaturation was performed at 95 °C for five min; 35 cycles of denaturation at 95 °C for 40 s; alignment, Table 1, 40 s; extension, 72 °C, 30 s; and a final extension at 72 °C for four min. The amplicons of the *GDF9* and *BMP15* genes were separated by gel electrophoresis on a 2.5% agarose gel in Tris-borate-EDTA or TBE running buffer at 1% (IBI Scientific, Dubuque, Iowa, USA) at 80 volts for 80 min in each case. A 100-1000 bp molecular marker was used (Promega©, Madison, Wisconsin, USA). The gel was stained with Gel Red® (Biotium, Hayward, California, USA), which was then added to the agarose gel. Three µL of amplicon was placed in each well, plus three µL of Green GoTaq® Flexi buffer (Promega©, Madison, Wisconsin, USA) was added. The gel was visualized in a Quantum® photo-documenter using the Vision Capt ® software.

Polymorphisms and genotypes in the *GDF9* and *BMP15* genes by PCR and sequencing

To confirm the mutations and genotypes found in the *BMP15* and *GDF9* genes using the T-ARMS-PCR technique, amplification of exon 2 of *GDF9* and *BMP15* was conducted through a final point PCR for subsequent sequencing. The reaction contained GoTaq® Colorless Master Mix

Table 1. Sequences used to amplify and identify the polymorphisms and genotypes of genes *GDF9* and *BMP15* in Pelibuey ewes using the T-ARMS-PCR methodology.

Gene	Mutation	Primer	Sequence 5´→3´	Product size (bp)
GDF9	*G4*	IF(G)	296 TTCACATGTCTGTAAATTTTACATGTGAGG 325	M= 212, W= 261, C= 417, TA= 50 °C"
		IR(A)	350 GCTGAAGATGCTGCAGCTGGTCGTT 325	
		OF	90 CAACAACTCCATTTCTTTTCCCTTTCCTG 118	
		OR	506 TAGGCAGATAGCCCTCTC TTCTGGTCAG 479	
	G6	IF(A)	573 CAGCTCTGAATTGAAGAAGCCTCGGA 598	M= 193, W= 223, C= 362, TA= 52 °C"
		IR(G)	625 ATTCACTCAGATTGACTGAAGCTGGCAC 598	
		OF	403 TATCTGAACGACACAAGTGCTCAGGCTT 430	
		OR	764 CTGGGACAGTCCCCTTTACAGTATCGAG 737	
	G8	IF(T)	763 AGGGCGGTCGGACATCGGTATGGATT 788	M= 146, W= 108, C= 198, TA= 55 °C"
		IR(C)	817 TGATGTTCTGCACCATGGTGTGAACCGTAG 788	
		OF	710 GGATTGTGGCCCCACACAAATACAACCC 737	
		OR	907 CATCAGGCTCGATGGCCAAAACACTCAA 880	
BMP15	*Fec X^{G}*	IF (C)	363 CTTCTTGTTACTGTATTTCAATGACAATC 391	M= 112, W= 102, C= 158, TA= 48 °C"
		IR (T)	417 GAGAGGTTTGGTCTTCTGAACACTATA 391	
		OF	306 AAGAGGTAGTGAGGTTCTTGAGTTCT 331	
		OR	463 AGAGAAGAGAAGGGTCTTTTTCTGTA 438	
	Fec X^{L}	IF (A)	606 TGCTCCCCATCTCTATACCCCAAACTAATA 635	M= 204, W= 252, C= 398, TA= 52 °C"
		IR (G)	662 TGTAGTACCCGAGGACATACTCCCTGAC 635	
		OF	411 ACCTCTCCCTAAAGGCCTGAAAGAGTTT 438	
		OR	808 ACAAGATACTCCCATTTGCCTCAATCAG 781	

[Nucleotide specificity is indicated in parentheses. F= forward, R= Reverse, O= external (common), I= internal (specific allele), M= mutant, W= wild, C= control fragment and TA= temperature of alignment (Polley *et al*., 2010)].

2X (Promega© Madison, Wisconsin, USA), each primer (*BMP15*, exon 1: For-5'-AATCCTTCTTTGGGGACTGG-3' and Rev-5'-AGCCCTAAAGGGAAGCAAAT-3', and exon 2: For-5'- CCAGAAAAGCCCAACCAATC-3' and Rev-5'-AGTGTAGTACCCGAGGACAT-3', AH009593.2, (Galloway *et al*., 2000); *GDF9*; exon 2: For-5'-GGAGAAAAGGGACAGAAGC-3' and Rev- 5'-ACGACAGGTACACTTAGT-3', (Silva *et al*., 2010); 10 µM; IDT®, Illinois, USA), and trehalose dihydrate at 10% (Merck© KGaA 64271, Darmstadt, Germany). The tubes containing the fragments of the processed card and reaction mixture were placed in a Biometra® thermal cycler. The amplification conditions were as follows: *BMP15* (exon 1): initial denaturation at 95 °C for five min; 35 cycles of denaturation at 95 °C for 30 s, alignment at 54 °C for 40 s, and extension at 72 °C for 30 s; and a final extension at 72 °C for five min; (exon 2): initial denaturation at 94 °C for five min; 35 cycles of denaturation at 94 °C for 30 s, alignment at 54.8 °C for 40 s, and extension at 72 °C for 30 s; and a final extension at 72 °C for four min. *GDF9* (exon 2): initial denaturation at 93 °C for three min; 35 cycles of denaturation at 93 °C for 40 s, alignment at 56 °C for 40 s, and extension at 72 °C for 40 s; and a final extension at 72 °C for five min. The amplicons were separated by electrophoresis on a 1% agarose gel in Tris-borate-EDTA running buffer at 1% (TBE; IBI Scientific, Dubuque, Iowa, USA) at 80 volts for 40 min. A molecular marker of 250-10000 bp was used (Promega©, Madison, Wisconsin, USA). The gel was stained with Gel Red® (Bio-

tium, Hayward, California, USA), which was then added to the agarose gel. Three µL of the amplicon plus three µL of Green GoTaq® Flexi buffer (Promega©, Madison, Wisconsin, USA) were added to each well. The gel was visualized using a Quantum® photo-documenter with the Vision Capt® software. Finally, once the appearance of the genes in the agarose gel was confirmed, the amplicons obtained (10 µL) were sent to MACROGEN© (Seoul, South Korea) for cleaning and sequencing. The primers were the same as those used for the amplification of each gene.

Bioinformatic analysis of sequences

The quality of the sequences was analyzed using the software Sequencher® version 5.4.6 (Gene Codes Corporation, Ann Arbor, MI, USA, http://www.genecodes.com). From the sequences of each gene, a search was performed using Nucleotide BLAST of the National Center for Biotechnology Information, and those that presented the greatest similarity with those of this study were selected: for the *BMP15* gene, AH009593.2 and KT238844.1, whereas for *GDF9*, AF078545.2, and HE866499.1. From the sequences of each exon, together with the reference sequences, alignment was conducted to determine the degree of similarity and to detect mutations with their genotypes, using the MUSCLE® algorithm (Edgar, 2004) in MEGA 7® (Molecular Evolutionary Genetics Analysis, Kumar *et al*., 2016).

RESULTS AND DISCUSSION

Polymorphisms and genotypes in the *GDF9* and *BMP15* genes revealed by T-ARMS-PCR

In this study, the T-ARMS-PCR methodology allowed the identification of two specific mutations known in exon 2 of the gene *GDF9*, since fragments of 261 bp (in five out of 60 sheep) and 212 bp (in 57 out of 60 sheep) were identified for the polymorphism *G4*, and 223 bp (in 30 out of 60 sheep) and 193 bp (in 30 out of 60 sheep) for *G6*, respectively (Figure 1). In addition, none of the sheep presented a heterozygous genotype for these two variants. Polymorphism *G8* was not detected in the present study. On the other hand, in gene *BMP15*, only the wild forms of *FecX*^{G} and *FecX*^{L} polymorphisms were detected when amplifying fragments of 102 and 252 bp, respectively (Figure 1).

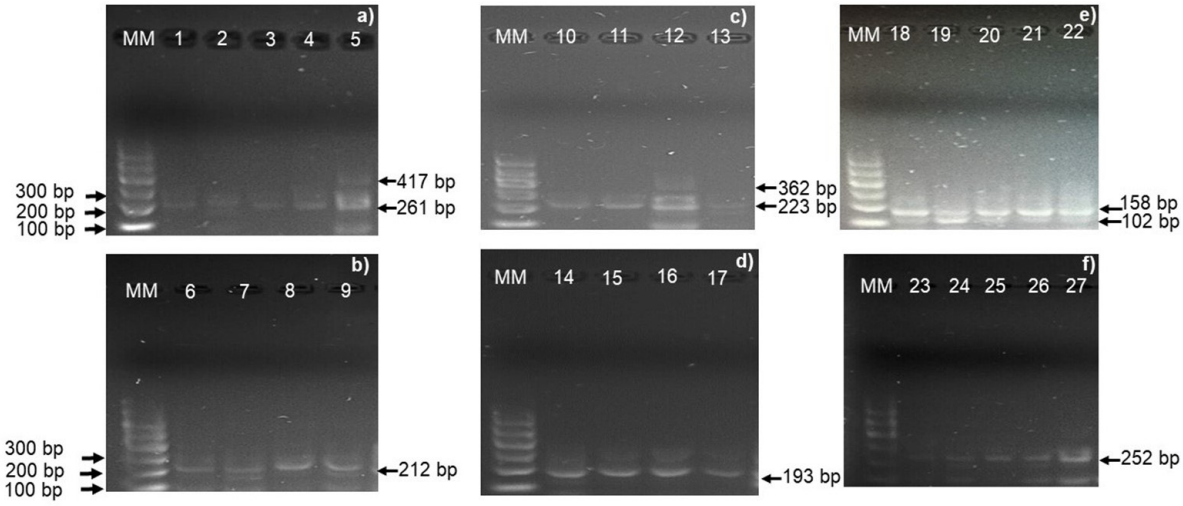

Figure 1. Polymorphisms and genotypes in the genes *GDF9* and *BMP15* identified by T-ARMS-PCR in Pelibuey ewes (MM= molecular marker). Polymorphism G4 with the genotypes a) wild (lanes 1 to 5: ewes with a fragment of 261 bp and control 417 bp) and b) mutated (lanes 6 to 9: ewes with a fragment of 212 bp). Polymorphism G6 with the genotypes c) wild (lanes 10 to 13: ewes with a fragment of 223 bp and control 362 bp) and d) mutated (lanes 14 to 17: ewes with a fragment of 193 bp). Polymorphism *FecX*^{G} in the wild form e) (lanes 18 to 22: ewes with a fragment of 102 bp, control 158 bp), and *FecX*^{L} in the wild form f) (lanes 23 to 27: ewes with a fragment of 252 bp).

Polymorphisms and genotypes in the *GDF9* and *BMP15* genes identified by sequencing

The sequences in this study had a similarity of 99.32 - 99.77% for *BMP15* and 99.67 - 99.45% for *GDF9*, with the sequences AH009593.2 and KT238844.1 for *BMP15*, and AF078545.2, and HE866499.1 for *GDF9*, respectively. Alignment of the sequences of gene *BMP15* from this study with those of the reference (AH009593.2, KT238844.1) did not reveal any change or mutation. The sequences from this study aligned with those of the reference (AF078545.2, HE866499.1) allowed the identification of SNP *G4* and *G6* in exon 2 of *GDF9*. In *G4*, guanine was substituted with adenine at position 721 (721 G→A) while, in *G6*, guanine was replaced with adenine at position 994 (994 G→A) (Figure

2). Likewise, this analysis confirmed the identification of wild-type and mutated genotypes in Pelibuey ewes. It is important to mention that ewes were not found to have the heterozygous genotype in polymorphisms *G4* and *G6* (Figure 2), nor was the mutation *G8* found using this methodology.

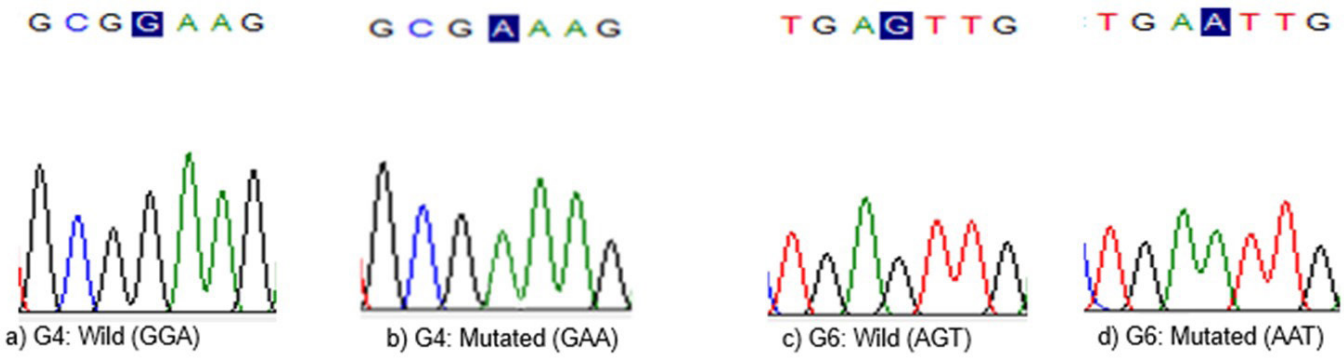

Figure 2. Electropherograms of SNP *G4* and *G6* obtained by sequencing exon 2 of the *GDF9* gene in Pelibuey ewes. Polymorphisms *G4* with a) wild and b) mutated genotypes, and *G6* with c) wild and d) mutated genotypes.

In polymorphism *G4*, mutant and wild alleles were detected with allelic frequencies of 0.08 and 0.92 while, in *G6*, wild and mutant alleles with allelic frequencies of 0.5, and 0.5, respectively, were detected.

SNP are changes or mutations in a nitrogenous base in the DNA sequence that can be used as molecular markers (Ahlawat *et al*., 2014). Currently, SNP are used to identify allelic variants and their genotypes (Ahlawat *et al*., 2014; Niciura *et al*., 2018). In this study, T-ARMS-PCR allowed the identification of polymorphism *G4*, and in the genotyping of the SNP, 5% of the sheep presented the mutant genotype and 95% of the wild-type genotype. Likewise, polymorphism *G6* was found in the genotype of the SNP, where 50% of the ewes had the wild-type genotype and the other 50% had the mutated or carrier genotype. The results obtained using the T-ARMS-PCR methodology in this study are in agreement with those reported by Polley *et al*. (2010), Roy *et al*. (2011), Dash *et al*. (2017), and Aboelhassan *et al*. (2021). The results of this study suggest that Pelibuey ewe is polymorphic in the specific *G4* and *G6* mutations of *GDF9*. It is important to mention that the polymorphism *G8* was not found in sheep in this study, and the absence of this allelic variant suggests that it was not present in ewes.

On the other hand, polymorphisms were not found in the gene *BMP15* using the T-ARMS-PCR methodology; only the wild variants of the SNP *FecX*^{G} and *FecX*^{L} were amplified in Pelibuey ewes. The results of this study support those reported by Polley *et al*. (2010) for Garole sheep, Roy *et al*. (2011) for Bonpala sheep, and Aboelhassan *et al*. (2021) for five Egyptian sheep breeds. However, they differ from those reported by Argüello-Hernández *et al*. (2014), who used the same methodology in sheep of Pelibuey breed. The lack of mutations in the gene *BMP15* in sheep in this study was perhaps because this gene is monomorphic and the wild allele is probably the one that predominates in these sheep (Salazar-Montes *et al*., 2013).

Sequence analysis of *GDF9* and *BMP15* showed an average 99.5% similarity with the sheep sequences reported in NCBI GenBank, suggesting that the sequences obtained in this study are broadly equal to those of other sheep. When comparing the sequences from exon 2 of *GDF9* obtained in this study with the reference sequences (accession AF078545.2 and HE866499.1), polymorphisms *G4* and *G6* were found. In the genotyping of these SNP, only the wild-type and mutated (homozygous) forms were found for each variant. In this study, the *G4* and *G6* polymorphisms identified through sequencing agreed with those reported in sheep of the Belclare, Cambridge, Mehraban (Hanrahan *et al*., 2004; Ahmadi *et al*., 2016), and Barki, Osseimi, Rahmani, Saudanez, and Awassi (Aboelhassan *et al*., 2021) breeds. Mutations were not found in the two codifying regions of *BMP15* (exons 1 and 2), according to the sequence analysis of this study compared to those of the reference (accession AH009593.2 and KT238844.1).

It should be noted that in both the T-ARMS-PCR methodology and sequencing, sheep were not found to have the heterozygous genotype in *GDF9*. The absence of heterosis in polymorphisms *G4* and *G6* in Pelibuey sheep indicates low genetic variation, which could be due to the Wahlund effect, which refers to a sub-population structure, mixture of populations, or possible endogamy, or may also be due to reduced flock (Kumar *et al*., 2007). The results obtained by the T-ARMS-PCR methodology in the search for and genotyping of polymorphisms were confirmed and validated with the results of sequencing DNA samples obtained from the same ewes of the Pelibuey breed. The results obtained by T-ARMS-PCR did not differ from those obtained by sequencing *BMP15* and *GDF9*. Finally, T-ARMS-PCR is a simple, fast, and easy methodology used to search

for SNP and genotypes in sheep, according to Polley *et al*. (2010), Niciura *et al*. (2018), and Aboelhassan *et al*. (2021). T-ARMS-PCR methodology and sequencing both allowed the identification of SNP and grouping of ewes of the Pelibuey breed according to their genotype.

CONCLUSION

The T-ARMS-PCR methodology allowed the identification of polymorphisms *G4* and *G6* and their wild-type and mutated genotypes in *GDF9*; however, sheep with the heterozygous genotype were not found, and no polymorphisms were found in the gene *BMP15*. This methodology was found to be rapid, reliable, and easy to apply for identifying SNP of interest.

Conflicts of interest

The authors declare that they have no conflicts of interest.

Acknowledgements

The authors thank the Mexican National Council for Science and Technology for funding the PhD studies of the first author, Universidad Autónoma Chapingo for the support provided in the use of the sheep, and Colegio de Postgraduados for financing this research. The authors also wish to thank the Lines of Generation and/or Application of Knowledge: Sustainable Management of Natural Resources (Campus SLP) and Efficient Livestock, Sustainable Well-being, and Climate Change (Campus Montecillo) of Colegio de Postgraduados.

REFERENCES

Aboelhassan, D. M., Darwish, A. M., Ali, N. I., Ghaly, I. S., & Farag, I. M. (2021). A study on mutation points of *GDF9* gene and their association with prolificacy in Egyptian small ruminants. *Journal of Genetic Engineering and Biotechnology*, *19*, Article 85. https://doi.org/10.1186/s43141-021-00181-8

Ahlawat, S., Sharma, R., Maitra, A., Roy, M., & Tantia, M. S. (2014). Designing, optimization and validation of tetra-primer ARMS PCR protocol for genotyping mutations in caprine Fec genes. *Meta Gene*, *2*, 439–449. https://doi.org/10.1016/j.mgene.2014.05.004

Ahmadi, A., Afraz, F., Talebi, R., Farahavar, A., & Vahidi, S. M. F. (2016). Investigation of *GDF9* and *BMP15* polymorphisms in Mehraban sheep to find the missenses as impact on protein. *Iranian Journal of Applied Animal Science*, *6*(4), 863–872. Retrieved from http://ijas.iaurasht.ac.ir/article_526632.html

Argüello-Hernández, H. J., Cortez-Romero, C., Rojas-Martínez, R. I., Segura-León, O. L., Herrera-Haro, J. G., Salazar-Ortiz, J., & Gallegos-Sanchez, J. (2014). Polimorfismos de la proteína 15 morfogénica ósea (*BMP15*) y su relación con el tipo de parto en la oveja Pelibuey. *Agrociencia*, *48*(1), 53–69. Retrieved from http://www.scielo.org.mx/scielo.php?script=sci_arttext&pid=S1405-31952014000100004

Bodin, L., Di Pasquale, E., Fabre, S., Bontoux, M., Monget, P., Persani, L., & Mulsant, P. (2007). A novel mutation in the bone morphogenetic protein 15 gene causing defective protein secretion is associated with both increased ovulation rate and sterility in Lacaune sheep. *Endocrinology*, *148*(1), 393–400. https://doi.org/10.1210/en.2006-0764

Bravo, S., Larama, G., Paz, E., Inostroza, K., Montaldo, H. H., & Sepúlveda, N. (2016). Polymorphism of the *GDF9* gene associated with litter size in Araucana creole sheep. *Animal Genetics*, *47*(3), 390–391.

COLPOS. (2016). Reglamento para el uso y cuidado de animales destinados a la investigación en el Colegio de Postgraduados. In *Reglamento para el uso y cuidado de animales en experimentación* (pp. 1–16).

Dash, S., Maity, A., Bisoi, P. C., Palai, T. K., Polley, S., Mukherjee, A., & De, S. (2017). Coexistence of polymorphism in fecundity genes BMPR 1B and *GDF9* of Indian Kendrapada sheep. *Exploratory Animal and Medical Research*, *7*(1), 33–38. Retrieved from http://www.animalmedicalresearch.org/

Davis, G. H. (2005). Major genes affecting ovulation rate in sheep. *Genetics Selection Evolution*, *37*, S11. https://doi.org/10.1186/1297-9686-37-S1-S11

Demars, J., Fabre, S., Sarry, J., Rossetti, R., Gilbert, H., Persani, L., Tosser-Klopp, G., Mulsant, P., Novak, Z., Drobik, W., Martyniuk, E., & Bodin, L. (2013). Genome-wide association studies identify two novel *BMP15* mutations responsible for an atypical hyperprolificacy phenotype in sheep. *PLoS Genetics*, *9*(4), e1003482. https://doi.org/10.1371/journal.pgen.1003482

Edgar, R. C. (2004). MUSCLE: Multiple sequence alignment with high accuracy and high throughput. *Nucleic Acids Research*, *32*(5), 1792–1797. https://doi.org/10.1093/nar/gkh340

Fabre, S., Pierre, A., Mulsant, P., Bodin, L., Di Pasquale, E., Persani, L., Monget, P., & Monniaux, D. (2006). Regulation of ovulation rate in mammals: contribution of sheep genetic models. *Reproductive Biology and Endocrinology*, *4*, 20. https://doi.org/10.1186/1477-7827-4-20

Galloway, S. M., McNatty, K. P., Cambridge, L. M., Laitinen, M. P. E., Juengel, J. L., Jokiranta, T. S., McLaren, R. J., Luiro, K., Dodds, K. G., Montgomery, G. W., Beattie, A. E., Davis, G. H., & Ritvos, O. (2000). Mutations in an oocyte-derived growth factor gene (*BMP15*) cause increased ovulation rate and infertility in a dosage-sensitive manner. *Nature Genetics*, *25*(3), 279–283. https://doi.org/10.1038/77033

Gootwine, E. (2020). Invited review : Opportunities for genetic improvement toward higher prolificacy in sheep. *Small Ruminant Research*, *186*, 106090. https://doi.org/10.1016/j.smallrumres.2020.106090

Hanrahan, J. P., Gregan, S. M., Mulsant, P., Mullen, M., Davis, G. H., Powell, R., & Galloway, S. M. (2004). Mutations in the genes for oocyte-derived growth factors *GDF9* and *BMP15* are associated with both increased ovulation rate and sterility in Cambridge and Belclare sheep (Ovis aries). *Biology of Reproduction*, *70*(4), 900–909. https://doi.org/10.1095/biolreprod.103.023093

Kumar, D., Sharma, R., Pandey, K. A., Gour, S. D., Malik, G., Ahlawat, S. P. S., & Jain, A. (2007). Genetic diversity and bottleneck analysis of Indian bellary sheep by microsatellite markers. *Russian Journal of Genetics*, *43*(9), 996–1005. https://doi.org/10.1134/S1022795407090050

Kumar, S., Stecher, G., & Tamura, K. (2016). MEGA7: Molecular Evolutionary Genetics Analysis Version 7.0 for Bigger Datasets. *Molecular Biology and Evolution*, *33*(1), 1870–1874. https://doi.org/10.1093/molbev/msw054

Lassoued, N., Benkhlil, Z., Woloszyn, F., Rejeb, A., Aouina, M., Rekik, M., Fabre, S., & Bedhiaf-Romdhani, S. (2017). FecXBar a novel *BMP15* mutation responsible for prolificacy and female sterility in Tunisian Barbarine sheep. *BMC Genetics*, *18*(1), 1–10. https://doi.org/10.1186/s12863-017-0510-x

Martinez-Royo, A., Jurado, J. J., Smulders, J. P., Martí, J. I., Alabart, J. L., Roche, A., Fantova, E., Bodin, L., Mulsant, P., Serrano, M., Folch, J., & Calvo, J. H. (2008). A deletion in the bone morphogenetic protein 15 gene causes sterility and increased prolificacy in Rasa Aragonesa sheep. *Animal Genetics*, *39*(3), 294–297. https://doi.org/10.1111/j.1365-2052.2008.01707.x

Moradband, F., Rahimi, G., & Gholizadeh, M. (2011). Association of polymorphisms in fecundity genes of *GDF9*, *BMP15* and *BMP15*-1B with litter size in iranian Baluchi sheep. *Asian-Australasian Journal of Animal Sciences*, *24*(9), 1179–1183. https://doi.org/10.5713/ajas.2011.10453

Muñoz-García, C., Vaquera-Huerta, H., Gallegos-Sánchez, J., Becerril-Pérez, C. M., Tarango-Arámbula, L. A., Bravo-Vinaja, Á., & Cortez-Romero, C. (2021). Influence of *FecG*^{E} mutation on the reproductive variables of Pelibuey ewes in the anestrus period. *Tropical Animal Health and Production*, *53*(2), 4–10. https://doi.org/10.1007/s11250-021-02755-7

Newton, C. R., Graham, A., Heptinstall, L. E., Powell, S. J., Summers, C., Kalsheker, N., Smith, J. C., Markham, A. F. (1989). Analysis of any point mutation in DNA. The amplification refractory mutation system (ARMS). *Nucleic Acids Research*, *17*(7), 2503–2516. https://doi.org/10.1093/nar/17.7.2503

Niciura, S. C. M., Cruvinel, G. G., Moraes, C. V., Bressani, F. A., Malago, J. W., Vieira, B. M., & de Chagas, A. C. S. (2018). PCR-based genotyping of SNP markers in sheep. *Molecular Biology Reports*, *45*(4), 651–656. https://doi.org/10.1007/s11033-018-4206-8

Nicol, L., Bishop, C. S., Pong-Wong, R., Bendixen, C., Holm, L.-E., Rhind, M. S., & McNeilly, S. A. (2009). Homozygosity for a single base-pair mutation in the oocyte- specific *GDF9* gene results in sterility in Thoka sheep. *Reproduction*, *138*(6), 921–933. https://doi.org/10.1530/REP-09-0193

Polley, S., De, S., Brahma, B., Mukherjee, A., Vinesh, P., Batabyal, S., Sing Arora, J., Pan, S., Kumar Samanta, A., Kumar Datta, T., & Goswami, S. L. (2010). Polymorphism of BMPR1B, *BMP15* and *GDF9* fecundity genes in prolific Garole sheep. *Tropical Animal Health and Production*, *42*(5), 985–993. https://doi.org/10.1007/s11250-009-9518-1

Roy, J., Polley, S., De, S., Mukherjee, A., Batabyal, S., Pan, S., Brahma, B., Kumar Datta, T., Goswami, S. L. (2011). Polymorphism of fecundity genes (FecB, FecX, and *FecG*) in the Indian Bonpala sheep. *Animal Biotechnology*, *22*(3), 151–162. https://doi.org/10.1080/10495398.2011.589239

SAGARPA (Secretaría de Agricultura, Ganadería, Desarrollo Rural, Pesca, y Alimentación) (2001). Norma oficial Mexicana NOM-062-ZOO-1999, Especificaciones técnicas para la producción, cuidado y uso de los animales de laboratorio. *Diario Oficial de La Federación*, *22 Agosto*, 107–165. Retrieved from https://www.gob.mx/cms/uploads/attachment/file/203498/NOM-062-ZOO-1999_220801.pdf

Salazar-Montes, A., Sandoval-Rodríguez, A., & Armendáriz-Borunda, J. (2013). *Biología molecular: fundamentos y aplicaciones en las ciencias de la salud* (S. A. de C. V McGraw-Hill Interamericana Editores, Ed.) (Primera ed). México. Pp. 338.

Silva, B. D. M., Castro, E. A., Souza, C. J. H., Paiva, S. R., Sartori, R., Franco, M. M., Azevedo, H. C., Silva, T. A. N. S., Vieira, J. P., Neves, E. O., & Melo, E. O. (2010). A new polymorphism in the *growth and differentiation factor 9* (*GDF9*) gene is associated with increased ovulation rate and prolificacy in homozygous sheep. *Animal Genetics*, *42*(1), 89–92. https://doi.org/10.1111/j.1365-2052.2010.02078.x

Souza, C. J. H., McNeilly, A. S., Benavides, M. V., Melo, E. O., & Moraes, J. C. F. (2014). Mutation in the protease cleavage site of *GDF9* increases ovulation rate and litter size in heterozygous ewes and causes infertility in homozygous ewes. *Animal Genetics*, *45*(5), 732–739. https://doi.org/10.1111/age.12190

Strauss III, J. F., Williams, C. J. (2019). Ovarian Life Cycle. In J. F. Strauss & R. L. Barbieri (Eds.), *Yen & Jaffe's Reproductive Endocrinology: Physiology, Pathophysiology, and Clinical Management: Eighth Edition* (pp. 167-205. e9). Elsevier Inc. https://doi.org/10.1016/B978-0-323-47912-7.00008-1

Våge, I. D., Husdal, M., Kent, P. M., Klemetsdal, G., & Boman, A. I. (2013). A missense mutation in growth differentiation factor 9 (*GDF9*) is strongly associated with litter size in sheep. *BMC Genetics*, *14*(1), 1–8. https://doi.org/10.1186/1471-2156-14-1

Ye, S., Dhillon, S., Ke, X., Collins, A. R., & Day, I. N. M. (2001). An efficient procedure for genotyping single nucleotide polymorphisms. *Nucleic Acids Research*, *29*(17), e88. https://doi.org/10.1093/nar/29.17.e88

Austral Journal of Veterinary Science

Austral J Vet Sci 55, 189-196 (2023)
https://doi.org/10.4206/ajvs.553.05

ORIGINAL ARTICLE

Diagnostic value of patellofemoral parameters in small breed dogs with medial patellar luxation: a tangential X-ray study

Radka Stayova Garnoeva[1*]

[1] Department of Veterinary Surgery, Faculty of Veterinary Medicine, Trakia University, 6000 Stara Zagora, Bulgaria

Article History
Received: 30.01.2023
Accepted: 04.08.2023
Published: 28.09.2023

Corresponding author
*Radka Stayova Garnoeva
dr.garnoeva@abv.bg

ABSTRACT. Knowing the diagnostic value of radiological patellofemoral parameters is important for evaluating the status of small-breed dogs with medial patellar luxation (MPL). This retrospective survey was conducted in four small dog breeds (Mini Pinscher, Pomeranian, Chihuahua, and Yorkshire terrier) on 46 healthy stifle joints and 72 joints with grade II and III MPL. The following morphometric parameters were measured on tangential radiographs: trochlear sulcus angle, lateral and medial trochlear inclination angles, trochlear depth, horizontal and vertical patellar diameters, length of the lateral and medial patellar facets, lateral and medial facet angles, Wiberg angle, congruence angle, and axial linear patellar displacement. Receiver operating characteristic (ROC) analysis was performed to evaluate the cut-off values, sensitivity, and specificity of the parameters associated with MPL. The trochlear sulcus angle and trochlear depth were capable of consistently identifying the MPL-affected joints (AUCs > 0.9). The parameters describing the position of the patella within the trochlear groove (congruence angle and axial linear patellar displacement) were found to be the most accurate, with an AUC of over 0.990 and a sensitivity/specificity of over 94%. The patellar morphology parameters had no diagnostic value in distinguishing between healthy and MPL stifles.

Keywords: patella; luxation; radiology; ROC analysis; trochlea; morphology; congruence.

INTRODUCTION

Medial patellar luxation (MPL) is a common orthopaedic condition in dogs (Di Dona *et al*., 2018). However, its pathogenesis is still not completely understood. Most cases are considered developmental, with anatomical deformities leading to pelvic limb malalignment and stifle extensor mechanism deficiency, such as coxa vara/valga, smaller anteversion angle, distal external femoral torsion, internal proximal tibial torsion, patella alta, and shallow trochlear groove (Perry & Dejardin, 2021; Sasaki *et al*., 2022). The breed is the most significant risk factor for the development of MPL (Kalff *et al*., 2014). Dogs from small breeds are about 12 times more susceptible than large breeds, particularly Pomeranians, Yorkshire Terriers, Chihuahuas, Poodles, Bichons and Pinschers (Bound *et al*., 2009; O'Neill *et al*., 2016).

Medial patellar luxation in dogs can develop without clinical signs. Assessment of the possibility of its progression to clinical disease is valuable for dog owners with regard to informed decision making regarding pet health (Farrell, 2022). The diagnosis is routinely based on clinical signs and imaging findings (Linney *et al*., 2011). The results of the orthopedic examination, however, depend strongly on the experience of veterinarians in diagnosing MPL, especially in grade II cases when the patella may only be temporarily located within the sulcus.

Apart from identification of the patellar position within the trochlear groove, radiography of the stifle joints with MPL may confirm or reject the presence of secondary osteoarthritis and cranial cruciate ligament damage. Accurate and sensitive radiological parameters are, therefore, important for assessing the condition of bone structures and making adequate decisions regarding the necessary surgical intervention (Marino & Loughlin, 2010).

Receiver operating characteristic (ROC) analysis is an approved method for evaluating and comparing the diagnostic value of radiological examinations (van Erkel & Pattynama, 1998). Over the past decade, it has been increasingly used not only in radiology but also in clinical biochemistry (Glazkov *et al*., 2020; Nahm, 2022). ROC analysis was designed to assess the overall diagnostic performance of a test, to determine an object from the study sample as either positive or negative based on a specific classifier, and to calculate the optimal cut-off value showing the best diagnostic performance. ROC curves were also used to compare the performance of two or more diagnostic tests.

In human medicine, there are numerous studies on patellofemoral diagnostic imaging parameters, and the use of ROC analysis to outline those that seem most relevant in the diagnosis of patellar instability (Ridley *et al*., 2016; Prakash *et al*., 2016; Geraghty *et al*., 2022; Kim & Parikh, 2022). To date, in dogs, ROC analysis data on sensitivity, specificity, and cut-off values have been reported only for trochlear groove morphometric parameters in small and large breeds (Longo *et al*., 2023) and proximodistal patellar position indices (Murakami *et al*., 2023); however, there

are no data on parameters of patellar morphology and patellofemoral alignment. This information seems valuable, as lameness affecting the opposite limb might have been missed in cases of bilateral MPL. In addition, half of the asymptomatic dogs with grade II MPL have been reported to develop chronic lameness or require surgery later in life (Hamilton *et al*., 2020).

The aim of this retrospective tangential radiological study was to identify parameters of trochlear anatomy, patellar anatomy, and patellofemoral congruence that differ significantly between healthy small-breed dogs and dogs with medial patellar luxation grades II and III, their cut-off values, and to assess their clinical diagnostic usefulness.

MATERIAL AND METHODS

Study cohort

The present single-observer retrospective survey was performed using tangential radiographs of 46 healthy stifle joints and 72 joints with grade II and III medial patellar luxation. All animals were of four small breeds: Mini Pinscher, Pomeranian, Chihuahua, and Yorkshire terrier.

The control group included 23 dogs (10 female and 13 male) who were referred to the clinic for prophylactic orthopedic examination or for minor interventions requiring anesthesia, mostly dental procedures. The median age of the dogs at the first presentation was 12 months (range, 8–28 months), and the median body weight was 2.6 kg (from 0.9–4.0 kg). The breed distribution was 12 Mini Pinschers, four (4) Pomeranians, three (3) Chihuahuas, and four (4) Yorkshire terriers. Both limbs of the animals were radiographed and measured, and 24 healthy stifles were examined from Mini Pinschers, eight (8) from Pomeranians, six (6) from Chihuahuas, and eight (8) from Yorkshire terriers. The inclusion criteria for the healthy joint group were a negative patellar displacement test (for detection of patellar subluxation or ligament laxity) and dancing patella test (for detection of joint effusion), as described by Verez-Fraguela *et al.* (2017), symmetrical femoral and gluteal muscles of both limbs, and lack of signs of long-term proprioceptive dysfunction.

The medial patellar luxation group included 43 dogs (17 Mini Pinschers, 12 Pomeranians, 10 Chihuahuas, and 4 Yorkshire terriers) diagnosed by physical examination and radiography. The MPL grade was determined according to Putnam's routine clinical classification – 41 of joints as grade II MPL and the other 31 as grade III MPL. In dogs with bilateral luxation, both stifles were included, whereas only the affected joint was included in dogs with unilateral luxation. Dogs were of similar age (median; range – 14 months; 9-72 months) and body weight (median; range – 2.7 kg; 1-5.7 kg) as controls. The male-to-female ratio was 18/25. Of the 72 stifle joints from the MPL group, 44 were from female dogs and 28 were from male dogs. The breed distribution was 30 joints from Mini Pinschers, 19 joints from Pomeranians, 18 joints from Chihuahuas, and five (5) joints from Yorkshire terriers. Informed consent was obtained from the owners of all patients involved in the study.

Measurements

After sedation, radiographs were obtained in a tangential (skyline) view using Bucky Diagnost CS4 stationary X-ray equipment (Philips, Bucky Diagnost CS4, Holland) with an iQ-CR ACE acquisition station and iQ-VIEW/PRO version 2.7. software. The exposure data was uniform at 50 kV and 10 mA. Patients were positioned according to the vertical position of the X-ray tube; in ventral recumbency, the examined stifle was flexed as much as possible. After palpation of the distal femur and patella, the X-ray beam was centered at the distal femur level between the condyles. All measurements were performed by a single observer using the image analysis system of the X-ray equipment software.

The morphometric parameters selected for the evaluation of trochlear morphology were trochlear sulcus angle (Brattstroem, 1964), lateral and medial trochlear inclination angles (Laurin *et al*., 1978), and trochlear depth (Pfirrmann *et al*., 2000) (Figure 1). Patellar morphology was assessed using the horizontal and vertical patellar diameters (Staubli *et al*., 1999), length of the lateral and medial patellar facets (Wiberg, 1941), lateral and medial facet angles (Jimenez *et al*., 2021), and Wiberg angle (Wiberg, 1941) (Figure 2). Two parameters, congruence angle (Merchant *et al*., 1974) and axial linear patellar displacement (Urch *et al*., 2009), were used to describe patellofemoral alignment in the axial plane (Figure 3).

Statistical analysis

The measurements are reported as median values and the minimum-maximum range. The Shapiro-Wilk test was used to evaluate the normality of data distribution. The Mann-Whitney U-test was used to compare the differences in numerical parameters between healthy joints and joints with medial patellar luxation at a level of $P < 0.05$. The Chi-square test was used to assess the association between MPL and categorical variables (sex and breed). A non-parametric receiver operating characteristic (ROC) curve analysis was performed using the recommended algorithm of DeLong *et al.* (1988) to calculate optimal cut-off values of parameters distinguishing healthy and medial patellar luxation joints on the basis of the Youden J statistic, the areas under the ROC curves (AUCs) as measures of diagnostic parameter accuracy, and the sensitivity and specificity of classifiers. The interpretation of the AUC as a measure of diagnostic accuracy was as follows: 0.90–1: excellent diagnostic test; 0.80–0.90: good diagnostic test; 0.70–0.80: fair diagnostic test; 0.60–0.70: poor diagnostic test; and 0.50–0.60: fail (Nahm, 2022). All statistical analyses were performed using MedCalc 15.8 (Belgium).

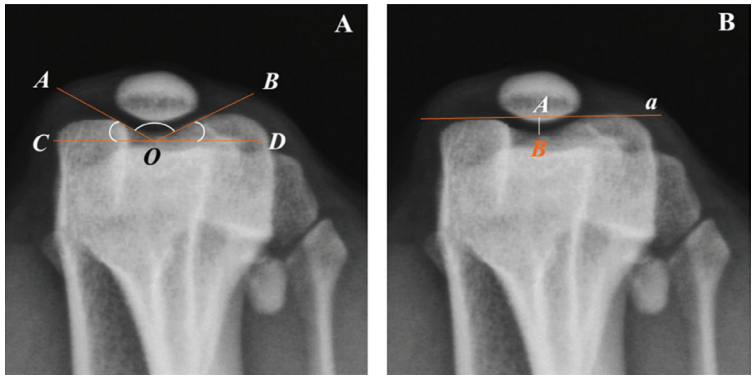

Figure 1. Tangential view of normal Pomeranian stifle. A) The sulcus angle (∠*AOB*) is formed by lines connecting the lateral and medial femoral condyles with the trochlear bottom. The lateral (∠ *BOD*) and medial (∠ *AOC)* trochlear inclination angles are formed by the lines tangential to the posterior condyle (*CD*) and the line passing from the sulcus center to the lateral (*BO*) and medial (*AO*) condyles; B) trochlear depth (*AB*) is the segment between the point of interception of the line passing through both trochlear facets (*a*) and the perpendicular line drawn from the trochlear bottom.

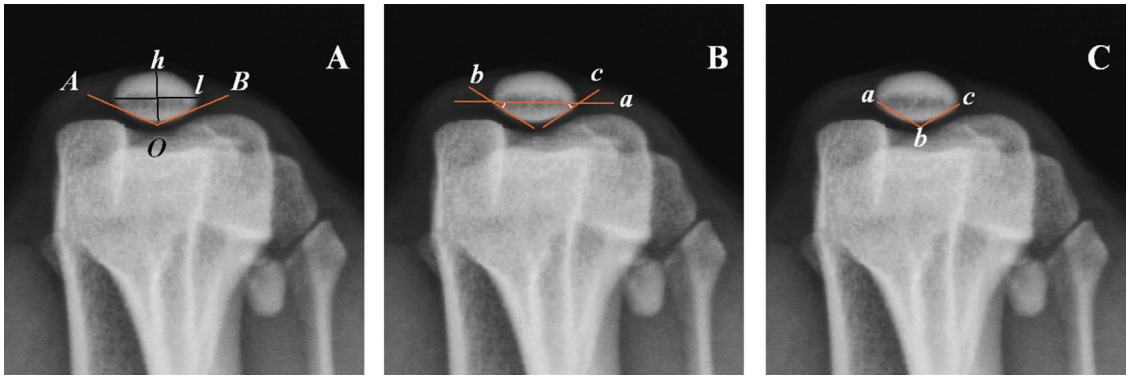

Figure 2. Tangential view of a normal Pomeranian stifle. A) The Wiberg angle (∠*AOB*) is formed by the medial and the lateral patellar facet tangents. The length between the most medial and the most lateral patellar edges corresponds to the horizontal patellar diameter (*l*), and the length between the farthest anterior and posterior patellar poles corresponds to the vertical patellar diameter or height (*h*); B) the lateral patellar facet angle is formed between the patellar horizontal diameter (line *a*) and the lateral patellar facet tangent (*c*); the medial patellar facet angle is formed between line *a* and the medial patellar facet tangent (*b*); C) lateral (*ab*) and medial (*bc*) patellar facets were measured from the patellar apex to the most lateral and medial edges of the patella, respectively.

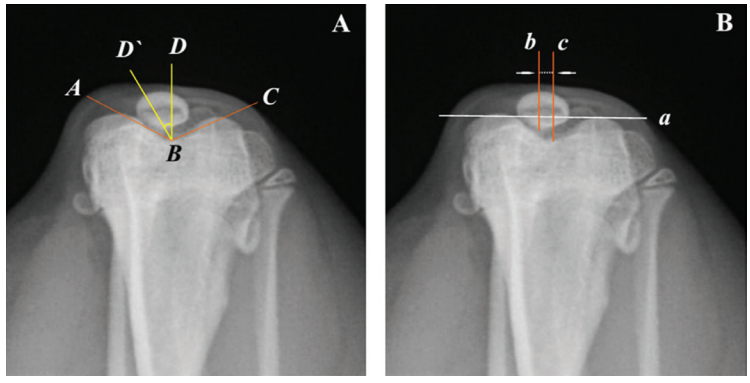

Figure 3. Tangential view of a Chihuahua stifle with grade II luxation. A) The congruence angle (∠DBD`) is formed between the sulcus angle bisector (BD) and the line passing through the trochlear bottom and the most posterior patellar edge (BD`); B) linear axial patellar displacement is the distance between two perpendiculars to the line connecting the femoral condyles (a): one from the trochlear groove bottom (c) and another from the most posterior patellar edge (b).

RESULTS

Analysis of the association between signalment data and the presence/absence of MPL showed no statistically significant effects of breed (P = 0.42), age (P = 0.09), or sex (P = 0.38).

The patellofemoral parameters measured in both joint groups are presented in Table 1. All the studied parameters of trochlear anatomy and patellofemoral alignment were significantly different between the groups. Among the patellar morphological parameters, the horizontal patellar diameter, lateral patellar facet length, and lateral patellar facet angle did not demonstrate significant between-group differences (Table 1).

The results of the ROC analysis (Table 2) showed that the sulcus angle and trochlear depth had excellent diagnostic value, as seen from the areas under the ROC curve (AUCs) (Figure 4). The cut-offs of these parameters had a sensitivity of over 90% (92.45% for sulcus angle and 98.1% for trochlear depth); therefore, they were deemed capable of reliably distinguishing medial patellar luxation joints. The lateral and medial inclination angles were defined as poor diagnostic classifiers.

The parameters of patellar morphology did not have high diagnostic value, as their AUC values corresponded to the definition of a poor diagnostic test, except for the Wiberg angle, which was interpreted as a fair diagnostic test.

According to the results, the two indices of patellofemoral alignment in the axial plane (congruence angle and axial linear patellar displacement) corresponded to the definition of excellent diagnostic tests. The congruence angle exhibited maximum sensitivity and specificity of 100% (Table 2, Figure 5).

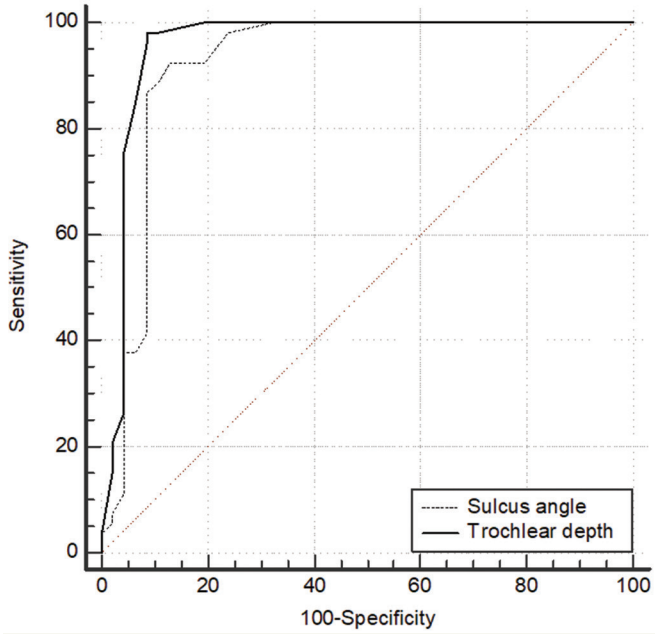

Figure 4. ROC curves of sulcus angle (AUC = 0.920; P < 0.001) and trochlear depth (AUC = 0.956; P < 0.001) as trochlear morphology parameters distinguishing healthy from MPL-affected joints.

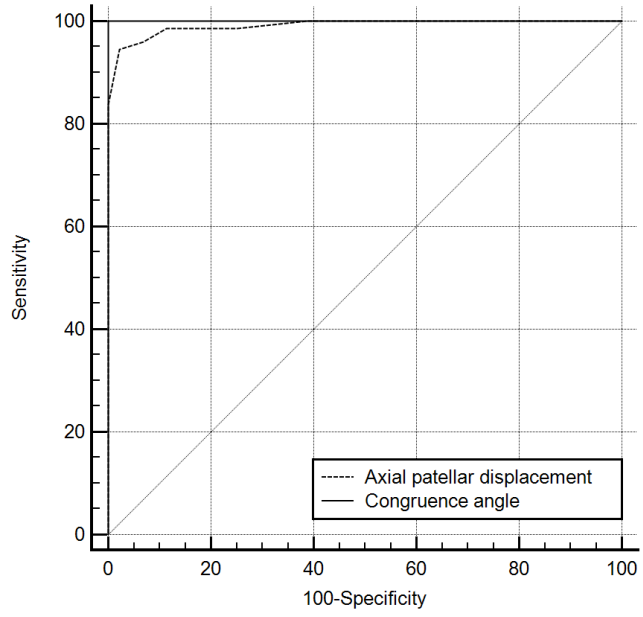

Figure 5. ROC curves of the congruence angle (AUC = 1.000; P < 0.001), axial linear patellar displacement (AUC = 0.990; P < 0.001), medial facet length (AUC = 0.991; P < 0.001), and medial facet angle (AUC = 0.956; P < 0.001) as patellofemoral alignment parameters distinguishing healthy joints from MPL-affected joints.

DISCUSSION

In dogs from small breeds, patellar luxation occurs as a consequence of complex morphological musculoskeletal abnormalities affecting the entire pelvic limb, but the pathogenetic role of the shallow trochlear groove (Longo *et al*., 2023) and medial femoral condyle hypoplasia (Garnoeva, 2021) is thought to be the leading cause. Therefore, tangential radiographs of canine stifles are preferred for satisfactory evaluation of trochlear groove depth and shape.

In diagnostic practice, the aim of ROC analysis is to choose objective parameters that will yield maximum true positives and true negatives and minimize false positive and false negative results. The sensitivity of a parameter is a measure of its ability to correctly identify pathological states (in our case, the presence of medial patellar luxation) and its specificity to correctly identify the lack of pathology. In a clinical setting, it is especially important not to "miss" positive cases and to reduce false-negative results as much as possible.

Table 1. Trochlear, patellar, and patellofemoral alignment parameters in both joint groups. Values are presented as medians (ranges).

	"Healthy joints (n = 46)"	"MPL joints (n = 72)"	*P*
Trochlear parameters			
Lateral trochlear inclination angle (°)	29.5 (12.0-39.0)	25.0 (11.0-35.0)	< 0.0001
Medial trochlear inclination angle (°)	28.0 (14.0-35.0)	23.0 (9.0-32.0	0.0002
Sulcus angle (°)	122.0 (112.0-153.0)	136.0 (126.0-160.0)	< 0.0001
Trochlear depth (mm)	2.2 (0.7-3.1)	1.1 (0.5-1.9)	< 0.0001
Patellar parameters			
Horizontal patellar diameter (mm)	5.1 (2.7-7.6)	5.3 (2.5-6.6)	0.6493
Lateral patellar facet angle (°)	37.0 (26.0-52.0)	36.0 (28.0-69.0)	0.8809
Lateral patellar facet length (mm)	2.6 (1.7-4.4)	2.8 (1.3-4.3)	0.4741
Medial patellar facet angle (°)	34.0 (18.0-51.0)	38.0 (28.0-58.0)	0.0285
Medial patellar facet length (mm)	2.6 (1.6-4.8)	3.0 (1.0-4.1)	0.0099
Patellar thickness (mm)	3.1 (1.8-5.0)	2.8 (1.3-4.1)	0.0012
Wiberg angle (°)	123.0 (112.0-136.0)	131.0 (110.0-178.0)	< 0.0001
Patellofemoral alignment parameters			
Axial linear patellar displacement (mm)	0.2 (0.1-0.8)	1.2 (0.3-11.5)	< 0.0001
Congruence angle (°)	-3.0 (-10.0 to -1.00)	-30.5 (-123.0 to -14.0)	< 0.0001

Table 2. Areas under the ROC curves (AUC), cut-off values, sensitivity, and specificity of the studied patellofemoral parameters.

	AUC	Cut-off value	Cut-off sensitivity	Cut-off specificity
Trochlear parameters				
Sulcus angle (°)	0.920***	> 129	92.45	86.96
Lateral trochlear inclination angle (°)	0.763***	≤ 25	58.49	86.96
Medial trochlear inclination angle (°)	0.723**	≤ 23	54.72	84.78
Trochlear depth (mm)	0.956***	< 1.6	98.1	91.3
Patellar parameters				
Patellar thickness (mm)	0.678***	≤ 3.7	97.14	32.61
Medial patellar facet angle (°)	0.620*	> 37	54.29	65.22
Medial patellar facet length (mm)	0.642*	< 2.7	68.57	65.22
Wiberg angle (°)	0.738***	< 129	58.57	76.09
Patellofemoral alignment parameters				
Congruence angle (°)	1.000***	≤ -14	100	100
Axial patellar displacement (mm)	0.991***	> 0.7	94.59	97.73

* $P < 0.05$; ** $P < 0.01$; *** $P < 0.001$.

AUC is widely used to measure the accuracy of diagnostic tests. The ROC curves closer to the upper-left corner of the graph denote the tests with higher accuracy. The ideal ROC curve had an AUC of 1.0. Curves closer to the 45° diagonal were considered to have low accuracy and were meaningless diagnostic tools. Therefore, in general, acceptable classifiers must have AUCs greater than 0.8 (Nahm, 2022).

In human medicine, many studies have performed ROC analysis on patellofemoral parameters associated with patellar luxation to report their cut-off values, sensitivity, and specificity (Hedgecock *et al*., 2022; Geraghty *et al*., 2022; Kim & Parikh, 2022). In canine orthopaedics, ROC analysis has been used to evaluate parameters related to developmental diseases, such as hip dysplasia (Gaspar *et al*., 2016) and medial elbow coronoid disease (Hersh-Boyle *et al*., 2021). In dogs with patellar luxation, only the cut-off values of femoral trochlear morphological parameters (Longo *et al*., 2023) and indices of proximodistal patellar position (Murakami *et al*., 2023) have been reported.

In the CT study by Longo *et al*. (2023), the cut-off value for sulcus angle in small-breed dogs was > 134°, with a sensitivity and specificity of 80% and 100%, respectively. These values were comparable to those in the present tangential X-ray study: the cutoff value for the sulcus angle was > 129°, the sensitivity was 92.45%, and the specificity was 86.96%. The differences in cutoff values may be explained by the different imaging techniques used. A similar difference was reported in a comparative study of human sulcus angles evaluated by radiography (145°) and magnetic resonance imaging (158°), which concluded that, although sometimes underestimated, radiography was also reliable for the diagnosis of trochlear dysplasia (Donaldson *et al*., 2012).

In a human study, Geraghty *et al*. (2022) provided information on the sensitivity and specificity of parameters measured on radiographs between 2010 and 2022 to evaluate patellar instability. The results confirmed that trochlear depth, sulcus angle, and lateral and medial inclination angles were highly sensitive and specific parameters of trochlear dysplasia predisposing patients to patellar luxation.

The present study is the first to evaluate the diagnostic value and cutoffs of parameters of patellar morphology and patellofemoral alignment in small-breed dogs with medial patellar luxation. The results demonstrated that the best diagnostic parameters were those describing the translation of the patella in the sulcus: congruence angle and linear axial patellar displacement, both with AUCs over 0.99 and sensitivity over 94%. The congruence angle showed the maximum possible sensitivity and specificity (100% each).

In men, only a few radiological parameters were found to be accurate for diagnosing patellar luxation. In a study of 1392 stifle joints with patellar luxation and a control group of 1525 healthy joints, statistically significant differences ($P < 0.0001$) were observed in the patellar height, lateral patellar facet angle, and trochlear sulcus angle (Smith *et al*., 2011). The congruence angle showed only a slight difference between the healthy and diseased joints. The trochlear groove depth was outlined as one of the most accurate parameters for patellar instability in an overview by Ridley *et al*. (2016). The high variability between the healthy and instability groups as a cause of the low specificity is discussed.

In a radiological study to determine the reference values of patellofemoral parameters in Koreans (Prakash *et al*., 2016), ROC analysis showed that the most important indices of patellar instability were trochlear depth (AUC = 0.852), increased congruence angle (AUC = 0.985) and patellar tilt (AUC = 0.974). These results are consistent with data from the present study.

The limitations of the present study were mainly related to the small number of dogs in the study cohort. A larger number of dogs, both healthy and with patellar luxation, would increase the reliability of the results and yield more precise deviation thresholds. With data from a larger population, breed- and sex-specific thresholds may be calculated. Despite efforts to reduce external influences (use of standardized procedures and protocols, uniform exposure data, and regular technical maintenance of radiography equipment), the effects of systemic and random observational errors were not investigated in this study. The participation of more observers can reduce subjective measurement errors owing to the identification of osseous landmarks on radiographs.

CONCLUSION

In dog stifles with medial patellar luxation, the calculation of indices "sensitivity" and "specificity" allowed defining optimum cut-offs of diagnostic imaging parameters of trochlear morphology and patellofemoral alignment with regard to the optimization of therapeutic strategies.

Of all the analyzed tangential radiological patellofemoral parameters, congruence angle, axial linear patellar displacement, sulcus angle, and trochlear depth had the highest sensitivity and specificity. Based on the areas under the ROC curves, they were determined to be excellent diagnostic tests with AUCs > 0.9. The most sensitive parameters were those describing the position of the patella within the trochlear groove: the congruence angle and linear axial patellar displacement, both with AUCs > 0.99, and sensitivity > 94%, which indicated that they were the most reliable for distinguishing stifles of dogs from small breeds with medial patellar luxation from healthy stifles. The patellar morphology parameters had no practical diagnostic value. In conclusion, evaluation of trochlear groove morphology and patellofemoral alignment on tangential radiographs is recommended in dogs suspected to have low-grade medial patellar luxation with respect to treatment decision-making, as well as in sexually mature, clinically healthy dogs from susceptible small breeds, especially in breeding animals.

DECLARATIONS

Competing interests statement

The author declares no competing interests.

Ethics statement

The study was performed after obtaining informed consent from the owners of the participating dogs.

Author contributions

Conceptualization, methodology, measurements, analysis, original draft preparation, review and editing, and visualization – RG.

Acknowledgements

This research was supported by the Bulgarian Ministry of Education and Science under the National Program "Young Scientists and Postdoctoral Students-2".

REFERENCES

Bound, N., Zakai, D., Butterworth, S. J., & Pead, M. (2009). The prevalence of canine patellar luxation in three centres. Clinical features and radiographic evidence of limb deviation. *Veterinary Comparative Orthopaedics & Traumatology*, *22*(1), 32–37.

Brattstroem, H. (1964). Shape of the intercondylar groove normally and in recurrent dislocation of patella: a clinical and X-ray anatomical investigation. *Acta Orthopaedica Scandinavica*, *68*, 1-148.

DeLong, E. R., DeLong, D. M., & Clarke-Pearson, D. L. (1988). Comparing the areas under two or more correlated receiver operating characteristic curves: a nonparametric approach. *Biometrics*, *44*(3), 837–845. https://doi.org/10.2307/2531595

Di Dona, F., Della Valle, G., & Fatone, G. (2018). Patellar luxation in dogs. *Veterinary Medicine: Research & Reports*, *9*, 23-32. https://doi.org/10.2147/VMRR.S142545

Donaldson, O. W., Heal, J., Mulford, J., Wakeley, C. J., & Eldridge, J. D. J. (2018). Does the plain radiograph accurately predict trochlear dysplasia [Abstract]. Orthopaedic Proceedings, 94-B, 61.

Farrell, M. (2022). The natural history of developmental patellar dislocation in dogs. *Archives of Orthopaedics*, *3*, 27-32.

Garnoeva, R. S. (2021). Evaluation of trochlear dysplasia in dogs with medial patellar luxation - comparative studies. *Acta Scientiae Veterinariae*, *49*, 1845. https://doi.org/10.22456/1679-9216.118579

Gaspar, A. R., Hayes, G., Ginja, C., Ginja, M. M., & Todhunter, R. J. (2016). The Norberg angle is not an accurate predictor of canine hip conformation based on the distraction index and the dorsolateral subluxation score. *Preventive Veterinary Medicine*, *135*, 47-52. https:/doi.org/10.1016/j.prevetmed.2016.10.020.

Geraghty, L., Humphries, D., & Fitzpatrick, J. (2022). Assessment of the reliability and validity of imaging measurements for patellofemoral instability: an updated systematic review. *Skeletal Radiology*, *51*, 2245-2256. https://doi.org/10.1007/s00256-022-04110-9

Glazkov, A. A., Kulikov, D. A., & Glazkova, P. A. (2020). Assessing diagnostic accuracy of quantitative data in biomedical studies using descriptive statistics and standardized mean difference. *Mathematical Biology and Bioinformatics*, *15*, 416–428. https://doi.org/10.17537/2020.15.416

Hamilton, L., Farrell, M., Mielke, B., Solano, M., Silva, S., & Calvo, I. (2020). The natural history of canine occult Grade II medial patellar luxation: an observational study. *Journal of Small Animal Practice*, *61*, 241-246. https://doi.org/10.1111/jsap.13093

Hedgecock, J., Cheng, C., Solomito, M., & Pace, J. (2020). Risk factors for patellar instability using a quantitative analysis of trochlear dysplasia. *Orthopaedic Journal of Sports Medicine*, *8*(6). https://doi.org/10.1177/2325967120S00344

Hersh-Boyle, R. A., Chou, P. Y., Kapatkin, A. S., Spriet, M., Filliquist, B., Garcia, T. C., & Marcellin-Little, D. J. (2021). Comparison of needle arthroscopy, traditional arthroscopy, and computed tomography for the evaluation of medial coronoid disease in the canine elbow. *Veterinary Surgery*, *50*(1), O116-O127. https://doi.org/10.1111/vsu.13581

Jimenez, A. E., Levy, B. J.,Grimm, N. L., Andelman, S. M., Cheng, C., Hedgecock, J. P., Cohen, A., & Pace, J. L. (2021). Relationship between patellar morphology and known anatomic risk factors for patellofemoral instability. *Orthopaedic Journal of Sports Medicine*, *9*(3). https://doi.org/10.1177/2325967120988690

Kalff, S., Butterworth, S. J., Miller, A., Keeley, B., Baines, S., & McKee, W. M. (2014). Lateral patellar luxation in dogs: a retrospective study of 65 dogs. *Veterinary Comparative Orthopaedics & Traumatology*, *27*(2), 130–134. https://doi.org/10.3415/VCOT-13-05-0064

Kim, H. K., & Parikh, S. (2022). Patellofemoral instability in children: imaging findings and therapeutic approaches. *Korean Journal of Radiology*, *23*(6), 674–687. https://doi.org/10.3348/kjr.2021.0577

Laurin, C. A., Levesque, H. P., Dussault, R., Labelle, H., & Peides, J. P. (1978). The abnormal lateral patellofemoral angle: a diagnostic roentgenographic sign of recurrent patellar subluxation. *Journal of Bone Joint Surgery*, *60*(1), 55-60.

Linney, W. R., Hammer, D. L., & Shott, S. (2011). Surgical treatment of medial patellar luxation without femoral trochlear groove deepening procedures in dogs: 91 cases (1998–2009). *Journal of the American Veterinary Medical Association*, *238*(9), 1168-1172. https://doi.org/10.2460/javma.238.9.1168.

Longo, F., Memarian, P., Knell, S. C., Contiero, B., & Pozzi, A. (2023). Computed tomographic measurements of the femoral trochlea in dogs with and without medial patellar luxation. *Veterinary Surgery*, *52*(3), 395-406. https://doi.org/10.1111/vsu.13903

Marino, D. J., & Loughin C. A. (2010). Diagnostic imaging of the canine stifle: A review. *Veterinary Surgery*, *39*(3), 284-295. https://doi.org/10.1111/j.1532-950X.2010.00678.x

Merchant, A. C., Mercer, R. L., Jacobsen, R. H., & Cool, C. R. (1974). Roentgenographic analysis of patellofemoral congruence. *Journal of Bone Joint Surgery (American)*, *56*(7), 1391-1396.

Murakami, S., Shimada, M., & Hara, Y. (2023). Examination of proximodistal patellar position in dogs with the stifle at full extension. *Veterinary Comparative Orthopedics and Traumatology*. https://doi.org/10.1055/s-0043-1764317. Advance online publication.

Nahm, F. S. (2022). Receiver operating characteristic curve: overview and practical use for clinicians. *Korean Journal of Anesthesiology*, *75*(1), 25-36. https://doi.org/10.4097/kja.21209.

O'Neill, D. G., Meeson, R. L., Sheridan, A., Church, D. B., & Brodbelt, D. C. (2016). The epidemiology of patellar luxation in dogs attending primary-care veterinary practices in England. *Canine Genetics and Epidemiology*, *3*, 4. https://doi.org/10.1186/s40575-016-0034-0

Perry, K. L., & Dejardin L. M. (2021). Canine medial patellar luxation. *Journal of Small Animal Practice*, *62*(5), 315-335. https://doi.org/10.1111/jsap.13311

Pfirrmann, C. W., Zanetti, M., Romero, J., & Hodler, J. (2000). Femoral trochlear dysplasia: MR findings. *Radiology*, *216*(3), 858-864. https://doi.org/10.1148/radiology.216.3.r00se38858

Prakash, J., Seon, J-K., Woo, S-H., Jin, C., & Song, E-K. (2016). Comparison of radiological parameters between normal and patellar dislocation groups in Korean population: A rotational profile CT-based study knee. *Knee Surgery & Related Research*, *28*(4), 302–311. https://doi.org/10.5792/ksrr.16.010

Ridley, T. J., Hinckel, B. B., Kruckeberg, B. M., Agel, J., & Arendt, E. A. (2016). Anatomical patella instability risk factors on MRI show sensitivity without specificity in patients with patellofemoral instability: A systematic review. *Journal of ISAKOS*, *1*(3), 141-152. https://doi.org/10.1136/jisakos-2015-000015

Sasaki, A., Hidaka, Y., Mochizuki, M., Honnami, M. (2022). Computed tomographic measurements of the sulcus angle of the femoral trochlea in small-breed dogs with and without medial patellar luxation. *Veterinary Comparative Orthopedics and Traumatology*, *35*(5), 314-320. https://doi.org/10.1055/s-0042-1749151

Smith, T. O., Davies, L., Toms, A. P., Hing, C. B., & Donell, S. T. (2011). The reliability and validity of radiological assessment for patellar instability. A systematic review and metaanalysis. *Skeletal Radiology*, *40*, 399-414. https://doi.org/10.1007/s00256-010-0961-x.

Staubli, H. U., Durrenmatt, U., Porcellini, B., & Rauschning, W. (1999). Anatomy and surface geometry of the patellofemoral joint in the axial plane. *Journal of Bone Joint Surgery (British)*, *81-B*(3), 452-458. https://doi.org/10.1302/0301-620x.81b3.8758

Urch, S. E., Tritle, B. A., Shelbourne, K. D., & Gray, T. (2009). Axial linear patellar displacement: a new measurement of patellofemoral congru-

ence. *American Journal of Sports Medicine*, *37*(5), 970-973. https://doi.org/10.1177/0363546508328596

van Erkel, A. R., & Pattynama, P. M. (1998). Receiver operating characteristic (ROC) analysis: Basic principles and applications in radiology. *European Journal of Radiology*, *27*(2), 88–94. https://doi.org/10.1016/s0720-048x(97)00157-5

Verez-Fraguela, J. L., Kostlin, R., Reviriego, R. L., Peris, S. C., Margallo, F. M., & Gargallo J. U. (2017). *Orthopaedic Pathologies of the Stifle Joint*. Milano. Edra Spa.

Wiberg, G. (1941). Roentgenographic and anatomic studies on the femoropatellar joint. *Acta Orthopaedica Scandinavica*, *12*(1-4), 319-410. https://doi.org/10.3109/17453674108988818

Austral Journal of Veterinary Science

Austral J Vet Sci 55, 197-202 (2023)
https://doi.org/10.4206/ajvs.553.06

SHORT COMMUNICATION

Comparisons of β2-microglobulin, apolipoprotein A1, and immunoglobulins (IgG and IgM) detected in the serum and urine from individual cats

Michio Katagi[1,2], Haruka Imatomi[2], Yasushiko Tsuchida[3], Kinya Katayama[4], Yasunaga Yoshikawa[1], Koichi Orino[1*]

[1] Laboratory of Veterinary Biochemistry, School of Veterinary Medicine, Kitasato University, 23-35-1 Higashi, Towada, Aomori 034-8628, Japan.

[2] Katagi Animal Hospital Kawagoe Animal Medical Center, 565-5 Matoba, Kawagoe, Saitama 350-1101, Japan.

[3] Gori Veterinary Clinic, 1-1-8 Yasuhara, Hirosaki, Aomori 036-8162, Japan.

[4] Laboratory of Biomolecular Chemistry, School of Veterinary Medicine, Nippon Veterinary and Life Science University, 1-7-1 Kyonancho, Musashino, Tokyo 180-8602, Japan.

Article History
Received: 15.11.2022
Accepted: 11.07.2023
Published: 23.10.2023

Corresponding author
* Koichi Orino
orino@vmas.kitasato-u.ac.jp

ABSTRACT. The detection of serum and urinary proteins is important for normal conditions, but comparisons of individual serum and urine proteins are rarely performed. The aim of this study was to examine β2-microglobulin (β2-MG), apolipoprotein A-I (ApoA-I), and immunoglobulins (IgG and IgM) in the serum and urine of cats with chronic kidney disease and lower urinary tract disease (LUTD), in addition to healthy cats. Serum and urine samples were analyzed by sodium dodecyl sulfate–polyacrylamide gel electrophoresis, followed by immunoblotting for β2-MG, ApoA-I, IgG, and IgM. The molecular weight of serum β2-MG was greater than the predicted molecular weight (11,472 Da), and different types of modified β2-MGs were detected in the urine of healthy and diseased cats, including the original type, in addition to the grycocylated and partially digested types. Serum and urinary ApoA-I molecular weights were lower than the predicted molecular weight (28,943 Da), and high levels of urinary ApoA-I were detected in LUTD cats, although urinary ApoA-I was not detected in healthy cats. Under non-reducing conditions, the H-chains of urinary IgM pentamers and IgG monomers were detected in healthy cats. These results suggest that urinary β2-MG is modified in a different manner from serum β2-MG, urinary ApoA-I is a potential marker of LUTD, and urinary IgM pentamer, IgG monomer, and their H-chains are found after glomerular filtration, even in healthy conditions.

Keywords: apolipoprotein A-I, immunoglobulins, serum, urine, β2-microglobulin.

INTRODUCTION

In felines, detection of urinary proteins is important for the diagnosis of kidney disease. Although large amounts of albumin (67 kDa) are present in the plasma of cats, levels are negligible in the glomerular filtrate due to selective glomerular permeability, and the small quantity of albumin in the glomerular filtrate is almost completely reabsorbed by the proximal tubular epithelial cells, resulting in a detection level of < 1 mg/dL in normal urine (Kovarikova, 2015). β2-Microglobulin (β2-MG), composed of a single polypeptide with a molecular weight of 11.8 kDa, is associated with major histocompatibility complex I on the surface of all nucleated cells (Argyropoulos *et al*., 2017; Cobbin *et al*., 2013). Glomerular-filtered β2-MG is reabsorbed and catabolized in proximal convoluted tubules (Argyropoulos *et al*., 2017). Impairment of this system is used to diagnose kidney disease based on the presence of β2-MG in the urinary protein because of the lack of endocytosis mediated by the megalin-cubilin complex (Argyropoulos *et al*., 2017; Cobbin *et al*., 2013). Urinary β2-MG is thought to be glycosylated based on the detection of multiple proteins compared to recombinant feline β2-MG (Hoshi, 2014). However, the mechanism of circulating β2-MG glycosylation has not been fully characterized. Apolipoprotein A-I (ApoA-I), with a molecular weight of 28 kDa, is the primary high-density lipoprotein (HDL). ApoA-I is reabsorbed after glomerular filtration by tubular epithelial cells via Apo and HDL receptors and transporters (Clark *et al*., 2019; Nielsen *et al*., 2016). In humans, children with kidney disease have detectable levels of urinary ApoA-I depending on the underlying disease (Clark *et al*., 2019).

Immunoglobulin G (IgG), which has a high molecular weight (160 kDa), can enter the urine in some amounts via neonatal Fc receptor–mediated transcytosis that occurs in the glomerular basement membrane (Akilesh *et al*., 2008), but can be a marker of glomerular impairment (Kovarikova, 2015).

Kidney and lower urinary tract diseases (LUTDs) are common in cats; therefore, it is important to accurately diagnose acute and chronic renal diseases (Kovarikova, 2015; Gomes *et al*., 2018; Lekcharoensuk *et al*., 2001). Acute kidney injury (AKI) causes sudden renal dysfunction leading to acute renal failure, which is associated with high morbidity and mortality rates (Kovarikova, 2015). Chronic kidney disease (CKD) is diagnosed in 15-30% of geriatric cats, and its prevalence increases in cats over 15 years of age (Brown *et al*., 2016; Cobbin *et al*., 2013). A considerable amount of data is available regarding the detection of urinary proteins as a means of diagnosing common kidney

diseases in felines during the early stages of the disease, but there is relatively limited data concerning comparisons of serum and urinary proteins in individual normal cats. To further characterize the differences in specific proteins (β2-MG, ApoA-I, IgG, and IgM) between serum and urine, these proteins were characterized using serum and urinary samples from normal cats, including CKD and LUTD cats.

MATERIALS AND METHODS

Chemicals

Rabbit anti-human β2-MG and ApoA-I antibodies were purchased from Abcam (Cambridge, MA, USA) due to immunological cross-reactions between humans and cats and Proteintech Group Inc. (Chicago, IL, USA), respectively. Polyclonal goat antibodies specific for cat IgG Fc fragment and IgM were purchased from Bethyl Laboratories (Montgomery, TX, USA). Alkaline phosphatase (ALP)-conjugated rabbit and goat IgG antibodies were purchased from MP Biomedicals (Irvine, CA, USA) and Southern Biotechnology Associates, Inc. (Birmingham, AL, USA), respectively. Bovine serum albumin (BSA) was purchased from Roche Life Sciences, Inc. (San Francisco, CA, USA). All other reagents were of analytical grade.

Blood and urine

The following cat breeds were used in this study: American shorthair, Japanese cat (domestic short hair), Maine Coon, Siamese, and mixed. Serum and urine samples were collected by centrifugation after collecting blood and urine directly into sterilized tubes from 12 healthy cats, including five kittens, four cats with CKD, and three cats with LUTD, as diagnosed by veterinarians. The concentration of protein in the urine was determined using a Pierce BCA protein assay kit according to the microtiter method, with BSA as the standard. All experiments were conducted following the established guidelines for animal welfare and approved by the Committee on the Ethics of Animal Experiments of Kitasato University (permit No.:20-048).

Sodium dodecyl sulfate-polyacrylamide gel electrophoresis (SDS-PAGE) and immunoblotting

Serum and urine samples were appropriately diluted with phosphate-buffered saline (150 mM NaCl, 20 mM sodium phosphate [pH 7.2]) and sample buffer with or without 40 mM dithiothreitol (DTT) was added. SDS-PAGE was performed according to the method described by Laemmli (1970) using a 4.5% stacking gel and a 12% running gel.

The amount of protein loaded on the SDS-PAGE gels varied from 4.8 μg/lane to 3.2 μg/lane for serum samples and from 4.0 μg/lane to 0.68 μg/lane for urine samples, which serum and urine samples were diluted finally 20-fold and 1.25-fold diluted.

Proteins separated by SDS-PAGE were transferred onto polyvinylidene fluoride membranes at 12 V for 12 min using an Invitrogen iBlot 2 Gel Transfer Device (Carlsbad, CA, USA). Briefly, the transferred proteins were incubated with rabbit anti-human β2-MG and ApoA-I antibodies, goat anti-cat IgG Fc fragment, and IgM, followed by ALP-conjugated polyclonal antibodies specific for rabbit or goat IgG (Fc) to detect primary antibodies. ALP-conjugated antibodies bound on the membrane were detected using 100 mM Tris-HCl (pH 7.6) containing 5 mM $MgCl_2$, 0.39 mM nitro blue tetrazolium, and 0.38 mM 5-bromo-4-chloro-3-indolylphosphate.

RESULTS AND DISCUSSION

Table 1 shows the results of the biochemical characterization of serum and urine samples from 12 healthy cats (Nos. 1-12), four cats (Nos. 13-16) with CKD, and three cats (Nos. 17-19) with LUTD. Except for cat No. 6, the healthy cats exhibited no azotemia based on either one or both of the following IRIS guideline criteria: serum creatinine ≤ 1.6 mg/dL and/or SDMA < 14 μg/dL (Hall *et al.*, 2018), the blood urea nitrogen (BUN) level of healthy cats was within the reference range (17-39 mg/dL) (Hall *et al.*, 2018). CKD was diagnosed based on serum creatinine levels of > 2.3 mg/dL (Boyd *et al.*, 2008; Ernst *et al.*, 2018).

β2-MG in the serum samples of 12 healthy cats was detected as a single band (17 kDa) by SDS-PAGE under reducing conditions via immunological cross-reaction with human β2-MG. The molecular weight of serum β2-MG was higher than that calculated based on its amino acid sequence (11,472 Da; accession no.: NM_001009876.1). In this study, the detection of β2-MG bands in Nos. 5 and 6 is shown as representative data, including all bands detected as described below (Figure 1A). In samples from five healthy cats (Nos. 2, 4-6, and 12), the molecular weight of β2-MG was slightly higher (18 kDa) than that observed in the other samples (Nos. 5 and 6). Urinary β2-MG was not detected in three healthy cats (Nos. 3, 7, and 11), but the protein was detected as a band that co-migrated with serum β2-MG in three healthy cats (Nos. 4, 10, and 12). An additional band (20 kDa) was also detected in three healthy cats (Nos. 1, 2, and 8), with two isoforms of serum β2-MG (17- and 18-kDa bands). Additionally, in three healthy cats (Nos. 5, 6, and 9), urinary β2-MG was detected at a lower molecular weight (15 kDa), with two or three more β2-MG bands, as previously described (Figure 1A). In cats with CKD, urinary β2-MG was observed as a 17- (No. 14) or 20-kDa (No. 13) band, or both bands (No. 16), in addition to a band (17 kDa) that co-migrated with serum β2-MG, except for cat No. 15, as described in healthy cats (Figure 1A). LUTD cats also demonstrated 18- and 20-kDa bands, with one band showing serum β2-MG, except for No. 18 (Figure 1A). In a previous study, urinary β2-MG exhibited a ladder pattern on immunoblotting with a monoclonal antibody against recombinant feline β2-MG, although only one band of purified recombinant feline β2-MG was detected, suggesting glycosylation of serum β2-MG (Hoshi, 2014). This study also revealed patterns of glycosylation in

Table 1.
Biochemical characterization of the serum and urine of healthy cats and cats with CKD or LUTD

N°	Breed	Diagnosis	Sex	Age (years)	TP (g/dL)	Alb (g/dL)	Ht (%)	BUN (mg/dL)	Cre (mg/dL)	SDMA (µg/dL)	GOT (U/L)	GPT (U/L)	Urinary protein (µg/mL)	UPC
1	D	Healthy	M (C)	0.5	6.8	3.3	31.4	27	0.7	ND	21	ND	613	ND
2	JC	Healthy	M	0.5	6.4	3	34.6	31	1.1	ND	36	116	215	ND
3	D	Healthy	M	0.6	6.1	3.1	40.7	24	1.5	ND	24	55	954	ND
4	MC	Healthy	M	0.5	6.6	3.3	36	28	1.1	ND	ND	ND	215	ND
5	BS	Healthy	M	0.6	6.3	3.3	39	20	1	ND	8	40	787	ND
6	MC	Healthy	M	2.6	6.8	2.8	38.4	27	2	ND	ND	ND	903	ND
7	D	Healthy	M(C)	12.6	7.9	3.3	ND	25	1.4	9	ND	ND	34	0.1
8	MC	Healthy	F	2	9.7	3.1	34.6	30	0.9	ND	29	ND	271	ND
9	JC	Healthy	M	14	ND	ND	35.7	25	1.5	11	16	25	572	<0.2
10	JC	Healthy	M	10	7.5	3.2	45	21	1.1	12	ND	30	516	<0.2
11	JC	Healthy	M	5	ND	ND	35.7	11	1.5	8	ND	ND	299	<0.2
12	JC	Healthy	F(S)	6	7.8	3	46.6	23	1.5	13	ND	71	253	<0.2
13	D	CKD	M(C)	6	7.5	3.3	24.5	<130	13.1	ND	22	31	89	0.18
14	JC	CKD	F(S)	17	7.7	3.3	38.4	<130	12.7	ND	50	48	206	0.12
15	D	CKD	M(C)	6	7.3	3.1	36.7	22	2.6	ND	ND	78	444	0.11
16	D	CKD	F(S)	9	7.4	3.5	39.4	38	3	13	ND	58	187	0.1
17	JC	Cystitis, CKD	M(C)	2	7.2	3.7	41.6	96	7.4	ND	21	ND	2,495	ND
18	D	Cystitis	M(C)	0.5	7.1	3.2	30.5	25	1	ND	36	179	283	ND
19	JC	Urolirhiasis, CKD	F(S)	15	7.9	3.4	30.7	56	3.3	ND	31	63	2,239	0.29

C: castrated; S: spayed; TP: total protein; Alb: albumin; Ht: hematocrit; BUN: blood urea nitrogen; Cre: serum creatinine; SDMA: serum symmetric dimethylarginine; GOT: glutamic-oxaloacetic transamidase; GPT: glutamic-pyruvic tranamidase; UPC: urine protein to creatinine ratio; ND: no data; JC: Japanese cat; MC: Maine Coon; BS: British shorthair; D: Domestic long- or short-hair cat.

serum and urinary β2-MG. Urinary β2-MG differs from serum β2-MG in some healthy cats (nos. 1, 2, 5, 6, 8, and 9). The lower molecular weight form of urinary β2-MG (15 kDa) found in only four healthy cats (Nos. 1, 5, 6, and 9) was expected to be the bona fide form of β2-MG. These unmodified and higher-molecular-weight β2-MG bands (18 and 20 kDa) may have been produced by glycosylation or de-glycosylation after the glomerular passage. Although β2-MG is a marker of damage to the proximal tubules, it was detected in healthy cats with SDMA levels within the normal range (Table 1). However, the presence of β2-MG is likely to be independent of age and/or urinary protein levels. Further studies are needed to examine more diseased cats regarding the lack of glomerular reabsorption of modified β2-MG; however, β2-MG appears to be a predictive marker of kidney dysfunction (Kovarikova, 2015).

Circulating feline ApoA-I was detected in all cats, including healthy cats and cats with kidney diseases, based on immunological cross-reactions with human ApoA-I, as shown in the sera of LUTD cats (Figure 1B). The apparent molecular weight of ApoA-I was 24 kDa, which is lower than that calculated from the predicted amino acid sequence (28,943 Da; ENSFCAG00000018483). However, ApoA-I was not detected in the urine of the healthy cats (Supplementary Data 1). ApoA-I was detected in the urine of the two cats with CKD (Supplementary Data 1), whereas abundant ApoA-I was strongly detected in LUTD cats. Circulating lipoproteins and their constituents, known as apolipoproteins, are urinary markers of CKD (Clark *et al.*, 2019; Nielsen *et al.*, 2016). Filtered ApoA-I is reabsorbed by the receptors of both megalin and cubilin in the proximal tubules (Nielsen *et al.*, 2016). ApoA-I was also detected in two cats with CKD, indicating that ApoA-I may be a marker of CKD in cats and humans (Clark *et al.*, 2019). Abundant ApoA-I was detected in the urine of three cats with LUTD with urolithiasis or cystitis, also indicating that urinary ApoA-I can be a marker of LUTD. However, the mechanism by which ApoA-I enters the urine of cats with LUTD remains unclear, although hematuria has not been examined.

Immunoblotting analysis of normal cat serum (C) using anti-IgM and anti-IgG Fc antibodies was performed under non-reducing conditions using SDS-PAGE (Figure 1C). Under non-reducing conditions, many bands were detected at 172, 155, 90, 82, 68, 49, 37, and 27 kDa, with the 85-kDa band strongly detected as the IgM H-chain, as indicated by the dotted arrow. Under non-reducing conditions, the IgM pentamer was strongly detected at a molecular weight > 250 kDa, although many protein bands were also observed (161, 148, 85, and 50 kDa). In the case of IgG, the H-chain was detected as a major band (50 kDa) in addition to a 31-kDa band under reducing conditions (Supplementary Data 2), and the IgG monomer was detected at a molecular weight of > 250 kDa in addition to a 50-kDa band under non-reducing conditions, as indicated by the dotted arrow. However, no bands were detected when the blot was probed with only the ALP-conjugated secondary antibody (data not shown), although many bands were detected for unknown reasons in the IgM and IgG analyses, as previously described. Identification of the H-chains of both IgM and IgG was enabled by comparing the analyses of IgM and IgG in normal feline serum under reducing and non-reducing conditions. Although urine samples from six healthy cats (Nos. 1-6) were used as representative data (Figure 1C), including normal feline serum (C), the IgM pentamer was identified as a faint band in the urine samples of eight healthy cats with the primary 45- and 33-kDa bands except for Nos. 1, 6, 7, and 9, and the IgM H-chain (85 kDa) was also detected in eight urine samples, except for Nos. 7-10, as indicated by dotted arrows under non-reducing conditions. In addition, under non-reducing conditions, IgG monomers were detected in the urine of seven healthy cats, except for Nos. 3-5, 7, and 12, and a 50-kDa band identified as the IgG H-chain was detected with a 31-kDa band in the urine of nine healthy cats, except Nos. 7 and 12. Under non-reducing conditions, each H-chain of IgM (μ-chain) and IgG (γ-chain) with molecular weights of 85 kDa and 50 kDa, respectively, migrated more rapidly than the H-chains of IgM and IgG under reducing conditions (Supplementary Data 2). In CKD cats (Nos. 13-16), a band corresponding to the IgM H-chain (90 kDa) was detected in addition to bands at 48 and 33 kDa, which were detected as major bands under reducing conditions. Under non-reducing and nonreducing conditions, IgM H chains and monomers were observed in cats with CKD and LUTD. Under reducing or nonreducing conditions, the IgG H-chain (55 kDa) and monomer were also observed in urine samples from cats with CKD and LUTD, but the IgG monomer was not detected in cat No. 19 (Supplementary Data 2).

Both IgG and IgM exhibited separated H-subunits, even in control serum samples and in the urine of diseased and healthy cats under non-reducing conditions. Filtered IgG is removed from the glomerular basement membrane to protect against accumulation in the glomerular barrier (Akilesh *et al.*, 2008; He *et al.*, 2020). Polymeric immunoglobulins (e.g., IgM and IgA) are likely to be secreted into the renal tubules as a result of kidney injury (Wei & Wang, 2021). In cats with CKD or LUTD, kidney injury is associated with the detection of immunoglobulins (IgM and IgA), rather than IgG reabsorption (Tencer *et al.*, 1998).

CONCLUSION

β2-MG, a marker of kidney tubular damage, was detected in healthy cats even with normal SDMA levels. Urinary β2-MG was detected as multiple bands on SDS-PAGE, probably due to glycosylation and protein cleavage. Although ApoA-I was not detected in the urine of healthy cats, it was strongly detected in cats with LUTD. In this study, detection of urinary IgG and IgM revealed the probability of detection in all cats even under normal conditions. These immunoglobulins can be separately divided into H- and L-chains from IgG and IgM molecules in circulation and/or after glomerular passage. This report provides preliminary data that yields new insights into the detection of urinary and serum proteins.

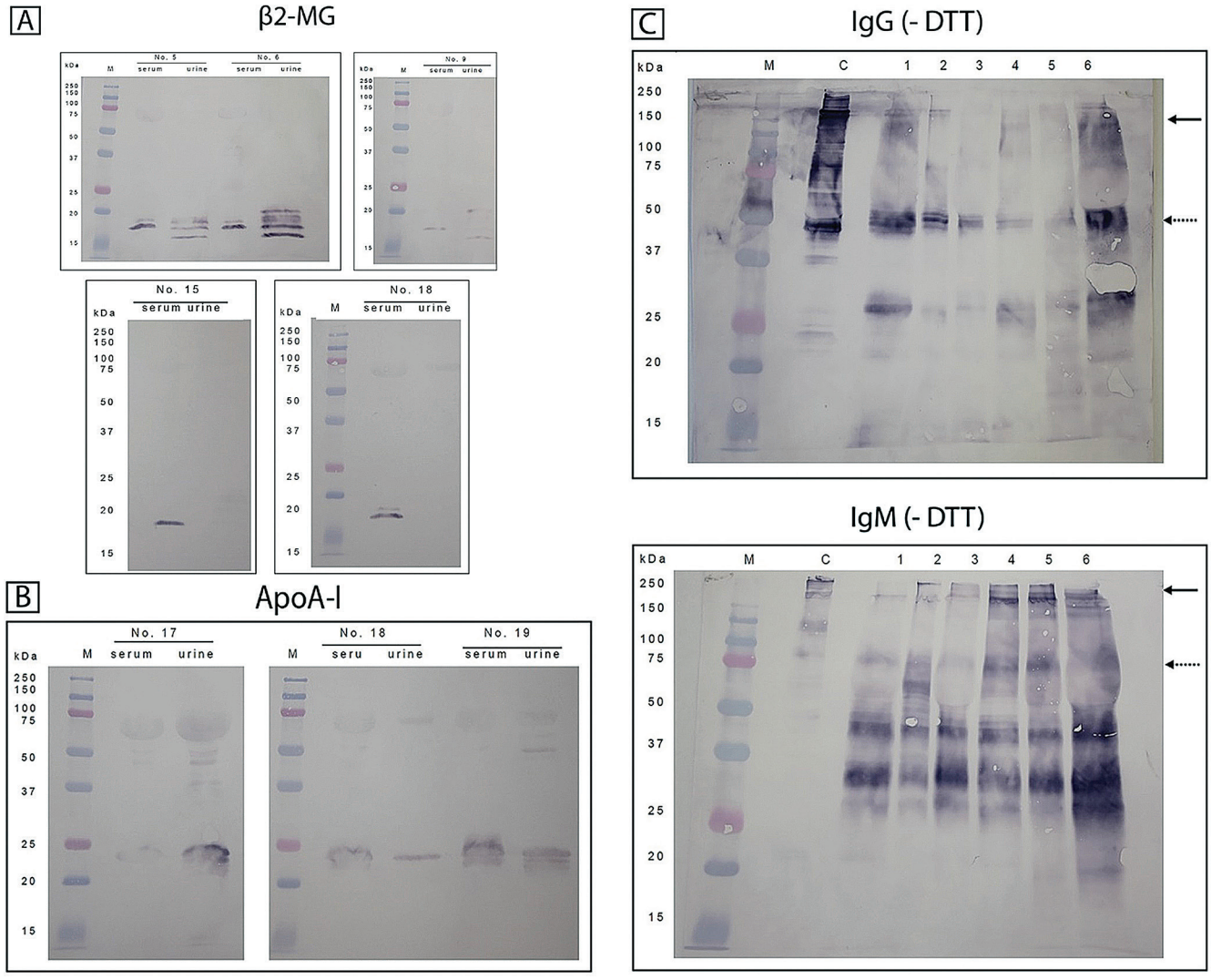

Figure 1.
Immunoblot analyses of the serum and urine of healthy and sick cats using antibody to human β2-MG antibody, human ApoA-I antibody or antibody to feline IgM μ-chain and IgG Fc fragment (γ-chain). A) and B) Serum and urine samples were diluted 40-fold and 1.25-fold with preparation buffer, respectively, and 20-μL aliquots were applied to SDS-PAGE gels followed by immunoblotting. C) Immunoblot analyses of the serum and urine of healthy cats (Nos. 1-6) using antibody to feline IgM μ-chain and IgG Fc fragment (γ chain). Urine samples of healthy cats were diluted 1.25-fold and with preparation buffer in the absence of DTT (-DTT), and 20-μL aliquots were applied to SDS-PAGE gels followed by immunoblotting as described in the "MATERIALS AND METHODS". The feline serum sample was used as a control sample (C). Arrows indicate H-chain of IgM or IgG and IgM pentamer or IgG monomer in the absence of DTT, and dotted arrows indicate H-chain of IgM or IgG detected. M represents marker proteins.

DECLARATIONS

Author contributions

Conceptualization, K. O., M. K., and Y. Y.; methodology, K. O. and M. K.; validation, K. O., M. K., and Y. Y.; formal analysis, K. O. and M. K.; investigation, K. K., M. K., H. I., and Y. T.; data curation, K. O., M. K., and H. I.; supervision, K. O.; writing-original draft, M. K.; writing-review and editing, K. O. All authors have read and agreed to the published version of the manuscript.

Ethics statement

All experiments were conducted following the established guidelines for animal welfare and approved by the Committee on the Ethics of Animal Experiments of Kitasato University (permit no.:20-048).

Conflict of interest

Authors declare no conflict of interests for this article.

REFERENCES

Akilesh, S., Huber, T. B., Wu, H., Wang, G., Hartleben, B., Kopp, J. B., Miner, J. H., Roopenian, D. C., Unanue, E. R., & Shaw, A. S. (2008). Podocytes use FcRn to clear IgG form the glomerular basement membrane. *Proceeding of the National Academy of Sciences of the United States of America, 105*(3), 967-972. https//doi.org/10.1073/pnas.0711515105

Argyropoulos, C. P., Chen, S. S., Ng, Y. H., Roumelioti, M. E., Shaffi, K., Singh, P. P., & Tzamaloukas, A. H. (2017). Rediscovering beta-2 microglobulin as a biomarker across the spectrum of kidney diseases. *Frontiers in Medicine*, *4*, 73. http://doi.org/10.3389/fmed.2017.00073

Boyd, L. M., Langston, C., Thompson, K., Zivin, K., & Imanishi, M. (2008). Survival in cats with naturally occurring chronic kidney disease (2000-2002). *Journal of Veterinary Internal Medicine*, *22*(5), 1111-1117. http://doi.org/10.1111/j.1939-1676.2008.0163.x

Brown, C. A., Elliott, J., Schmiedt, C. W., & Brown, S. A. (2016). Chronic kidney disease in aged cats: clinical features, morphology, and proposed pathogeneses. *Veterinary Pathology*, *53*(2), 309-326. https://doi.org/10.1177/0300985815622975

Clark, A. J., Jabs, K., Hunley, T. E., Jones, D. P., VanDeVoorde, R. G., Anderson, C., Du, L., Zhong, J., Fogo, A. B., Yang, H., & Kon, V. (2019). Urinary apolipoprotein AI in children with kidney disease. *Pediatric Nephrology*, *34*(11), 2351-2360. http://doi.org/10.1007/s00467-019-04289-5

Cobbin, A. R., Blois, S. L., Kruth, S. A., Abrams-Ogg, C. G., & Dewey, C. (2013). Biomarkers in the assessment of acute and chronic diseases in the dog and cat. *Journal of Small Animal Practice*, *54*(12), 647-655. https://doi.org/10.1111/jsap.12150

Ernst, R., Ogeer, J., McCrann, D., Cross, J., Strong-Townsend, M., Frils, H., Coyne, M., Clements, C., Drake, C., & Murphy, R. (2018). Comparative performance of IDEXX SDMA test and the DLD SDMA ELISA for the measurement of SDMA in canine and feline serum. *PLOS One*, *13*, e0205030. https://doi.org/10.1371/journal.pone.0205030

Gomes, V. D. R., Ariza, P. C., Borges, N. C., Shultz, F. J., Jr., & Floravanti, M. C. S. (2018). Risk factors associated feline urolithiasis. *Veterinary Research Communications*, *42*(1), 87-94. https://doi.org/10.1007/s11259-018-9710-8

Hall, J. A., Yerramilli, M., Obare, E., Yerramilli, M., & Jewell, D. E. (2014). Comparison of serum concentrations of symmetric dimethylarginine and creatinine as kidney function biomarkers in cats with chronic kidney disease. *Journal of Veterinary Internal Medicine*, *28*(6), 1676-1683. https://doi.org/10.1111/jvim.12445

He, T., Siwy, J., Metzger, J., Mullen, W., Mischak, H., Schanstra, J. P., Zürbig, P., & Jankowski, V. (2020). Associations of urinary polymeric immunoglobulin receptor peptides in the context of cardio-renal syndrome. *Scientific Reports*, *10*, Article 8291. https://doi.org/10.1038/s41598-020-65154-2

Hogan, I., Doherty, M., Fagan, J., Kennedy, E., Conneely, M., Crowe, B., & Lorenz, C. (2016). Optimization of the zinc sulfate turbidity test for the determination of immune status. *Veterinary Records*, *178*(7), 161-169. https://doi.org/10.1136/vr.103401

Hoshi, F. (2014). United States Patent No. 8,716,453 B2, Available online: https://patentimages.storage.googleapis.com/5f/37/16/bc0b2883b3d9b6/US8716453.pdf

Kobayashi, N., Suzuki, Y., Tsuge, T., Okumura, K., Ra, C., & Tomino, Y. (2002). FcRn-mediated transcytosis of immunoglobulins in human renal proximal tubular epithelial cells. *American Journal of Physiology-Renal Physiology*, *282*(2), F358-F365. https://doi.org/10.1152/ajprenal.0164.2001

Kovarikova, S. (2015). Urinary biomarkers of renal function in dogs and cats: a review. *Veterinární Medicína*, *60*(11), 589–602. https://doi.org/10.17221/8527-VETMED

Laemmli, U. K. (1970). Cleavage of structural proteins during the assembly of the head of bacteriophage T4. *Nature*, *227*, 680-685. http://doi.org/10.1038/227680a0

Lekcharoensuk, C., Osborne, C. A., & Lulich, J. P. (2001). Epidemiologic study of risk factors for lower urinary tract diseases in cats. *Journal of the American Veterinary Medical Association*, *218*(9), 1429-1435. https://doi.org/10.2460/javma.2001.218.1429

Nielsen, R., Christensen, E. I., & Birn, H. (2016). Megalin and cubilin in proximal tubule protein reabsorption: from experimental models to human disease. *Kidney International*, *89*(1), 58-67. http://doi.org/10.1016/j.kint.2015.11.007

Sarrias, M. R., Padilla, O., Monreal, Y., Carrascal, M., Abian, J., Vives, J., Yélamos, J., & Lozano, F. (2004). Biochemical characterization of recombinant and circulating human Spα. *Tissue Antigens*, *63*(4), 335-344. http://doi.org/10.1111/j.0001-2815.2004.00193.x

Tencer, J., Torffvit, O., Thysell, H., Rippe, B, & Grubb, A. (1988). Proteinuria selectivity index based upon alpha 2-macroglobulin or IgM is superior to the IgG based index in differentiating glomerular diseases. *Kidney Internatinal*, *54*(6), 2098-2105. http://doi.org/10.1046/j.1523-1755.1998.00205.x

Wei, H., & Wang, J. Y. (2021). Role of polymeric immunoglobulin receptor in IgA and IgM transcytosis. *International Journal of Molecular Sciences*, *22*(5), 2284. https://doi.org/10.3390/ijms22052284

White, J. D., Malik, R., & Norris, J. M. (2011). Feline chronic kidney disease: can we move from treatment to prevention? *The Veterinary Journal*, *190*(3), 317-322. https://doi.org//10.1016/j.tvjl.2010.12.011

Austral Journal of Veterinary Science

Austral J Vet Sci 55, 203-207 (2023)
https://doi.org/10.4206/ajvs.553.07

CASE REPORT

Vertebral osteomyelitis associated with *Enterococcus faecalis* in Broiler Breeders in Chile

Leandro Cádiz[1,2], Miguel Guzmán[1,2], Fernando Navarrete[2], Paulina Torres[2], Héctor Hidalgo[2*]

[1] Núcleo de Investigaciones Aplicadas en Ciencias Veterinarias y Agronómicas, NIAVA. Facultad de Medicina Veterinaria y Agronomía, Universidad de las Américas, Campus Maipú, 5 de abril 620, Santiago, Chile.

[2] Laboratorio de Patología Aviar, Departamento de Patología Animal, Facultad de Ciencias Veterinarias y Pecuarias, Universidad de Chile, Santiago 8820808, Chile.

Article History
Received: 31.03.2023
Accepted: 12.07.2023
Published: 10.10.2023

Corresponding author
*Héctor Hidalgo
hhidalgo@uchile.cl

ABSTRACT. Vertebral osteomyelitis is a re-emerging disease characterized by inflammation and necrosis of the thoracic vertebral body, caused by *Enterococcus cecorum*. Here, we report the first case of vertebral osteomyelitis caused by *Enterococcus faecalis* in Broiler Breeders, in Chile, which also causes infections in humans and is resistant to multiple antimicrobials, representing a risk to public health.

Keywords: poultry, public health, infections, zoonosis.

Vertebral osteomyelitis (VO), or enterococcal spondylitis, is a re-emerging disease that affects broilers and breeders worldwide (Souillard *et al*., 2022). Although there are several causative agents of VO, including *Escherichia coli* and *Staphylococcus aureus*, species of the genus *Enterococcus*, particularly *E. cecorum*, are the most commonly identified (Braga *et al*., 2018). VO is characterized by inflammation and necrosis of the free thoracic vertebral body (T4). As a result, there is compression of the spinal cord and an alteration in the mobility of affected birds, which eventually die because of dehydration or starvation. The posture described as "sitting on their hocks," characterized by the extension of legs cranially and support from the tibiotarsal-metatarsal joints, is the classic clinical sign of this disease (Borst *et al*., 2017), which occurs more frequently in males than in females (Braga *et al*., 2018).

The genus *Enterococcus* belongs to the *Enterococcaceae* family. It is composed of ubiquitous gram-positive coccoid bacteria, catalase-negative, non-spore-forming, facultative anaerobes frequently found in the environment, and is part of the normal gastrointestinal (GI) tract microbiota in humans and animals, including birds and poultry. The main *Enterococcus* species associated with VO in poultry are *E. cecorum*, *E. faecium*, *E. hira, and E. faecalis*. The incidence of *Enterococcus*-associated diseases in poultry has increased in recent years, causing significant economic losses to the poultry industry (Souillard *et al*., 2022).

The first cases of VO due to *E. cecorum* infection were described in 2002 in farms in the Netherlands (Devriese *et al*., 2002) and the United Kingdom (Wood *et al*., 2002). Subsequently, cases have been reported in Belgium (De Herdt *et al*., 2009), Hungary (Makrai *et al*., 2011), and Germany (Jung & Rautenschlein, 2014). The disease has also been reported in North America, several US states (Pennsylvania, Washington, North Carolina, South Carolina, Arkansas, Mississippi, Alabama, and California) (Borst *et al*., 2012), and Canada (Stalker *et al*., 2010). In South America, vertebral osteomyelitis due to infection by other pathogens such as *E. coli*, *S. aureus* and *E. faecalis* has been reported in broilers in Brazil (Braga *et al*., 2016). *E. faecalis* is associated with several diseases affecting the poultry industry, including omphalitis, endocarditis, septicemia, and amyloidosis (Souillard *et al*., 2022). Here, we report a case of vertebral osteomyelitis caused by *Enterococcus faecalis* infection in broiler breeders in Chile based on *pre-* and *post-mortem* findings, bacterial cultures, biochemical characteristics, and molecular analysis.

Sudden onset of lameness and subsequent complete paralysis was reported in 67 male broiler breeders between six and 11 weeks of age on a farm with approximately 4,000 birds in Chile's Valparaíso Region. Nine live birds were obtained from Universidad de Chile's Avian Pathology Laboratory. They were prostrate, depressed, and sitting on their hocks (figure 1). The birds were euthanized by cervical dislocation, and *post-mortem* examination revealed a nodular mass in the free thoracic vertebral body (T4) (figure 2A). Sagittal section of the spine revealed vertebral osteomyelitis with necrosis and caseous material in the vertebral body (figure 2B). Some birds also presented with detachment of the coxofemoral articular cartilage, femoral head necrosis, femur osteomyelitis, and pericarditis.

Samples from vertebral lesions and femoral head necrosis were obtained aseptically, plated on tryptone soy agar with 5% blood and MacConkey agar, and incubated for 24 hours at 37°C under microaerophilic conditions. At 24 h post-incubation, cultures from the vertebral lesions and

Figure 1.
Broiler breeder prostrate, depressed and sitting on its hocks.

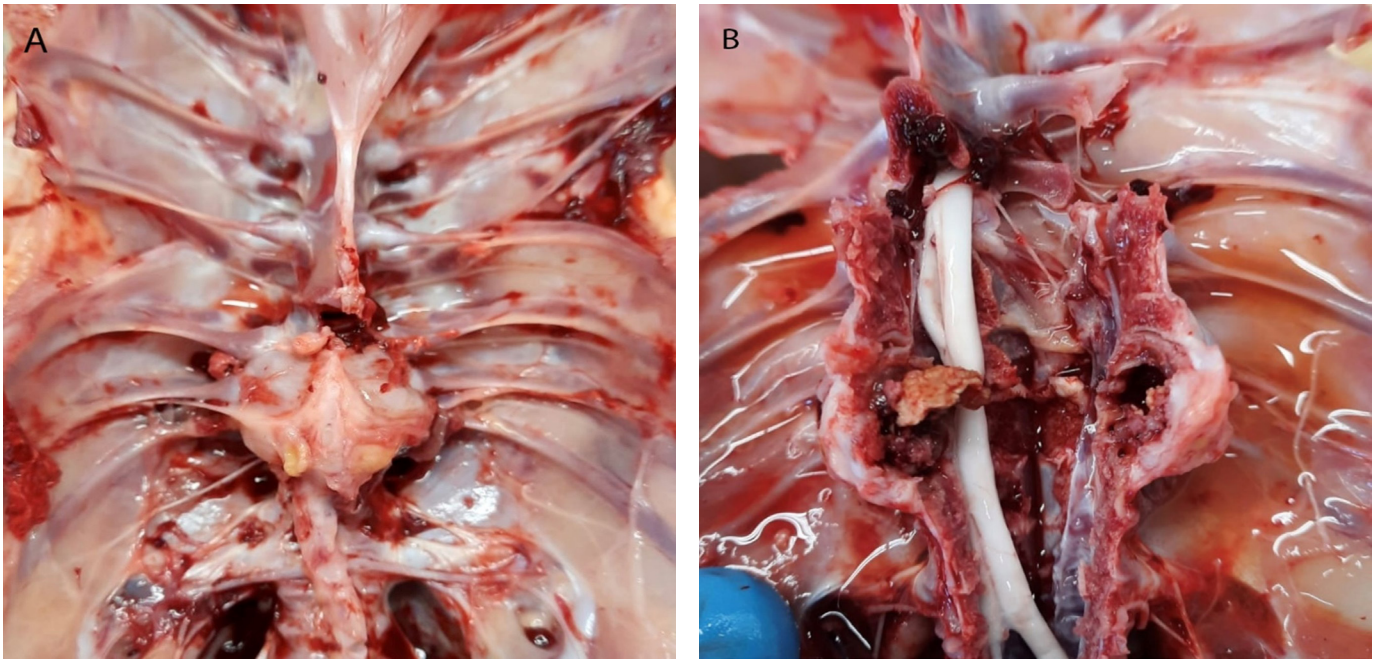

Figure 2.
A) Nodular mass in the free thoracic vertebral body (T4). B) Vertebral lesion with necrosis and caseous material after performing the sagittal section of the spine.

femoral head necrosis presented cream-colored, smooth-edged, very small, non-hemolytic colonies of up to 1.5 mm on blood agar plates (figure 3). No bacterial growth was observed on MacConkey agar plates.

Subsequently, pure subcultures were generated from single colonies on blood agar plates. The following day, the subcultures were processed for Gram staining, catalase reaction, and biochemical tests using the Vitek® 2 Compact identification system, according to the manufacturer's instructions (BioMerieux, Marcy-l'Étoile, France). Based on the characteristics of the colonies, Gram staining, and biochemical tests, the isolates obtained from vertebral lesions and femoral head necrosis corresponded to *E. faecalis*, which was confirmed by PCR. For this purpose,

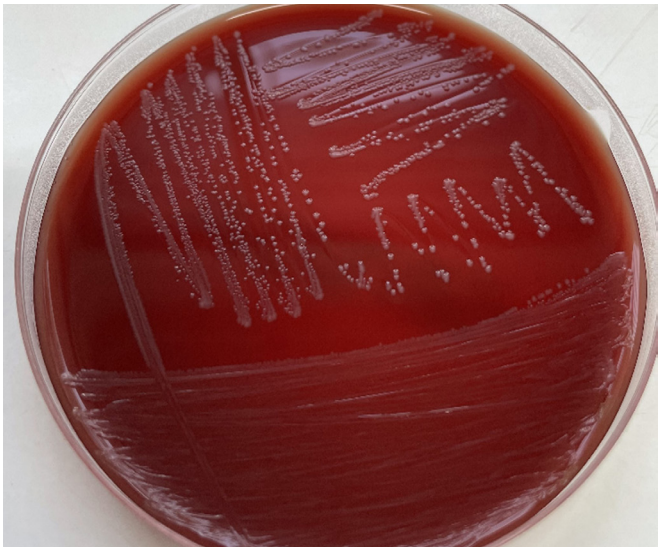

Figure 3.
Culture of *Enterococcus faecalis* on tryptone soy agar with 5% blood.

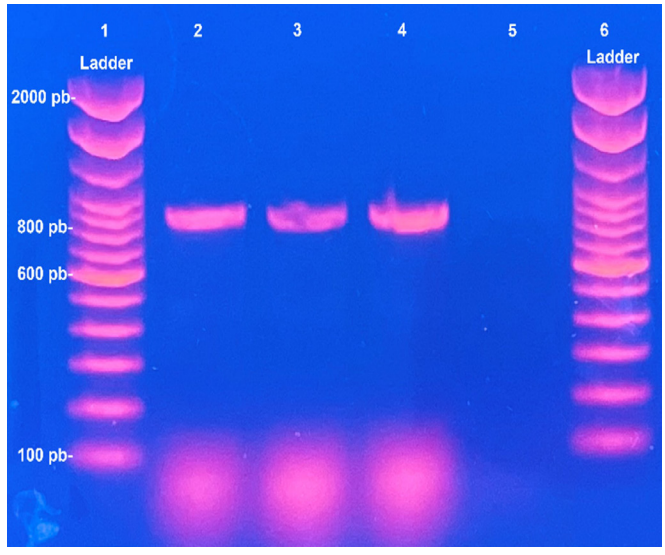

Figure 4.
Detection of *Enterococcus faecalis* by PCR. Lane 1:100 bp DNA Ladder. Lanes 2-4: *Enterococcus faecalis* DNA. Lane 5: Negative control. Lane 6:100 bp DNA Ladder.

Table 1.
Antibiogram results for *Enterococcus faecalis* isolates from vertebral lesions.

Antimicrobial	Inhibition halo (mm)	Interpretation
Amoxycillin	25	Sensitive
Colistin	0	Resistant
Enrofloxacin	21	Sensitive
Streptomycin	0	Resistant
Florfenicol	20	Sensitive
Fosfomycin	10	Resistant
Fosfomycin + Tylosin	0	Resistant
Lincomycin	0	Resistant
Lincomycin-Spectinomycin	10	Resistant
Norfloxacin	15	Intermediate
Oxytetracycline	0	Resistant
Sulfadoxine-Trimethoprim	22	Sensitive
Sulfisomidine	0	Resistant
Tiamulin	0	Resistant
Tylosin	0	Resistant

bacterial DNA was extracted according to the manufacturer's instructions using the PureLink™ Genomic DNA Mini Kit (Invitrogen, Massachusetts, United States). An 803-bp portion of the tuf gene was amplified using the primers EfisF: ATGCCGACATTGAAAGAAAAAATT and EfisR: TCAATCTTTGGTTCCATCTCT under previously reported conditions (Mahmoudpour *et al.*, 2007) (figure 4). An antibiogram (Kirby-Bauer test) was performed to determine the antimicrobial susceptibility of *E. faecalis* isolated from the vertebral lesions. The results are presented in Table 1.

This case report describes for the first time a case of vertebral osteomyelitis associated with *E. faecalis* in broiler breeders in Chile. This result is interesting because most reports have shown an association between vertebral osteomyelitis and *E. cecorum* infection in broilers and broiler breeders (Braga *et al.*, 2018). The case reported here affects broiler breeders between six and 11 weeks of age, which coincides with previous reports (age range: 5-13 weeks) and correlates with a period of rapid skeletal development in birds (Braga *et al.*, 2018). The *E. faecalis* strain isolated in this study was resistant to 10 of the 15 antimicrobials tested, indicating multidrug resistance. Furthermore, given the difficulty in achieving adequate concentrations of these drugs in the spine, the therapeutic options for affected birds are clearly diminished and treatment is longer than usual (Pöntinen *et al.*, 2021).

The origin and pathogenesis of vertebral osteomyelitis due to *Enterococcus* infection remains largely unknown (Borst *et al.*, 2017). However, predisposing factors such as immunosuppression, rapid bird growth, stocking density, and heat stress are thought to contribute to the susceptibility of poultry to enterococcal infections (Schreier *et al.*, 2022). In *Gallus domesticus*, the last cervical vertebra and first three thoracic vertebrae are fused into a notarium structure. After notarium, the fourth thoracic vertebra (T4) was the only mobile thoracic vertebra. The remaining thoracic and lumbar vertebrae are fused with the sacral vertebrae in a structure known as the *sinsacrum*. As the only mobile vertebra, T4 is subjected to high mechanical stress and microtrauma, predisposing it to infection (Braga *et al.*, 2018). The most likely explanation is that *E. faecalis*, normally present in the intestine, enters through

hematogenous dissemination due to a compromised or damaged intestinal barrier resulting from infection with other infectious agents, such as *E. coli* or *Eimeria* species. Consequently, when combined with the aforementioned environmental factors, any condition that disrupts the intestinal barrier may predispose an *Enterococcus*-associated infection (Jung & Rautenschlein, 2014).

Vertebral osteomyelitis caused by *E. faecalis* could have a significant economic impact on the poultry industry, including increased mortality in breeders, poor feed conversion ratios, and increased slaughterhouse condemnation in broilers (De Herdt *et al*., 2008). Minimizing the predisposing factors described above appears to be critical for preventing this disease. *Enterococcus* species are zoonotic agents that play an important role in nosocomial diseases (Pöntinen *et al*., 2021). They easily acquire antimicrobial resistance (AMR) determinants and thus play a key role in the dissemination of AMR. Humans can acquire enterococci from several sources, including environmental and animal food sources, contaminated with intestinal microbiota. Antimicrobial use in animal production systems (poultry, cattle, and pigs) is a major risk factor in the selection of AMR, and the poultry industry contributes the most to the dissemination, selection, and persistence of antimicrobial resistance in human populations, thereby increasing the risk to public health (Abreu *et al*., 2023).

Studies that allow phenotypic and genetic characterization of this bacterium would make it possible to adequately understand and control the disease and, in turn, reduce the role of the poultry industry as a source of *E. faecalis* strains and AMR.

DECLARATIONS

Acknowledgements

This study was funded by the Avian Pathology Laboratory, Department of Animal Pathology, Faculty of Veterinary and Animal Sciences, Universidad de Chile.

Competing interests

The authors declare that they have no competing interests.

REFERENCES

Abreu, R., Semedo-Lemsaddek, T., Cunha, E., Tavares, L., & Oliveira, M. (2023). Antimicrobial Drug Resistance in Poultry Production: Current Status and Innovative Strategies for Bacterial Control. *Microorganisms*, *11*(4), 953. https://doi.org/10.3390/microorganisms11040953

Borst, L. B., Suyemoto, M. M., Robbins, K. M., Lyman, R. L., Martin, M. P., & Barnes, H. J. (2012). Molecular epidemiology of *Enterococcus cecorum* isolates recovered from enterococcal spondylitis outbreaks in the southeastern United States. *Avian Pathology: Official Journal of the W.V.P.A*, *41*(5), 479–485. https://doi.org/10.1080/03079457.2012.718070

Borst, L. B., Suyemoto, M. M., Sarsour, A. H., Harris, M. C., Martin, M. P., Strickland, J. D., Oviedo, E. O., & Barnes, H. J. (2017). Pathogenesis of Enterococcal Spondylitis Caused by *Enterococcus cecorum* in Broiler Chickens. *Veterinary Pathology*, *54*(1), 61–73. https://doi.org/10.1177/0300985816658098

Braga, J., Martins, N. R., & Ecco, R. (2018). Vertebral Osteomyelitis in Broilers: A Review. *Brazilian Journal of Poultry Science*, *20*(3), 605–616. https://doi.org/10.1590/1806-9061-2017-0690

Braga, J. F., Silva, C. C., Teixeira, M. P., Martins, N. R., & Ecco, R. (2016). Vertebral osteomyelitis associated with single and mixed bacterial infection in broilers. *Avian Pathology: Official Journal of the W.V.P.A*, *45*(6), 640–648. https://doi.org/10.1080/03079457.2016.1193843

Herdt, P.D., Defoort, P., Steelant, J., Swam, H., Tanghe, L., Goethem, S.V., & Vanrobaeys, M. (2009). *Enterococcus cecorum* osteomyelitis and arthritis in broiler chickens. *Vlaams Diergeneeskundig Tijdschrift*, *78*, 44-48.

Devriese, L., Cauwerts, K., Hermans, K., & Wood, A. (2002). *Enterococcus cecorum* septicemia as a cause of bone and joint lesions resulting in lameness in broiler chickens. *Vlaams Diergeneeskundig Tijdschrift*, *71*(3), 219–221.

Jung, A., & Rautenschlein, S. (2014). Comprehensive report of an *Enterococcus cecorum* infection in a broiler flock in Northern Germany. *BMC Veterinary Research*, *10*, 311. https://doi.org/10.1186/s12917-014-0311-7

Mahmoudpour, A., Rahimi, S., Sina, M., Soroush, M. H., Shahi, S., & Asl-Aminabadi, N. (2007). Isolation and identification of *Enterococcus faecalis* from necrotic root canals using multiplex PCR. *Journal of Oral Science*, *49*(3), 221–227. https://doi.org/10.2334/josnusd.49.221

Makrai, L., Nemes, C., Simon, A., Ivanics, E., Dudás, Z., Fodor, L., & Glávits, R. (2011). Association of *Enterococcus cecorum* with vertebral osteomyelitis and spondylolisthesis in broiler parent chicks. *Acta Veterinaria Hungarica*, *59*(1), 11–21. https://doi.org/10.1556/AVet.59.2011.1.2

Pöntinen, A. K., Top, J., Arredondo-Alonso, S., Tonkin-Hill, G., Freitas, A. R., Novais, C., Gladstone, R. A., Pesonen, M., Meneses, R., Pesonen, H., Lees, J. A., Jamrozy, D., Bentley, S. D., Lanza, V. F., Torres, C., Peixe, L., Coque, T. M., Parkhill, J., Schürch, A. C., Willems, R. J. L., & Corander, J. (2021). Apparent nosocomial adaptation of *Enterococcus faecalis* predates the modern hospital era. *Nature Communications*, *12*(1), 1523. https://doi.org/10.1038/s41467-021-21749-5

Schreier, J., Rychlik, I., Karasova, D., Crhanova, M., Breves, G., Rautenschlein, S., & Jung, A. (2022). Influence of heat stress on intestinal integrity and the caecal microbiota during *Enterococcus cecorum* infection in broilers. *Veterinary Research*, *53*(1), 110. https://doi.org/10.1186/s13567-022-01132-y

Souillard, R., Laurentie, J., Kempf, I., Le Caër, V., Le Bouquin, S., Serror, P., & Allain, V. (2022). Increasing incidence of *Enterococcus*-associated diseases in poultry in France over the past 15 years. *Veterinary Microbiology*, *269*, 109426. https://doi.org/10.1016/j.vetmic.2022.109426

Stalker, M. J., Brash, M. L., Weisz, A., Ouckama, R. M., & Slavic, D. (2010). Arthritis and osteomyelitis associated with *Enterococcus cecorum* infection in broiler and broiler breeder chickens in Ontario, Canada. *Journal of Veterinary Diagnostic Investigation*, *22*(4), 643–645. https://doi.org/10.1177/104063871002200426

Wood, A. M., MacKenzie, G., McGiliveray, N. C., Brown, L., Devriese, L. A., & Baele, M. (2002). Isolation of *Enterococcus cecorum* from bone lesions in broiler chickens. *The Veterinary Record*, *150*(1), 27.

The Editorial Committee acknowledge the reviewers of Volume 55, 2023

ACOSTA, Gerardo
ALCALA-CANTO, Yasmin
ARIAS, J. Ignacio
ARIAS, J. Luis
ARIAS, Rodrigo
BARRIO, Elena
BERESFORD, Tom
BLAKEWAY, Stephen
BRAVO, Silvana
BRONSON, Ellen
BRUNDAGE, Cord
CARVALLO, Francisco
CHELLADURAI, Jesudoss
CELIKELOGLU, Koray
CITEK, Jindrich
CORTÉS-HINOJOSA, Galaxia
DADARAO, Shirish
DATZ, Craig
DE LIMA, Renato
DIAS, Ricardo
DOMENIS, Lorenzo
ELFATIK, Mohamed
FIORELLO, Christene
FULTON, Mick
GALECIO, Sebastián
GARCIA; Elena
GIANGASPERO, Annuniziata
GUZMAN, Miguel
HADDY, Emily
HEO, Suyoung
HERMOSILLA, Carlos
HERNÁNDEZ, Felipe
HERNÁNDEZ, Mariano
HERRERA, Emilio
IBAÑEZ, Rodrigo
JARAMILLO, Jairo
JONES, Ronald
JONES, Sarah
JONES-MCVEY, Rosalie
KENUBIH, Ambaya
KNOTEK, Zdenek
LANDAETA, Carlos
LARRIEU, Edmundo
LIU, Shou
LOPEZ, Claudia
LUNA, Daniela
MANFREDI, Ma. Teresa
MASRI, María
MANSO, Helio
MEDINA, Paul
MENDALE-PUNTER, Mathilde
MORALES, Abelardo
MORALES, Elizabeth
MORAN, Gabriel
MURAKAMI, Sawako
NAVARRO, Grisel
NEIRA, Víctor
ORTEGA, Rene
OYARZUN, Pablo
PALKHADE, Rajendra
PAPPA, Eleni
PARKES, Rebecca
PEREZ, Barbara
PINTO, Hudson
RAMIREZ, Galia
RAFFO, Eduardo
REIS, Thaisa
RETAMAL, Patricio
RIZZI, Chiara
ROGERS, Suzanne
ROLDAN, Antonio
SAENZ, Leonardo
SALGADO, Miguel
SANTURTUN, Eduardo
SCARABUCCI, Patricia
SCHUMACHER, John
SHURBE, Mesfin
SIRANGANATHAN, Nammalwar
SOBRERO, Raúl
SOZA, Paula
STEUER, Pamela
TABYNOV, Kairat
TADICH, Tamara
TALUKDER, Anup
THIEMANN, Alexandra
TORRES, Cristian
UBERTI, Benjamín
ULLOA, Cesar
VALENZUELA, Carolina
VERGARA, Fernando
VERHAAR, Nicole
VERJAN, Noel
VILA, Fernando
ZUÑIGA, Ma. Paz

Universidad Austral de Chile
Facultad de Ciencias Veterinarias

VOLUME 55 / VALDIVIA - CHILE / 2023 / Nº 3